



MINISTRY OF AVIATION SUPPLY

AERONAUTICAL RESEARCH COUNCIL

CURRENT PAPERS

Flow Unsteadiness and Model  
Vibration in Wind Tunnels at  
Subsonic and Transonic Speeds

*by*

*D. G. Mabey*

*Aerodynamics Dept., R.A.E., Bedford*

LONDON: HER MAJESTY'S STATIONERY OFFICE

1971

PRICE £1.30p NET



FLOW UNSTEADINESS AND MODEL VIBRATION IN WIND TUNNELS AT  
SUBSONIC AND TRANSONIC SPEEDS

by

D. G. Mabey

SUMMARY

Flow unsteadiness and model vibration in the RAE 3ft × 3ft tunnel have impeded static and dynamic measurements at subsonic and transonic speeds. The unsteadiness was measured with pressure transducers both in the 3ft × 3ft tunnel and a 1/9 scale model of this tunnel and good agreement obtained.

For the closed 3ft × 3ft tunnel, successive modifications to the balance section and diffuser derived from tests of the model tunnel have reduced the unsteadiness at subsonic speeds to an acceptable level for dynamic tests.

The unsteadiness in the slotted tunnels operated by diffuser suction originated in the extraction region and was reduced in the 3ft × 3ft tunnel by covering the slots with perforated screens. The unsteadiness was still higher than in the closed tunnel and just acceptable in the 0.91m × 0.69m (3ft × 2.2ft) working section and unacceptable in the 0.91m × 0.91m (3ft × 3ft) working section.

The perforated and closed working sections of the model tunnel had nearly the same unsteadiness and a similar result was achieved with the new perforated working section for the 3ft × 3ft tunnel in the frequency range normally of interest (from 20 to 900 Hz). Edge-tones generated at low unit Reynolds number were eliminated by a modification to the hole geometry.

Some comparative pressure fluctuation measurements in other closed, slotted and perforated tunnels are included in Appendices.

---

\* Replaces RAE Technical Report 70184 - ARC 32716.

<u>CONTENTS</u>		<u>Page</u>
1	INTRODUCTION	3
2	EXPERIMENTAL DETAILS	3
	2.1 Wind tunnels	3
	2.1.1 Closed section	4
	2.1.2 Top and bottom slotted section	4
	2.1.3 Slotted section	4
	2.1.4 Perforated section	5
	2.1.5 Model tunnel	5
	2.2 Pressure fluctuation measurements	5
	2.3 Model vibration measurements	7
	2.4 Flow visualization	8
3	RESULTS	9
	3.1 Closed working section	9
	3.2 Top and bottom slotted section	11
	3.3 Slotted working section	11
	3.4 Origin of unsteadiness in the model tunnel	12
	3.5 Perforated section	15
4	DISCUSSION	20
	4.1 Unsteadiness in slotted sections with diffuser suction	20
	4.2 Unsteadiness in perforated sections with diffuser suction	21
5	CONCLUSIONS	22
	Appendix A Adverse effect of corner half slots	25
	Appendix B Unsteadiness measurements in other slotted tunnels	26
	Appendix C Unsteadiness measurements in other perforated tunnels with 60° inclined holes	28
	Appendix D Unsteadiness measurements in 3 large wind tunnels	30
	Tables 1-4	32-35
	Symbols	36
	References	37
	Illustrations	Figures 1-46
	Detachable abstract cards	-

## 1 INTRODUCTION

The unsteadiness of airflow in wind tunnels is important because, if the model response excited by the unsteadiness is excessive, it may prevent the accurate measurement of overall forces (such as drag) or impede dynamic measurements (such as wing buffeting or flutter tests).<sup>(1)</sup> The desirable level of tunnel unsteadiness is zero for all frequencies; the acceptable level is normally determined by the type of tunnel test programme. The RAE 3ft x 3ft tunnel has been used for wing buffeting<sup>1</sup> and flutter tests, and some modifications were required to achieve an acceptable level of tunnel unsteadiness. This Report describes the modifications to the tunnel and the levels of unsteadiness achieved.

Fig.1 illustrates the principal sources of flow unsteadiness in transonic tunnels. Many of these sources were encountered in the RAE 3ft x 3ft tunnel and some useful reductions in unsteadiness were achieved by modifications to the tunnel described in sections 2 and 3; Tables 1 to 4 provide a summary of the principal configuration changes. The work is complex as it involves measurements both in the 3ft x 3ft tunnel and a 1/9 scale model of the 3ft x 3ft tunnel over a long period. The general reader may prefer to turn directly to sections 3.4, 3.5, 4 and 5 for details of the origin of the unsteadiness, a discussion of the principal results and the conclusions.

Some comparative pressure fluctuation measurements in other closed, slotted and perforated tunnels are included in Appendices. These measurements, together with wing buffeting measurements in several wind tunnels, furnish criteria to assess the suitability of wind tunnels for buffeting tests. The tunnel unsteadiness criteria appropriate to two levels of wing buffeting are illustrated in Fig.2; these buffeting levels are

(1) light buffeting associated with vortex type separations as on highly swept and slender wings, and

(2) heavy buffeting associated with separations on unswept wings.

Fig.2 shows the present limitations on buffeting tests imposed by the RAE 3ft x 3ft tunnel working sections.

## 2 EXPERIMENTAL DETAILS

### 2.1 Wind tunnels

The 3ft x 3ft wind tunnel was described in Refs.2 to 4, but these descriptions are not adequate for the present objective because the working

sections and diffuser have been substantially modified to reduce the tunnel unsteadiness. The modified tunnel is now described.

### 2.1.1 Closed section (Table 1)

The closed 0.91m × 0.91m (3ft × 3ft) working section is fitted with flat subsonic or contoured supersonic liners<sup>2,3</sup> (Fig.3). Downstream of the closed working section is the supersonic balance section which originally had a centre body with a bluff base to form a constant area supersonic diffuser and to shield the flow spoilers. The bluff base of this centre body caused a large flow separation in the mobile diffuser and considerable unsteadiness in the working section (3.1). To eliminate this separation a removable fairing was first inserted in the mobile diffuser. Subsequently the centre body and the flow spoilers were removed from the supersonic balance section. The wooden linings of the steel shell of the balance section were altered to provide a constant area diffuser without the centre body, Fig.3b, and a pair of flat plate spoilers fitted to the sidewalls of the mobile diffuser, Fig.3c. These diffuser spoilers may be used with any one of the four working sections.

### 2.1.2 Top and bottom slotted section (Table 2)

The 0.91m × 0.69m (3ft × 2.2ft) top and bottom slotted working section (Fig.4) is formed by inserting slotted liners over the subsonic liners of the closed working section and also utilizes the supersonic balance section. There are four complete slots 25 mm (0.98 in) wide and two corner half slots 12.5 mm (0.49 in) wide in these slotted liners. The lower surface of the complete slots was covered with perforated metal (Fig.4c-d) to reduce the flow unsteadiness (3.2). This small section is used for most transonic measurements in the 3ft × 3ft tunnel.

### 2.1.3 Slotted section (Table 3)

The large 0.91m × 0.91m (3ft × 3ft) transonic working section with four slotted walls (Fig.5) utilizes a special balance section<sup>4</sup>. Model vibration limits the use of this section<sup>5</sup> and the unsteady signal from strain gauge balances is sometimes sufficient to overload the ac amplifiers of the self levelling potentiometers and produce spurious readings<sup>6</sup>. Wing buffeting tests in this section are impeded by the high level of wing vibration at zero incidence<sup>1</sup>. This working section has one complete slot on every side 61 mm (2.38 in) wide and half slots 30.5 mm (1.19 in) wide in every corner of the top and bottom liners. The lower surface of these slots was also covered with

perforated metal (Fig.5c-d) to reduce the flow unsteadiness (3.3), but this is still higher than with the top and bottom slotted section.

#### 2.1.4 Perforated section (Table 4)

The reduction in unsteadiness obtained by covering the slots with perforated metal suggested that a transonic tunnel with fully perforated walls would have low unsteadiness. Hence a perforated working section  $0.91 \text{ m} \times 0.82 \text{ m}$  ( $3 \text{ ft} \times 2.7 \text{ ft}$ ) was constructed for the  $3 \text{ ft} \times 3 \text{ ft}$  tunnel (Fig.6). This perforated working section has  $9.5 \text{ mm}$  ( $0.375 \text{ in}$ ) diameter holes drilled at  $60^\circ$  to the vertical to ensure good shock cancellation at the design Mach number  $M = 1.2$ , as in the AEDC tunnels at Tullahoma. To ensure shock cancellation at intermediate Mach numbers from  $M = 1.0$  to  $1.2$  the wall porosity can be continuously varied from 0 to 6% by sliding thin perforated plates under the liners near the model as described by Felix<sup>7</sup>. Some extensive modifications to this section were required to achieve low unsteadiness; these modifications are described in section 3.5 and Table 4.

#### 2.1.5 Model tunnel

The  $4 \text{ in} \times 4 \text{ in}$  tunnel is a  $1/9$  scale model of the  $3 \text{ ft} \times 3 \text{ ft}$  tunnel which represents the contraction, working sections, balance sections and mobile diffuser illustrated in Figs.3-6. The closed and slotted working sections are to scale, but owing to an error the open area ratio of the  $4 \text{ in} \times 4 \text{ in}$  top and bottom slotted section is 16% instead of 8% as in the  $3 \text{ ft} \times 3 \text{ ft}$  tunnel. The  $4 \text{ in} \times 4 \text{ in}$  perforated working section is  $4 \text{ in} \times 3.56 \text{ in}$  (Fig.7) and the open area ratio is about 6% based on the hole diameter. Fig.8 shows the geometry of the holes in both the  $4 \text{ in} \times 4 \text{ in}$  and  $3 \text{ ft} \times 3 \text{ ft}$  perforated working sections.

## 2.2 Pressure fluctuation measurements

Owen has described the basic technique used for pressure fluctuation measurements in RAE wind tunnels<sup>8</sup>. The results are presented in nondimensional form by dividing the rms intensity of pressure fluctuations,  $\bar{p}$ , by the wind tunnel kinetic pressure  $q$ . A nondimensional frequency parameter  $n = fw/V$  is used (referred to as a Strouhal number when one particular frequency parameter predominates in the pressure fluctuation spectra), where  $f =$  frequency Hz (c/s),  $w =$  width of tunnel m (ft) and  $V =$  velocity in m/s (ft/s) and a nondimensional spectrum function  $F(n)$  such that

$$\overline{p^2}/q^2 = \int_{n=0}^{n=\infty} F(n) dn = \int_{\log n=-\infty}^{\log n=\infty} nF(n) d(\log n) \quad .$$

In buffeting investigations the presentation of excitation spectra in terms of  $\sqrt{nF(n)}$  against  $\log n$  is useful and this form is adopted here. Owen's previous pressure fluctuation measurements in the 3ft  $\times$  3ft tunnel<sup>9</sup> may have been subject to some interference from the model base flow or the support sting in the subsonic and transonic regions. To eliminate this possibility the present measurements were made with a pressure transducer flush with a sidewall or a slat. (The principal transducer positions are shown in Figs.3-7.) The pressure transducer then receives additional excitation from the fully established wall turbulent boundary layer, but this represents a small, nearly constant correction at high frequency, which is often approximated by  $\overline{p}/q = 0.006$ . For a turbulent boundary layer the rms pressure fluctuations are given more precisely by  $\overline{p}/q \approx 2.5 \times$  the skin friction coefficient  $C_f$  and  $C_f$  is estimated to be about 0.002 to 0.003 for these tunnel boundary layers. No corrections were made to the spectra for the turbulent boundary layer pressure fluctuations or the size of the transducer relative to the boundary layer. In the perforated working section almost the same pressure fluctuations were simultaneously measured by transducers mounted flush with the bottom and side liners as on the cylindrical section of a 9 in long ogival nosed body mounted on the tunnel centre line. Hence the contribution of the wall boundary layer was small and the pressure fluctuation field approximately onedimensional across the tunnel. These comparative measurements were made simultaneously with sensitive transducers and low noise level amplifiers (see next paragraph).

Several RAE miniature differential pressure transducers<sup>10</sup> were used for these experiments. These transducers were of the capacitance type and were insensitive to accelerations. The first transducers used had a pressure range of  $\pm 14 \text{ kN/m}^2$  ( $\pm 2 \text{ lb/in}^2$ ) although later (November 1967) transducers with a pressure range  $\pm 4 \text{ kN/m}^2$  ( $\pm 0.6 \text{ lb/in}^2$ ) became available. The transducers with a pressure range of  $\pm 14 \text{ kN/m}^2$  ( $\pm 2 \text{ lb/in}^2$ ) were used in conjunction with a 20 kHz carrier system amplifier for the first measurements in the slotted sections of the 3ft  $\times$  3ft tunnel and in the model tunnel (Figs.12-27). The signal/noise ratio of this system was just adequate when the tunnel unsteadiness was high - typical rms signals wind on were about 60-100 mV and the wind off noise was about 28 mV (some of this was near the carrier frequency). From November 1967, however, 400 kHz amplifiers were used for the measurements in the perforated section and comparative measurements in the slotted and closed sections



(Figs.28 to 38). These gave typical rms signals of 500 mV (or 1 V with the transducer with a pressure range of  $\pm 4 \text{ kN/m}^2$  ( $\pm 0.6 \text{ lb/in}^2$ ) and the wind off noise was reduced to about 8 mV. These amplifiers and the sensitive transducers greatly improved the signal/noise ratio. The transducer output was recorded directly from 20 to 6300 Hz on a level recorder coupled to a Bruel and Kjaerspectrum analyser. The wind-on signal in dB (corrected for wind off noise at the appropriate frequency) was then converted directly to a voltage. The static calibration  $K$ , analyser bandwidth ratio  $\epsilon$ , the tunnel kinetic pressure  $q$  were then used to form  $\sqrt{nF(n)}$  thus

$$\sqrt{nF(n)} = (\text{voltage}) \times K/q\sqrt{\epsilon} .$$

Throughout these experiments the same analyser bandwidth ratio  $\epsilon = 0.12$  was used.

In the 3ft  $\times$  3ft tunnel a limited amount of data from 2 to 20 Hz was recorded manually using a Muirhead selective filter, for comparison with the model tunnel data at 20 to 180 Hz (i.e. the same frequency parameter). The 3ft  $\times$  3ft tunnel measurements were generally made at a total pressure  $P_t$  of  $98 \text{ kN/m}^2$  ( $14.3 \text{ lb/in}^2$ ) to ensure comparable accuracy with those in the model tunnel which runs at a total pressure about  $2 \text{ kN/m}^2$  ( $0.3 \text{ lb/in}^2$ ) below atmospheric pressure.

### 2.3 Model vibration measurements

The table shows typical vibration measurements taken on a cambered slender wing model mounted on an internal six component balance in the slotted transonic section at  $M = 0.40$ :

Balance component	Rms total stress/kinetic pressure
Normal force	19
Pitching moment	19
Side force	19
Yawing moment	19
Rolling moment	24
Axial force	570

These measurements illustrate the serious nature of the vibration problem particularly for axial force. (The natural frequency of model vibrations on

axial force balances in the 3ft  $\times$  3ft tunnel is generally within the range from 100 to 200 Hz.) The present measurements were on the axial force balance of a slender wing model (Fig.9) which vibrated badly in previous tests<sup>6</sup>. A slender wing was selected because its weak perturbation of the mean flow appeared to interfere with the movement of unsteady normal waves upstream through the working section only close to  $M = 1.0$  (section 2.4).

The axial force bridge was excited by 6 V dc ( $e$ ) and the rms voltage fluctuation ( $\bar{e}$ ) was measured with the equipment used in buffeting investigations<sup>1</sup>. The rms voltage fluctuation  $\bar{e}$  is converted to an rms balance stress  $\sigma$  by the relation

$$\bar{e}/e = \nu \sigma/E$$

where  $\nu$  = gauge factor = 2 for wire gauges

$\sigma$  = balance stress  $\text{kN/m}^2$  ( $\text{lb/in}^2$ )

$E$  = Young's modulus  $\text{kN/m}^2$  ( $\text{lb/in}^2$ ).

At constant Mach number the balance stress was proportional to the kinetic pressure  $q$  (implying only structural damping for this vibration mode) and the measurements were presented as curves of  $\sigma/q$ . To avoid changing the structural damping the model was not removed from the sting or quadrant during the comparative tests shown in Fig.12.

#### 2.4 Flow visualization

Oil flow photographs showed that the mean streamlines were comparable in the mixing regions of the 3ft  $\times$  3ft and 4in  $\times$  4in tunnels where the pressure fluctuations were generated. These mixing regions were the area of separated flow in the mobile diffuser downstream of the supersonic balance section (2.1.1) and the extraction region near the end of the slotted working sections (2.1.2 and 2.1.3) (Fig.10).

Some spark schlieren photographs with a vertical knife edge were taken in the top and bottom slotted working sections of the 3ft  $\times$  3ft and 4in  $\times$  4in tunnel (exposure about 1  $\mu\text{s}$ ). They showed nearly normal waves which formed in the extraction region and moved upstream into the working section from  $M = 0.80$  to  $M = 1.00$  (Fig.11). Above  $M = 1.0$ , photographs in the 4in  $\times$  4in tunnel showed that these waves were confined to the extraction region downstream of the terminal shock. In both tunnels high speed cine films of the waves taken with a Fastex camera at 3000 frames/s showed that they moved upstream through the working section with a wave velocity  $V_w$  given by

$$V_w = (1 - M) a$$

where  $a$  = velocity of sound. (Mach numbers derived from the measured wave velocity  $V_w$  were within  $\pm 0.002$  of the Mach numbers derived from the plenum chamber static pressure.)

Strong normal waves were also found in the closed working section with the diffuser fairing out; very weak, oblique waves of much higher frequency were observed with the mobile diffuser fairing in. A cine film showing these waves passing over the slender wing in the 3ft  $\times$  3ft tunnel is available.

### 3 RESULTS

Fig.12 summarizes reductions in tunnel unsteadiness  $[\sqrt{nF(n)}]$ , and model response  $[\sigma/q]$  achieved by the principal modifications to the closed and slotted working sections. The levels of unsteadiness and model response shown refer to axial force balance vibrations of the slender wing model (Fig.9) at a single frequency of 140 Hz. A complete picture covering all frequencies of the improvements achieved by the tunnel modifications can only be obtained by an examination of the unsteadiness spectra  $\sqrt{nF(n)} \text{ v } \log n$ . These spectra are now discussed.

#### 3.1 Closed working section (Table 1)

The principal source of unsteadiness in the closed working section was identified by tests in the model tunnel as the large separation in the mobile diffuser downstream of the base of the balance section centre body. The working section pressure fluctuations at  $M = 0.80$  (Fig.13) suggest that the excitation from the separation may have excited the first and second diffuser transverse organ pipe resonance frequencies (at 110 and 220 Hz) and weakly excited the third resonance at 360 Hz. The same effect was found at other Mach numbers with some variation of the relative intensity of the modes caused by variations in the predominant frequency of the excitation from the separation. (The base flow on the centre body was not twodimensional because its aspect ratio was only 3 and there were thick boundary layers on the walls. However, the predominant frequency at  $n = 0.38$  corresponds with a Strouhal number based on the width of the centre body of 0.16, a typical value for bluff bodies.)

A removable fairing to eliminate this separation was developed in the model tunnel and a similar fairing subsequently manufactured for the 3ft  $\times$  3ft tunnel. This fairing reduced the working section pressure fluctuations (Figs.13 and 14) and the axial force balance stress (Fig.12).

Two significant observations can be made from Fig.14. The first is that when the tunnel chokes (at  $M = 1.075$  with the tunnel empty because an excessive allowance was made for boundary layer growth in the working section) the excitation appears small because

$$\sqrt{nF(n)} \approx 0.0005$$

from  $n = 0.04$  to  $4.0$ . This signal includes the excitation from the sidewall boundary layer and hence the flow in the maximum section downstream of the aftercooler, honeycomb and screens is good<sup>11</sup>. (Later more accurate measurements with the improved instrumentation show that this level should be rather higher - about  $0.002$  to  $0.003$ .) The second observation is that at subsonic speeds, even with the diffuser fairing, there is a large low frequency component in the range from  $n = 0.02$  to  $0.08$  which disappears when the tunnel chokes. A similar low frequency component was found in the model tunnel and was higher with the centre body and diffuser fairing than with the unfaired centre body (Fig.15). One hypothesis to explain the origin of this low frequency unsteadiness was that the flow did not divide steadily on either side of the long centre body, but oscillated from side to side. (Low frequency unsteadiness of this type has been observed in bifurcated intake ducts<sup>29</sup>.) If this hypothesis was correct, it seemed possible that a very short centre body would reduce the low frequency unsteadiness. Hence the long centre body and diffuser fairing were removed from the model tunnel and replaced by a revised balance section without a centre body which incorporated nearly the same area distribution. This revised balance section reduced the low frequency excitation in the model tunnel (Fig.16) and hence was subsequently incorporated in the  $3\text{ft} \times 3\text{ft}$  tunnel (Fig.17). In the  $3\text{ft} \times 3\text{ft}$  tunnel the low frequency unsteadiness associated with the flow over the step and the rest of the return circuit is still relatively high, at subsonic speeds, with  $\sqrt{nF(n)} \approx 0.004$  (Fig.17).

The revised balance section for the  $3\text{ft} \times 3\text{ft}$  tunnel should also reduce model vibration at supersonic speeds, because in the model tunnel the revised balance section reduces the low frequency component of the pressure fluctuations at the quadrant (Fig.18) which arise from the movement of the terminal shock system. (The flow unsteadiness caused by the unfaired centre body in the  $3\text{ft} \times 3\text{ft}$  tunnel has vibrated the quadrant at  $M = 2.0$  and thus excited serious lateral oscillations at  $10$  to  $40$  Hz on several models).

### 3.2 Top and bottom slotted section (Table 2)

The unsteadiness in this section before modification was unacceptable for buffeting tests. Comparative buffeting measurements on Model B of Ref.1 showed that the unsteadiness in this working section was much higher than in the HS 2ft × 2ft slotted tunnel (Fig.10, Ref.1) which apparently had a similar slot configuration. Spark schlieren photographs confirmed that the waves in the 3ft × 3ft tunnel were stronger than those in the HS 2ft × 2ft tunnel. A comparison of the tunnels revealed only one difference which was believed to be significant (Appendix B). The 3ft × 3ft tunnel utilized deep perforated channel screens as developed for the temporary transonic section<sup>12</sup> whereas the HS tunnel had flat perforated screens immediately under the slots (Fig.40). This change in screen geometry would certainly alter the slow mixing process in the plenum chamber produced by the outflow through the slots and the more rapid mixing process in the extraction region produced by diffuser suction. Hence the channel screens of the 3ft × 3ft tunnel were replaced by flat screens and the model vibration at 140 Hz was immediately reduced (Fig.12). Schlieren photographs showed that the strength of the waves in the working section was also reduced, although their frequency was not altered.

Fig.19 shows the working section pressure fluctuations with flat screens. There is still a peak at about  $\sqrt{nF(n)} = 0.004$  at subsonic Mach numbers from  $M = 0.80$  to  $0.90$  at a frequency parameter  $n = 1.2$  (this corresponds with a frequency of 350 Hz at  $M = 0.80$ ). The later more accurate measurements, with the rear of the central slat cut away, give higher pressure fluctuations, e.g. Fig.38 shows  $\sqrt{nF(n)} = 0.007$  at  $M = 0.80$  for  $n = 1.2$ . At supersonic speeds the spectra are flatter and lower, although there are local peaks, e.g.  $\sqrt{nF(n)} = 0.003$  at  $n = 1.8$  at  $M = 1.10$ . These imply that the pressure fluctuations in the extraction region can be transmitted to the working section through the plenum chamber, perhaps by altering the initial expansion through the slots. Fig.19 also shows that the low frequency component (at  $n = 0.03$ ) is smaller over the complete Mach number range, than in the closed working section, (Fig.14) possibly because of the lower velocities in the diffuser.

### 3.3 Slotted working section (Table 3)

The first attempt to reduce the unsteadiness of this section with the same type of thin screens which had improved the top and bottom slotted section was successful, judged by vibration measurements on the slender wing. However fatigue cracks quickly started at the downstream end of the screens and they were replaced by thicker screens.

The new screens (Fig.5c) were 3.2 mm (0.125 in) thick. The hole diameter and open area ratio were not considered critical with respect to the unsteadiness and were increased from 2.16 mm (0.085 in) and 33% to 6.25 mm (0.25 in) and 50% respectively to improve the subsonic Mach number distribution. These screens achieved about the same reduction in model vibration as the thin screens (Fig.12) and reduced the tunnel unsteadiness at the peak ( $n \approx 0.6$  at  $M = 0.80$  to  $0.85$ ) by about 50% (Fig.20). However the slotted transonic section is still 2 to 3 times more unsteady than the top and bottom slotted section (comparing Figs.19 and 20) even allowing for the difference in spectra, probably because the wider slots permit more effective mixing in the slotted transonic section. Even with these improvements steady measurements may still be impossible on a particular model if the model/balance combination has an axial force frequency of about 100 to 200 Hz and low damping. Thus the slender wing still cannot be safely tested in this section at a reasonable Reynolds number (cf. the model response in the closed, top and bottom slotted sections and slotted transonic section Fig.12).

The unsteadiness in the slotted transonic sections in the 3ft  $\times$  3ft and 4in  $\times$  4in tunnels with the slots open is similar in character, although the 3ft  $\times$  3ft tunnel appears about 2 to 4 times as bad as the 4in  $\times$  4in tunnel (Fig.21).

#### 3.4 Origin of unsteadiness in the model tunnel

Pressure fluctuation measurements in the slotted transonic working section of the model tunnel were followed by comparative measurements at a series of different points down the diffuser with the slotted and perforated working sections. These measurements showed (Fig.22) that with the slotted working section there were large pressure fluctuations in the extraction region with a peak of  $\sqrt{nF(n)} = 0.036$  at  $n = 0.8$ . With the perforated working section the pressure fluctuations at the same point were small and the spectrum was flat with a level  $\sqrt{nF(n)} \approx 0.002$ . The large pressure fluctuations originating in the extraction region of the slotted working section rapidly decayed as the pressure transducer was moved downstream. There was a small increase in the weak pressure fluctuations associated with the perforated working section as the transducer moved downstream through the re-attachment point on the sidewalls (Fig.22) and the pressure fluctuations then decayed towards the end of the mobile diffuser. The general correspondence between the spectra measured in the extraction region (Fig.22a) and the working sections (Fig.23a) was good so that the extraction region was definitely identified as the origin of the unsteadiness.

High speed cine schlieren films taken of the flow in the extraction region of the top and bottom slotted section of the 4in  $\times$  4in tunnel suggested an hypothesis to explain the generation of the unsteadiness. (This region is included in the cine film). Two shear layers were visible, a steady shear layer from the slats and an unsteady flow from the slots which oscillated so that a re-attachment point appeared to move upstream and downstream in the diffuser. The perforated screens placed across the slots in the 3ft  $\times$  3ft tunnel probably inhibited this oscillation of the slot flow and hence reduced the pressure fluctuations (sections 3.2 and 3.3). The same argument would apply with greater force to the perforated working section. This hypothesis was also substantiated by a test made in the model tunnel. In this test, pressure fluctuations in the working section and extraction region were compared with the slots open (10% open area ratio) and with the slots closed by shaped inserts. The results (Fig.24) show a large reduction in pressure fluctuations both in the working section and in the diffuser when the slots are closed and the separation point fixed at the periphery of the working section. With the slots closed the pressure fluctuations at both points are almost identical with those measured with the perforated working section.

This test also confirms the previous result that with the closed working section (Fig.3) and the revised balance section there is no high frequency unsteadiness associated with the sudden enlargement to the mobile diffuser (Figs.16 and 17). This flow over the step has a fixed separation line and re-attaches to a fixed surface. In the original balance section although there were fixed separation lines from the bluff base of the centre body the flow did not re-attach, but formed a wake which moved down the centre of the diffuser. (The much smaller pressure fluctuations with the step in the side-wall compared to those with the bluff base on the centre line recall the reduction in pressure fluctuations, vortex shedding and base drag achieved by the insertion of splitter plates into the wakes of bluff bodies<sup>13</sup>.)

The pressure transducer could not detect any organ piping in the transonic balance section at streamwise stations (a) to (d) (Fig.22) when traversed vertically nor were any significant horizontal variations of pressure fluctuations detected in the extraction region with either the slotted or perforated working sections. Despite the absence of organ piping in the transonic diffuser there was a characteristic peak excitation frequency in all the slotted working sections (Figs.20, 21). This frequency is about the same

for all 3ft × 3ft and 4in × 4in working sections when expressed as a Strouhal number in terms of the slot width  $w_s$ , rather than the tunnel width  $w$  (Fig.25), with a fairly well defined range

$$0.030 \leq S^* \leq 0.040 \quad .$$

Fig.26 shows comparative measurements of plenum chamber pressure fluctuations for both slotted and perforated working sections. (Measurements are presented for positions 1 and 4 shown in Fig.22; position 1 was on the sidewall centre line at the same streamwise position as the reference static hole.) At position 1 the slotted tunnel has a peak of  $\sqrt{nF(n)} = 0.0053$  at  $n = 0.77$  (Fig.26a) compared to the extraction region which has a peak of  $\sqrt{nF(n)} = 0.036$  at  $n = 0.80$  (Fig.24a). In the plenum chamber of the perforated section there is no high frequency excitation and only a relatively small amount of low frequency excitation below  $n = 0.08$  similar to that in the slotted section. These spectra are not significantly different when the Mach number is increased to  $M = 1.04$  (Fig.26b). At position 4 upstream the high frequency excitation in the slotted section is about 40% of that at position 1, but the low frequency fluctuations are unaltered (Fig.26c and d). These measurements may be summarized by saying that in the plenum chamber the high frequency pressure fluctuations resemble those in the extraction region but attenuate fairly rapidly moving upstream whereas the low frequency component is not attenuated moving upstream.

An interesting comparison may be made between the pressure fluctuations in the slotted working section and plenum chamber.

<u>Mach number</u>	<u>Working section</u> <u>Fig.23</u>	<u>Plenum chamber</u> <u>Fig.26</u>
Subsonic	Peak $\sqrt{nF(n)} = 0.010$	Peak $\sqrt{nF(n)} = 0.0053$
$M = 0.80$	at $n = 0.60$	at $n = 0.77$
Supersonic	Peak $\sqrt{nF(n)} = 0.004$	Peak $\sqrt{nF(n)} = 0.0055$
$M = 1.03$	at $n = 0.5$	at $n = 0.65$

The table shows that at subsonic speeds the working section pressure fluctuations are greater than those in the plenum chamber. This is because at subsonic speeds the working section receives pressure fluctuations from the extraction region via the mainstream and the plenum chamber. However at



supersonic speeds the working section only receives pressure fluctuations from the extraction region via the plenum chamber, and there is probably some attenuation through the narrow slots. (The unsteadiness of the plenum chamber flow might induce additional unsteadiness by boundary layer movement on the liners.) Hence these measurements explain why the slotted working section is inferior to the perforated working section even at supersonic speeds (Fig.23), for the perforated working section has little unsteadiness in the extraction region, even less in the plenum chamber and little chance of radiating energy through the small inclined perforations into the working section.

The plenum chamber pressure fluctuation measurements show some attenuation moving upstream. According to the theory developed by Eggink<sup>14</sup> weak compression waves moving upstream through the working section at high subsonic speeds must intensify into shock waves and then be dissipated as heat. Hence the corresponding wall pressure fluctuations would first increase and then decrease. This theory was verified in the model tunnel top and bottom slotted working section by measuring the sidewall pressure fluctuations at  $M = 0.80$  as the transducer was moved upstream. The measurements (Fig.27) show a small initial increase in the peak pressure fluctuations just upstream of the ends of the slots (probably just significant) and then an almost monotonic decrease. There is no alteration in the frequency of peak excitation (about 1360 Hz) along the working section. The high speed cine film also suggests that the waves are attenuated moving upstream.

No normal waves could move upstream from the extraction region through the working section at supersonic speeds. Sidewall pressure fluctuation measurements at different positions were attempted at  $M = 1.11$  but were not repeatable because of large changes induced by small alterations in the test section Mach number ( $\pm 0.005$ ). The spectra measured were characterized by a large low frequency fluctuation from 20 to 200 Hz ( $\sqrt{nF(n)} \approx 0.005$ ) associated with the movement of the tunnel shock system of inclined waves; the spectra were very flat from 1000 to 2000 Hz with a general level  $\sqrt{nF(n)} = 0.0020$  (see lower half of Fig.27).

### 3.5 Perforated section (Table 4)

A low level of unsteadiness was expected for the 3ft  $\times$  3ft tunnel perforated working section on the basis of the model tunnel tests described above. However, during the first runs the tunnel was extremely noisy at speeds up to  $M = 0.70$  and large working section pressure fluctuations ( $\sqrt{nF(n)} \approx 0.10$ ) were measured which increased in frequency from 30 to 50 Hz

as speed increased. This phenomenon recalled the unsteadiness observed in a slotted water tunnel which was traced to edge-tones shed from the diffuser collectors and eliminated by changing the geometry of the collectors<sup>15</sup>. A similar process seemed possible with the perforated working section because the side collectors had a small leading-edge radius. Hence bluff side baffles were added to the side collectors and these reduced the audible noise and the working section pressure fluctuations (Fig.28). (No further improvement was obtained with more streamlined baffles.) These side baffles suppressed the shedding of vorticity inevitably associated with a stagnation point oscillation on the sharp collector nose. [No comparable unsteadiness was observed in the slotted transonic section with these collectors because the streamwise flow was then constrained to a few discrete areas downstream of the four complete slots (Fig.10).]

Significant unsteadiness remained at 50 Hz and another experiment\* was made to determine its origin. All the holes in the perforated working section were covered with adhesive tape and the working section pressure fluctuations reduced as anticipated (Fig.29). Then the tapes were removed progressively from every wall in the sequence illustrated; the unsteadiness at 50 Hz only returned when both sidewalls were uncovered (Fig.29b). (This effect was also observed in the plenum chamber.) This suggested that the generation of edge-tones depended on a symmetric sidewall configuration and also that the edge-tones might be influenced by the degree of interconnection between the side plenum chambers. Hence longitudinal wooden baffles were inserted in every corner of the plenum chamber. These reduced the unsteadiness at  $M = 0.60$  but introduced large pressure fluctuations and excessive external noise at other speeds. These solid baffles were then removed and perforated with 2 in diameter holes drilled halfway between the transverse venting holes spaced every 8 in along the longitudinal I beams (these venting holes are 4 in diameter). When the perforated corner baffles were inserted the pressure fluctuations at 50 Hz were reduced (Fig.30) and there was no increase in pressure fluctuations or external noise at other speeds. Perforated corner baffles are desirable to equalize small static pressure differences between the plenum chambers induced by lifting models.

For the next series of tests another pressure transducer was placed near the downstream end of the plenum chamber. Fig.31a shows that in the plenum

---

\*This was suggested by Mon. R. Destuynder in the light of comparable experiments in the ONERA 6ft tunnel<sup>16</sup>.

chamber the pressure fluctuations at 50 Hz were higher than those in the working section, suggesting resonance at the longitudinal organ pipe frequency (the 11 ft length corresponds with a closed/closed mode of 50 Hz). This hypothesis was confirmed by the insertion of a paper honeycomb at the end of the plenum chamber. This introduced attenuation between the diffuser and the plenum chamber and thus reduced the plenum chamber pressure fluctuations at 50 Hz. However, the honeycomb did not alter the working section pressure fluctuations (Fig.31b), indicating that the unsteadiness was excited in the diffuser or working section rather than the plenum chamber. The honeycomb was then removed because it interfered with the flow through the downstream end of the perforated liners and absorbed extra power. The honeycomb was replaced by a series of plenum chamber baffles wedged through the 4in diameter transverse venting holes. In the upstream part of the plenum chamber these baffles were set at  $45^\circ$  to produce high acoustic damping for the longitudinal mode. In the downstream part of the plenum chamber the baffles were set at zero incidence to provide some limited acoustic damping and to partially inhibit the unsteady lateral flow in the plenum chamber indicated by nylon tufts. These combined baffles reduced the plenum chamber pressure fluctuations more effectively than the honeycomb and also reduced the sidewall pressure fluctuations over a wider range (Fig.31c). This improvement probably came from a more stable plenum chamber flow although no noticeable improvement in steadiness of the nylon tufts was observed.

One other serious problem was encountered with this perforated section. When operated at low Reynolds numbers (e.g. as obtained when starting the tunnel or when running at high subsonic speeds but low density) strong high frequency edge-tones were emitted from the holes which seriously impeded dynamic measurements. Fig.32 shows how the pressure fluctuations at  $M = 0.80$  increased from  $\sqrt{nF(n)} = 0.004$  to 0.060 at the edge-tone frequency as the tunnel total pressure was reduced from 136 to 34  $\text{kN/m}^2$  (20 to 5  $\text{lb/in}^2$ ). The measured Strouhal number of these edge-tones (based on the hole diameter  $d$  rather than the tunnel width  $w$ ) did not vary much with Mach number although first, second and third modal frequencies could sometimes be distinguished (Fig.33). These Strouhal numbers can be predicted from Brown's formula<sup>17</sup> if we make two assumptions.

- (1) The effective jet velocity is the free stream velocity  $V$ .
- (2) The effective distance between the jet orifice and the sharp edge is the hole diameter  $d$ .

(The streamwise distance from the jet orifice to the sharp edge varies from 0 to  $2d$  round the periphery of these inclined holes. However there are obviously no edge-tones in the limit when this distance tends to zero so that the assumption of a weighted, effective mean value of  $d$  is not unreasonable.) With these assumptions and for  $V \geq 40$  cm/s and  $d = 0.95$  cm Brown's formula becomes:

$$S^* = fd/U = 0.0466j (1 - 40/V) (1 - 0.07d) \approx 0.0433j$$

where  $j = 1.0, 2.3, 3.8$ , give the frequencies corresponding with the first, second and third modes. The predicted edge-tone Strouhal numbers are then in fair agreement with the measurements for the first 3 modes (Fig.33a). The amplitude of the pressure fluctuations at the edge-tone frequency did not vary strongly with Mach number up to  $M = 0.70$  (Fig.33b) so that acoustic resonances at fixed frequencies in the plenum chamber, working section or diffuser (whose amplification factor would vary as frequency changed) could not influence this phenomenon. It is interesting to note that the Strouhal number derived from previous measurements<sup>18</sup> (Appendix C) in the ONERA 6ft  $\times$  6ft tunnel at  $M = 0.80$ ,  $P_t = 102$  kN/m<sup>2</sup> (14.8 lb/in<sup>2</sup>) agreed exactly with that measured in the RAE 3ft  $\times$  3ft tunnel at  $M = 0.80$ ,  $P_t = 34$  kN/m<sup>2</sup> (5 lb/in<sup>2</sup>) (Fig.33a) and that even the pressure fluctuation amplitudes were comparable ( $\sqrt{nF(n)} = 0.038$  and 0.050 respectively in Fig.33b) despite many detailed differences between the tunnels. Hence edge-tones from the holes were generating the pressure fluctuations in both facilities.

In both facilities the edge-tones were completely eliminated by taping over the wind swept surfaces. When one of the sidewalls of the RAE 3ft  $\times$  2.7ft tunnel was then untaped (Fig.34a), edge-tones were generated almost as strongly as with four walls untaped<sup>†</sup>. However, as this open sidewall was progressively taped over again, working upstream from the end of the liner, the pressure fluctuations were reduced and the unit Reynolds number for the onset of edge-tones was also reduced. This suggested that the effect of reducing unit Reynolds number was to increase the boundary layer thickness  $\delta^*$ , and

---

<sup>†</sup> Interference between the four walls produced this apparently anomalous result; large mutual interference effects were clearly demonstrated in additional experiments.

Detailed measurements of the boundary layer thickness in the corners of the working section would probably have been needed to interpret these anomalous pressure fluctuation measurements correctly.

that edge-tones were generated when  $\delta^*/d$  exceeded some critical value. As the tapes were extended upstream the boundary layer at the open holes just upstream of the tape became thinner at any given unit Reynolds number. Hence a progressively lower unit Reynolds number was required to achieve the critical value of  $\delta^*/d$  necessary to initiate edge-tones. A critical value of about  $\delta^*/d \geq 0.4$  to  $0.5$  can be inferred from the measurements given in Fig.34a.

Tests in the ONERA 6ft tunnel<sup>16</sup> showed that the edge-tones could also be eliminated by reducing the wall porosity from 6% to 3%. This variation of wall porosity was achieved, not by sealing 50% of the holes, but by moving perforated plates extending over the full length of the plenum chamber side of the top and bottom liners. A comparable experiment was made using the small length of variable porosity sidewall of the RAE 3ft  $\times$  2.7ft tunnel, the remaining walls being taped over. Fig.34b shows that the pressure fluctuations fell suddenly as the open area ratio was reduced from 3% to 2.2%. This modification was then applied over a wider area by sticking perforated cardboard underneath the rear 2 ft of the top and bottom liners from which the tapes were removed. The cardboard was displaced so as to give the desired open area ratio of 2.2% and a large reduction in pressure fluctuations was achieved (Fig.35a). Aluminium strips were subsequently used to modify every hole in the liners in this fashion. This modification virtually eliminated the edge-tones (Fig.35b) at the fundamental mode, although the third mode (Fig.33) still persisted.

An hypothesis to explain the generation of the edge-tones is suggested by the flow patterns found in individual holes (Fig.36). This shows a herring-bone pattern, indicative of a complex threedimensional shear layer separating from the upstream edge of the hole. The mean shear layer contains streamwise vorticity components of opposite sense on either side. Under certain conditions (e.g. as  $\delta^*/d$  increases), the mean shear layer may not reattach to the inner surface of the hole. The shear flow is probably always unsteady, but the degree of unsteadiness may be much greater when the mean shear layer does not reattach onto a solid surface. The mass flow into the hole would then vary strongly with time, which would generate stronger edge-tones from the downstream edge of the hole. The downstream movement of the variable porosity plate reduces the edge-tones either by permitting reattachment or by severely limiting the amplitude of the shear layer oscillation. There is not enough evidence to confirm this hypothesis, but the flow model inferred is at least consistent with Roshko's explanation<sup>13</sup> of the effect of splitter plates on the flow in the wake of bodies with a bluff base.

The movement of the variable porosity plate to the critical position should not greatly alter the outflow characteristics. With this flow model some low amplitude edge-tones will be generated by the transverse mixing of the turbulent boundary layer even without the shear layer oscillation. This inference is supported by the persistence of a low level first mode in the modified tunnel, even when the shear layers are stabilized (Fig.37). This low amplitude component could probably be eliminated by rounding the sharp leading-edge at the top of every hole. This modification would be a formidable task for 8000 holes. At supersonic speeds the rounded holes might introduce much stronger shock waves which would spoil the Mach number distribution.

Apart from the fairly low level residual pressure fluctuations corresponding with the first and third mode edge-tones, the pressure fluctuations now approach those measured with all the holes sealed on the wind swept surfaces (Fig.37). These pressure fluctuations vary from  $\sqrt{nF(n)} = 0.003$  to 0.006 in the frequency range from 20 to 1000 Hz. The pressure fluctuations only vary slightly with unit Reynolds number and are generally significantly lower than those recently measured to the same degree of accuracy in the top and bottom slotted section at subsonic and supersonic speeds (Fig.38).

#### 4 DISCUSSION

The principal features which may determine the unsteadiness in slotted or perforated working sections are now reviewed.

##### 4.1 Unsteadiness in slotted sections with diffuser suction

The measurements in section 3.4 showed that the unsteadiness came from the extraction region and was reduced by covering the slots with perforated metal. Both slotted sections are serviceable. The 3ft  $\times$  3ft section (Fig.5) is occasionally used for force measurements on large subsonic models but balance vibration problems are probable in the speed range from  $M = 0.75$  to 0.90, where accurate drag measurements are important. The 3ft  $\times$  2.2ft section (Fig.4) is used for most static and dynamic tests, although dynamic measurements are sometimes difficult and occasionally impossible at supersonic speeds.

The unsteadiness of other slotted tunnels operated with diffuser suction may be reduced by covering the slots with perforated metal screens as in the 3ft  $\times$  3ft tunnel (Figs.12 and 20) although this may alter the steady force interference corrections<sup>19</sup>. Moore and Wight have shown<sup>20</sup> that the large dynamic interference effects on a half model mounted in a top and bottom slotted tunnel can be reduced to small proportions at all speeds when perforated screens are

fitted behind the slots. Larger reductions in unsteadiness might be achieved if there is an optimum position for the screens, perhaps corresponding with the 'time-average' position of the dividing streamline of the slot flow. An optimum position for the screen may exist because the HS 2ft  $\times$  2ft working section with screens 18 mm (0.7 in) below the slots is superior to the RAE top and bottom slotted section with screens 13 mm (0.5 in) below the slots (Appendix B).

Measurements in the 3ft  $\times$  3ft tunnel suggest that even with screens beneath the slots the peak excitation frequency or Strouhal number associated with the slots width  $w_s$  is (Fig.25)

$$S^* = f w_s / V \approx 0.035 \quad ,$$

which is almost the same as the Strouhal number for the first edge-tone mode for perforated tunnels with  $60^\circ$  inclined holes (Fig.33a).

New slotted tunnels should incorporate a reasonably large number of narrow slots, because this will raise the peak excitation frequency above the range of balance frequencies (typically 50 to 300 Hz) and lower the peak amplitude. Thus comparing Figs.20 and 19 the peak amplitude at  $M = 0.80$  in the 3ft  $\times$  3ft tunnel falls from  $\sqrt{nF(n)} = 0.013$  with 6 slots to 0.004 with 10 slots (a reduction remains even after making a linear adjustment for the reduction in open area ratio from 10 to 8%). No waves have been observed in the NPL top and bottom slotted sections which have from 20 to 24 slots only about 5.1 mm (0.2 in) wide. A study of transonic similarity relations appropriate to tunnel interference parameters suggests that 6 to 8 slots per side are best<sup>21</sup> and open area ratios as low as 3% have been recommended<sup>22</sup> for tests up to  $M = 1.00$ .

The present tests also suggest that half slots in the corners of the working section introduce additional unsteadiness (Appendix A). Pressure fluctuations at the model can be further reduced by extending the working section downstream (Fig.27), but the tunnel would then require a somewhat higher pressure ratio.

#### 4.2 Unsteadiness in perforated sections with diffuser suction

Fig.37 shows that the unsteadiness of a perforated tunnel may be reduced to a level comparable with that of a closed tunnel by careful attention to the geometry of the plenum chamber, the extraction region and the holes

(cf. Figs.28 to 35). The unsteadiness of the perforated working section is generally lower than that of the top and bottom slotted working section except at frequencies above about 900 Hz where weak edge-tones persist (Fig.38). The improvement is particularly large at supersonic speeds where flutter tests were previously most difficult in the top and bottom slotted section (Fig.38c). The unsteadiness of both sections is of the same order as the unsteadiness measured in three much larger wind tunnels (Appendix D).

Perforated tunnels with  $60^\circ$  inclined holes may develop edge-tones if

$$\delta^*/d \geq 0.5$$

although other parameters may influence the edge-tones.

J. Lukasiwicz<sup>23</sup> recommended that  $\delta^*/d \leq 0.5$  to ensure linear interference characteristics for the cancellation of shock and expansion waves for perforated walls at transonic speeds. Goethert<sup>24</sup> suggests that reasonable interference characteristics can still be obtained if this criterion is relaxed and

$$\delta^*/d \leq 0.75 \quad .$$

However application of this criterion will allow the development of edge-tones as observed in the RAE 3ft  $\times$  3ft tunnel at low densities, the AEDC 16ft  $\times$  16ft tunnel and the ONERA 6ft  $\times$  6ft tunnel (Fig.42b and c). These edge-tones may be reduced by modifying the hole geometry as demonstrated first in the ONERA 6ft  $\times$  6ft tunnel and then in the RAE 3ft  $\times$  3ft tunnel. There will be probably only a small alteration in the tunnel calibration, and the lift and blockage corrections associated with this modification, because the hole flow characteristics should only be slightly modified (see the discussion of Fig.36 in 3.5).

## 5 CONCLUSIONS

Flow unsteadiness and model vibration in the 3ft  $\times$  3ft tunnel have impeded static and dynamic measurements at subsonic and transonic speeds. The unsteadiness was measured with pressure transducers in both the 3ft  $\times$  3ft tunnel and a 1/9 scale model of the 3ft  $\times$  3ft tunnel and good agreement obtained.

For the closed 3ft  $\times$  3ft tunnel successive modifications to the balance section and diffuser derived from tests of the model tunnel have reduced the unsteadiness at subsonic speeds (Figs.12 and 17).



The unsteadiness in the slotted tunnels operated by diffuser suction originated in the extraction region and was reduced in the 3ft × 3ft tunnel by covering the slots with perforated screens (Figs.12 and 20); the unsteadiness was still higher than in the closed tunnel.

The perforated and closed working sections of the model tunnel had nearly the same low level of unsteadiness and a similar result was achieved for the new perforated working section for the 3ft tunnel after some initial difficulties. These included the generation of edge-tones at low unit Reynolds number, which were eliminated by a modification to the hole geometry.



The author would like to thank Mr. G. F. McCanless for indicating (private communication, May 1971) that Brown's formula for the edge-tone frequency is quoted incorrectly on p.18, as in several text books on acoustics. The correct formula, given by Brown in Ref.19, has a constant

$$= 0.466$$

instead of a constant

$$= 0.0466$$

quoted on p.18.

Thus although the measured Strouhal numbers for  $60^\circ$  inclined holes are unaltered they are much lower than those predicted by the correct formula together with the assumptions made on p.17 (Fig.33a).

In retrospect it is probably unwise to try to predict a Strouhal number for a complex threedimensional flow under a thick boundary layer (Fig.36) directly from the edge-tone frequency excited by a twodimensional jet striking a sharp wedge, for Brown did not investigate the effects of variations in wedge angle or wedge inclination appropriate to jets. The fundamental question remains if  $60^\circ$  inclined holes really do emit edge-tones. McCanless discusses this question in some detail\*. He concludes that  $60^\circ$  inclined holes do emit edge-tones and that there is an analogy between the critical ratio of boundary layer thickness/hole diameter ( $\delta^*/d$ , p.22) at which the holes start to emit noise and the critical ratio of jet thickness/jet separation distance at which a sharp edge starts to generate edge-tones\*\*. McCanless also supports the critical ratio of  $\delta^*/d$  given on p.22 by additional experiments.

---

\*G. F. McCanless  
J. R. Boone

Noise reduction in transonic wind tunnels  
(paper in preparation).

\*\*K. Karamcheti *et al*

Some features of an edge-tone flow field.  
NASA SP 207 pp.275-304 (July 1969)



Appendix A

ADVERSE EFFECT OF CORNER HALF SLOTS

Some brief tests were made with 2 configurations of the model tunnel:

<u>Configuration</u>	<u>Open area ratio</u> %	<u>4 half slots</u>	<u>4 complete slots</u>
1	3.3	Open	Closed
2	6.7	Closed	Open

The working section unsteadiness was much higher for Configuration 1 than for Configuration 2 and extended over a wider frequency range (Fig.39) although the open area ratio was only 3.3% instead of 6.7%. Hence half slots in the corners of the working section apparently introduce excessive unsteadiness. One tentative explanation for this effect is illustrated in the small insert in Fig.39. The pair of vortices formed by flow into the plenum chamber from complete slots are equal in magnitude and opposite in sign; they probably diffuse rapidly in the extraction region giving zero total circulation. In contrast the single vortex formed from the corner half slot may persist in the corner of the diffuser inducing additional streamline curvature and momentum transfer and hence additional pressure fluctuations. (Even without the half slots strong secondary flows exist in corner boundary layers.)

In the 3ft x 3ft tunnel the half slots in the slotted transonic section are now covered with perforated screens and could be completely eliminated. With the top and bottom slotted section the corner half slots provide clearance to avoid damaging the side walls of the supersonic working section, and cannot easily be eliminated. For this reason they are not covered with perforated screens.

## Appendix B

### UNSTEADINESS MEASUREMENTS IN OTHER SLOTTED TUNNELS

This appendix presents observations made in 2 other slotted tunnels with diffuser suction.

The HS 2ft  $\times$  2ft tunnel at Hatfield<sup>25</sup> has 5 complete slots/side. Comparative buffeting tests on Model B of Ref.1 indicated that at the wing fundamental frequency of 280 Hz this 2ft  $\times$  2ft tunnel had much less unsteadiness than the unmodified RAE 3ft  $\times$  3ft tunnel which superficially had a similar slot geometry. (A detailed comparison made in Fig.40 suggested that the significant differences between the tunnels were the presence of perforated metal under the slots and the absence of corner half slots in the HS tunnel.) Spark schlieren photographs in August 1963 confirmed that there were only weak waves in the working section of the HS tunnel at subsonic speeds. The first wall pressure fluctuation measurements were made in December 1966 when the working size was 0.61 m  $\times$  0.61 m (2 ft  $\times$  2 ft). The tunnel total pressure was just below atmospheric. The initial measurements (Fig.41) were made without any recirculation of exhaust gases at a total temperature  $T_t$  of 16°C. The spectra are flat with a general level of  $\sqrt{nF(n)} = 0.0005$ . This level is about the same as that in the 3ft  $\times$  3ft tunnel with the closed working section and must be close to the practical limit. This unsteadiness is better than in the modified 3ft  $\times$  3ft top and bottom slotted section (Fig.19) and has a smaller Mach number variation. The measurements were continued with recirculation of exhaust gases and  $T_t = 84^\circ\text{C}$  (the normal transonic operating temperature used in the buffeting tests of Model B). There was no difference between the spectra at  $T_t = 84^\circ\text{C}$  and 16°C at the first test Mach number  $M = 0.50$  but the transducer then developed an electrical fault (attributed to the effects of temperature gradient in the transducer) and the tests were terminated. Since there was no difference between the spectra at  $T_t = 84^\circ\text{C}$  and 16°C at  $M = 0.50$  the differences at higher Mach numbers were probably small (owing to the relatively small increase in the maximum section velocity) and Fig.41 then represents a fair approximation to the working section unsteadiness at  $T_t = 84^\circ\text{C}$ . The values of excitation  $\sqrt{nF(n)} \cdot q$  at the wing bending frequency for Model B derived from these spectra show little variation from  $M = 0.50$  to 0.90 and explain the flat curve of wing response to tunnel unsteadiness in this tunnel (Fig.10, Ref.1).

The second set of measurements was made in February 1970 with improved instrumentation (2.2) when the working section size had been increased from 0.61 m × 0.61 m (2 ft × 2 ft) to 0.76 m × 0.61 m (2.5 ft × 2 ft). The tunnel unsteadiness is still quite low, despite the increased velocities in the maximum section, but shows some increase compared to the original measurements at M = 0.50 and 0.90, although being unchanged at M = 0.80.

The intermittent 20in × 20in in HS transonic tunnel at Woodford has 9 complete slots 11.7 mm (0.46 in) wide and 2 half slots/side and some spark schlieren photographs were taken in May 1964. The schlieren photographs (not reproduced here) clearly show strong normal waves in the working section at subsonic speeds but only weak inclined waves at supersonic speeds (cf. Fig.11 for the 3ft × 3ft tunnel). The principal wave frequency deduced at M = 0.83 is about 780 Hz, which gives a Strouhal number based on the slot width  $w_s$  of

$$S^* = f w_s / V = 0.033 .$$

This compares very well with the 3ft × 3ft tunnel values (Fig.25). The complete slots on the 20in × 20in tunnel are covered with perforated screens but the corner half slots are not covered. The existence of strong waves suggests that either the position of the perforated screen below the slots or the presence of half slots may be important. The model balance frequencies are much lower than the peak excitation frequency (780 Hz at M = 0.83) and there have been no balance fatigue failures. Small vibrations have been observed on some balance measurements.

Some spark schlieren photographs taken when the 20in × 20 in tunnel was driven by jet engines and had a poor temperature distribution also showed normal waves in the working section.

Appendix C

UNSTEADINESS MEASUREMENTS IN OTHER PERFORATED TUNNELS WITH 60° INCLINED HOLES

There was initially no information available on the unsteadiness of perforated tunnels operated with diffuser suction larger than the model RAE 4in × 4in tunnel. Measurements on a larger tunnel seemed desirable and so some tests in the AEDC 1ft × 1ft perforated tunnel at Tullahoma, USA were requested. This tunnel has similar hole geometry to that selected for the 3ft × 3ft tunnel; viz. 60° inclined holes and an open area ratio of 6%.

The working section wall pressure fluctuations were measured with 100% auxiliary suction (the normal operating condition as reported in the previous measurements of Ref.26) and then with 100% diffuser suction (obtained by extending the diffuser flaps). The measurements reported in a private communication show (Fig.42a) no significant difference between the total rms pressure fluctuations for the 2 tunnel operating conditions. This result implies that the extraction region of a perforated tunnel operated with diffuser suction makes only a small contribution to the working section unsteadiness. This is a valuable confirmation of the model tunnel results presented in Figs.22 and 23. The previous measurements in the AEDC 1ft × 1ft tunnel<sup>26</sup> suggested that the unsteadiness was concentrated at discrete frequencies associated with the compressors and was transmitted from the maximum section into the working section. There was no evidence of edge-tones, possibly because the pressure fluctuations above 1250 Hz were removed by a filter<sup>26</sup>. There is some evidence that edge-tones are generated by the inclined holes in the working section of the AEDC 16ft × 16ft tunnel. Thus Fig.42b, (based on Fig.13 of Ref.27) shows a Strouhal number of 0.052 at M = 0.60 and 0.70, which is almost identical with that measured in the 3ft × 3ft tunnel (cf. Fig.33a). The amplitude of the pressure fluctuations are  $\sqrt{nF(n)} = 0.027$  and 0.036 respectively, of the same order as those measured in the RAE 3ft × 3ft tunnel and the ONERA 6ft × 6ft tunnel (cf. Fig.33b). In the AEDC 16ft × 16ft tunnel the Strouhal number falls to 0.043 and  $\sqrt{nF(n)}$  falls to 0.011 at M = 0.80. This parallels the behaviour of the first edge-tone mode in the 3ft × 3ft tunnel shown in Fig.33. The total rms pressure fluctuations  $\bar{p}/q$  also appear to increase as total pressure is decreased (Fig.11, Ref.27). Although some of this increase may be attributed to the increased effect of electronic noise it may also reflect higher values of  $\sqrt{nF(n)}$  generated by larger areas of the sidewalls exceeding the critical ratio of  $\delta^*/d$  (cf. 3.5).



The ONERA 6ft  $\times$  6ft transonic tunnel at Modane operates with diffuser suction and has perforated walls with  $60^\circ$  inclined holes and an open area ratio of 6%. Wall pressure fluctuations were measured in this tunnel in preparation for some buffeting<sup>18</sup> measurements. Some typical spectra are shown in Fig.42c. The spectra are flat except from  $M = 0.68$  to  $0.90$  when there are large pressure fluctuations at 500 Hz from the edge-tones. A change in hole geometry subsequently eliminated these edge-tones<sup>16</sup>. The residual unsteadiness in the ONERA 6ft  $\times$  6ft perforated working section is characterized by flat spectra with a relatively low level of excitation. Comparable edge-tones were subsequently measured in the RAE 3ft  $\times$  3ft tunnel at low Reynolds numbers and eliminated by a similar change in hole geometry (3.5).

Some additional noise measurements in perforated tunnels with  $60^\circ$  inclined holes have been recently reported<sup>28,30,31</sup>. Ref.30 is particularly interesting, because the hole Strouhal number at  $M = 0.775$  is about 0.05 and the level  $\sqrt{nF(n)} = 0.05$ , closely resembling those measured in the RAE 3ft  $\times$  3ft and ONERA 6ft  $\times$  6ft tunnels.

Appendix D

UNSTEADINESS MEASUREMENTS IN 3 LARGE WIND TUNNELS

Some pressure fluctuations measured when assessing the suitability of 3 large wind tunnels for dynamic tests are presented. These measurements set the unsteadiness levels achieved in the RAE 3ft x 3ft tunnel in a wider perspective.

In the RAE 8ft x 6ft slotted transonic tunnel (operated with auxiliary suction at transonic speeds) the spectra (Fig.43), measured on the centre of a slat, up to  $M = 0.65$  are characterized by high peaks associated with the fan, which is immediately downstream of the working section. The peak frequencies are given by the relation

$$f(\text{Hz}) = N \times (\text{number of fan blades}) \times \text{fan rev/sec}$$

where  $N = 1, 2, 3$  etc.

The unsteadiness level at the peaks is high, e.g. at  $M = 0.65$

f Hz	N	$\sqrt{nF(n)}$
140	1	0.036
290	2	0.020
530	3	0.009

At  $M = 0.70$  and higher speeds these peaks are largely suppressed and the general level of unsteadiness falls to about  $\sqrt{nF(n)} = 0.005$ . Additional measurements were also made near the nose and at the maximum section of a NACA RM 12 model mounted on the tunnel centre line. Fig.44 shows a comparison between the pressure fluctuations measured near the nose of the body ~~and~~ on the tunnel side-wall. The agreement is fair at low values of unsteadiness and good at the much higher unsteadiness at the peak frequencies. Some differences must be expected because of the differing contributions to the measured pressure fluctuations from the boundary layer on the tunnel slat and from the boundary layer on the curved surface of the model. Interaction between the local constraints imposed by the model and its sting (supercriticalities and curvature) and the tunnel unsteadiness may also account for some of the differences. The unsteadiness level in this tunnel is too high for dynamic tests at the peak frequencies.

In the ARA 8ft x 9ft perforated transonic tunnel (also operated with auxiliary suction at transonic speeds) the sidewall pressure fluctuations decreased as the pressure transducer was moved upstream. To reduce any local influence of the sidewall boundary layer on the measured pressure fluctuations the NACA RM 12 model was tested at one streamwise position on the tunnel centre line. The pressure fluctuations measured at both points on the body were nearly identical. Fig.45 shows that these pressure fluctuations are typically  $\sqrt{nf(n)} = 0.002$  to  $0.003$  at subsonic speeds, except where there are peaks associated with the fan. At Mach numbers above  $M = 0.95$  the pressure fluctuations fall rapidly when the diffuser chokes. The low level of unsteadiness at most frequencies allows light buffeting to be detected fairly easily in this tunnel (e.g. model C of Ref.1).

In the RAE 8ft x 8ft closed subsonic/supersonic tunnel, sidewall pressure fluctuations were recently measured 1.45 m (4.75 ft) upstream of the model centre of rotation. Fig.46 shows that the spectra are generally flat, with a level of  $\sqrt{nf(n)} = 0.0005$  at small frequency parameters ( $n < 0.5$ ) increasing to about 0.0025 by  $n = 50$ . The low unsteadiness at small frequency parameters allows light buffeting to be detected easily in this tunnel at most Mach numbers. At constant speed, the tunnel unsteadiness generally shows no variation over a 4/1 range of unit Reynolds number.

SUMMARY OF PRINCIPAL DATA FOR THE RAE 3ft x 3ft TUNNEL

NB 'Low frequency' - 2 to 70 Hz } for 3ft tunnel  
 'High frequency' - 100 to 300 Hz }

Table 1

TUNNEL CONFIGURATION - CLOSED WORKING SECTION (Fig.3)

Remarks	3ft x 3ft tunnel	4in x 4in tunnel	Tunnel comparison
Date	1956 - October 1963	1956 - July 1963	
Low frequency	Moderate	Moderate	
High frequency	Very high	Very high	
Type of spectra	Very peaky	Very peaky	Good
Figures	13	Not presented	15

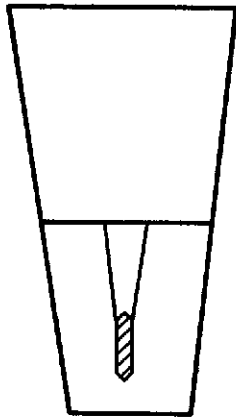
  

Date	October 1963 - September 1966	July 1963 - July 1966	
Low frequency	Moderate	Moderate	
High frequency	Low	Low	
Type of spectra	Fairly flat	Fairly flat	Good
Figures	14	16	cf. 14 and 16
Note 1			

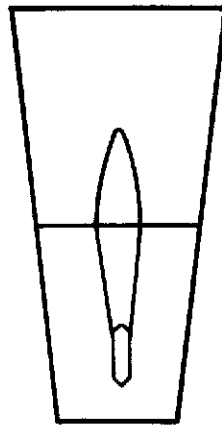
Date	November 1966	July 1966	
Low frequency	Low	Low	
High frequency	Low	Low	
Type of spectra	Flat	Flat	Good
Figures	17	16	cf. 16 and 17
Note 2			

(1) Centre body with no mobile diffuser fairing (Fig.3a)

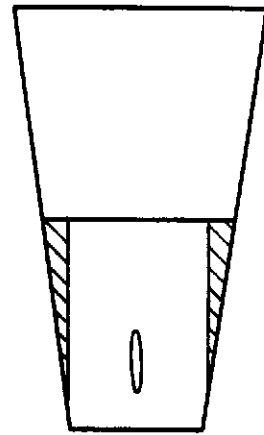


Balance section  
Mobile diffuser

(2) Centre body with mobile diffuser fairing (Fig.3a)



(3) Revised balance section  
 - no centre body  
 - no diffuser fairing (Fig.3b)



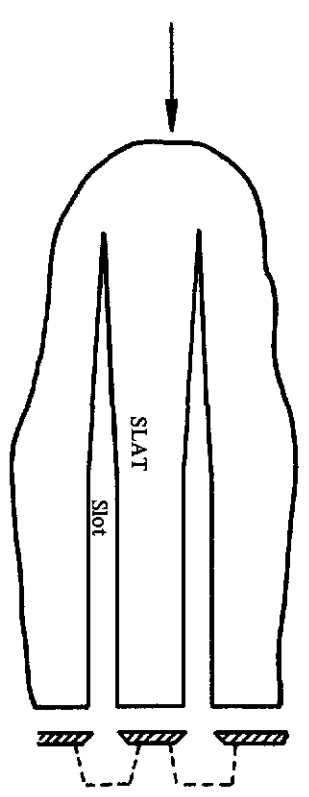
NOTE 1 This fairing (1.2) reduced the pressure ratio required to drive the tunnel by about 0.02 over the Mach number range from M = 0.4 to 1.6, and by about 0.01 at M = 2.0  
 NOTE 2 Up to M = 1.5 the pressure ratio required for configurations 1.3 and 1.1 were identical. However the pressure ratio required at M = 2.0 is 1.84 instead of 1.81

Table 2

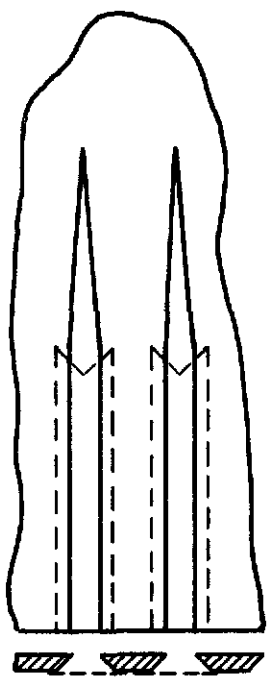
TUNNEL CONFIGURATION - TOP AND BOTTOM SLOTTED SECTION (Fig. 4)

Remarks	3ft x 3ft tunnel	4in x 4in tunnel	Tunnel comparison
Date	July 1960 - December 1964	July 1960	Direct comparison impossible because open area ratio of 4in tunnel was made 16% in error compared to the 3ft tunnel's 8%
Low frequency	?	Low	
High frequency	? probably high deduced from severe vibration	Moderate - high	
Type of spectra	Probably very peaky	Peaky	
Figure	-	Not presented	

(1) Slots with channel screens (Fig. 4c)



(2) Slots with flat screens (Fig. 4d)



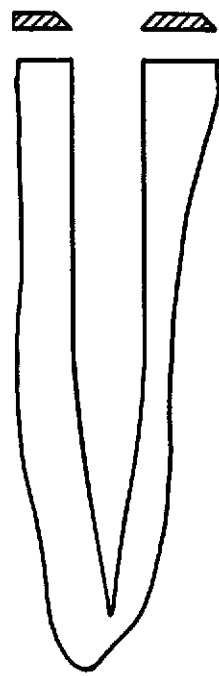
Date	January 1965	Not tried
Low frequency	Low	-
High frequency	Moderate	-
Type of spectra	Peaky	-
Figure	-	-

Table 3

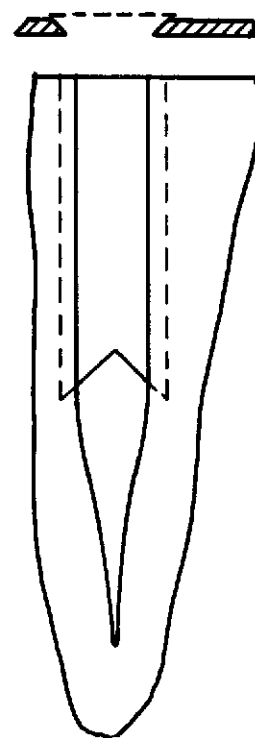
TUNNEL CONFIGURATION - SLOTTED TRANSONIC SECTION (Fig.5)

<u>Remarks</u>	<u>3ft x 3ft tunnel</u>	<u>4in x 4in tunnel</u>	<u>Tunnel comparison</u>
Date	December 1958 - July 1965	December 1958	
Low frequency	Low	Low	
High frequency	Very high	Very high	
Type of spectra	Very peaky	Very peaky	Fair
Figures	20	23	24

(1) Slots open (Fig.5c)



(2) Slots with flat screens (Fig.5d)

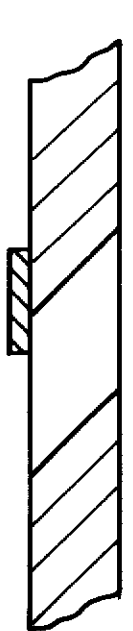
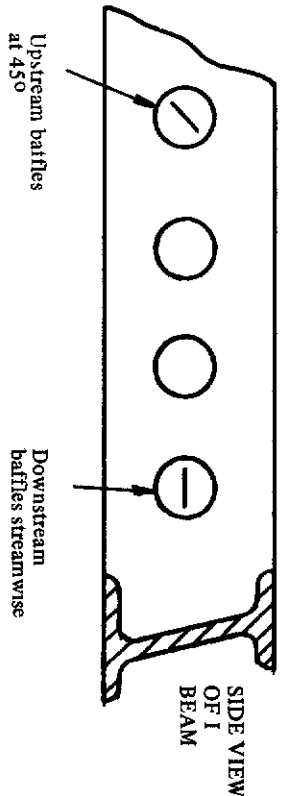
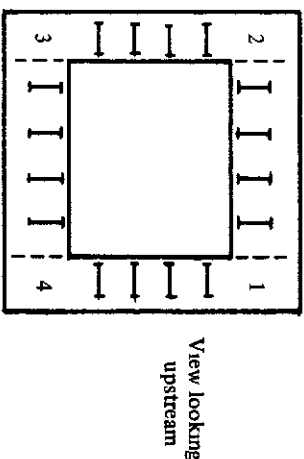
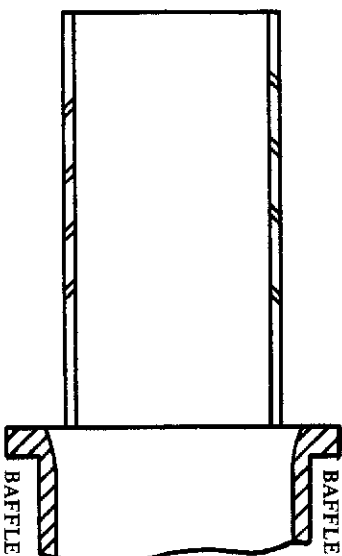
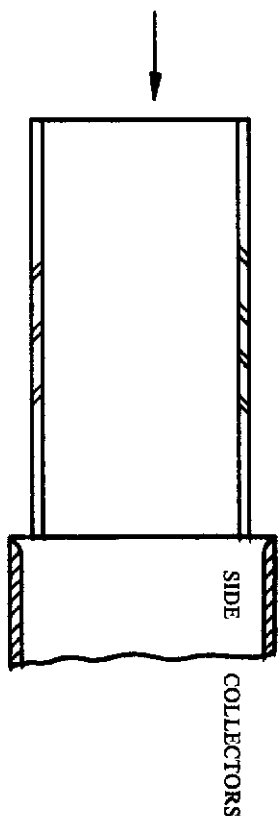


Date	August 1965	Not tried	
Low frequency	Low	-	
High frequency	High	-	
Type of spectra	Peaky	-	
Figure	20	-	

Table 4

TUNNEL CONFIGURATION - PERFORATED TRANSONIC SECTION (Figs. 6 and 7)

Remarks	3ft x 3ft tunnel		4in x 4in tunnel	
	Date	Low frequency	Date	Low frequency
(1) Side collectors without baffles	November 1967	Very high	Not tried	-
		High frequency		-
		Type of spectra		-
		Figure		-
		28		-
(2) Side collectors with baffles	November 1967	Moderate	January 1966	Low
		Low frequency		Low
		High frequency		Very flat
		Type of spectra		23
		Figures		
		28		
(3) with addition of 4 perforated corner baffles	December 1967	Fairly low	Not tried	-
		Low frequency		-
		High frequency		-
		Type of spectra		-
		Figure		-
		30		-
(3) + addition of plenum chamber baffles	February 1968	Low	Not tried	-
		Low frequency		-
		High frequency		-
		Type of spectra		-
		Figure		-
		31		-
(4) + treatment of 60° inclined holes	October 1968	Elimination of edge-tones at low Reynolds number	Not tried	-
		Date		-
		October 1968		-
		Elimination of edge-tones at low Reynolds number		-
		Figures		-
		32 to 36		-



SYMBOLS

a	velocity of sound m/s (ft/s)
$C_f$	local skin friction coefficient
d	hole diameter m (ft)
E	Young's modulus $N/m^2$ (lb/in <sup>2</sup> )
$\bar{e}, e$	rms and steady voltages
f	frequency Hz (c/s)
F(n)	contribution to $\bar{p}^2/q^2$ in frequency band $\Delta f$
$\sqrt{nF(n)}$	$p/q(\epsilon)^{\frac{1}{2}}$
K	static calibration of pressure transducer
M	Mach number
N	number of fan blades
n	frequency parameter = $f w/V$
p	pressure fluctuation in a band $\Delta f$ at frequency $f = \text{voltage} \times K$
$\bar{p}$	rms pressure fluctuations $N/m^2$ (lb/in <sup>2</sup> )
$\frac{\bar{p}^2}{q^2}$	$= \int_{\log n = -\infty}^{\log n = \infty} nF(n) d(\log n)$
$P_t$	total pressure $N/m^2$ (lb/in <sup>2</sup> )
q	kinetic pressure = $\frac{1}{2} \rho V^2$ $N/m^2$ (lb/in <sup>2</sup> )
S*	Strouhal number $fd/V$ ; $fw_s/V$
V	free stream velocity m/s (ft/s)
$V_w$	wave velocity m/s (ft/s)
w	width of tunnel m (ft)
$w_s$	width of slot m (ft)
$\epsilon$	analyser bandwidth ratio $\Delta f/f$
$\sigma$	balance stress $N/m^2$ (lb/in <sup>2</sup> )
$\rho$	density $kg/m^3$ (lb/in <sup>3</sup> )
$\nu$	gauge factor (2 for wire strain gauges)



REFERENCES

<u>No.</u>	<u>Author(s)</u>	<u>Title, etc.</u>
1	D.G. Mabey	Comparison of seven wing buffet boundaries measured in wind tunnels and in flight. ARC CP 840 (1964)
2	D.E. Morris	Calibration of the flow in the working section of the 3ft x 3ft tunnel, National Aeronautical Establishment. ARC CP 261 (1954)
3	J.B. Scott-Wilson D.I.T.P. Llewelyn-Davies	The development of an improved diffuser for the 3ft x 3ft tunnel, Royal Aircraft Establishment. ARC CP 308 (1956)
4	E.P. Sutton M.T. Caiger A. Stanbrook	Performance of the 36 x 35in slotted transonic working section of the RAE Bedford 3ft wind tunnel. ARC R & M 3228 (1960)
5	E. Huntley	Details of the fatigue failure of a wind tunnel drag balance. RAE Technical Memorandum Aero 641 (1959)
6	L.C. Squire	Further experimental investigations of the characteristics of cambered gothic wings at Mach numbers from M = 0.4 to 2.0. ARC R & M 3310 (1961)
7	A.R. Felix	Variable porosity walls for transonic wind tunnels. Unpublished paper Supersonic Tunnel Association meeting 1964
8	T.B. Owen	Techniques of pressure fluctuation measurements employed in the RAE low-speed wind tunnels. RAE Technical Memorandum Aero 565 (AGARD Report 172, ARC 20780) (1958)

REFERENCES (Contd.)

<u>No.</u>	<u>Author(s)</u>	<u>Title, etc.</u>
9	T.B. Owen	An interim note on measurements of airflow unsteadiness in several RAE wind tunnels. RAE Technical Memorandum Aero 634 (ARC 20936) (1959)
10	W.R. MacDonald	A sub-miniature differential pressure transducer for use in wind tunnel models. RAE Technical Note Inst 169 (1961)
11	D.G. Mabey	Aerodynamically induced vibration in coolers. RAE Technical Report 65098 (1965) Journal Roy. Aero. Soc., December 1965
12	E.P. Sutton	The development of slotted working section liners for transonic operation of the RAE Bedford 3 ft wind tunnel. ARC R & M 3085 (1955)
13	A. Roshko	On the wake and drag of bluff bodies. J. Aer. Sci., Vol.22, p.124-132, February 1955
14	H. Eggink	On unsteady processes in high speed tunnels. Völkenrode Translations RT 948, September 1947
15	J.L. King	Instability <u>in</u> slotted wall tunnels. Journ. Fluid Mech., Vol.4, p.283, July 1958
16	J.M. Christophe J.M. Loniewski	Reduction of pressure fluctuations in a transonic test section. ONERA unpublished
17	G.B. Brown	The vortex motion causing edge-tones. Physical Society 49, p.493 (1937)
18	D.G. Mabey	RAE unpublished
19	D.R. Holder	Upwash interference on wings of finite span in a rectangular wind tunnel with closed side walls and porous-slotted floor and roof. ARC R & M 3395 (1965)

REFERENCES (Contd.)

<u>No.</u>	<u>Author(s)</u>	<u>Title, etc.</u>
20	A.W. Moore K.C. Wight	On achieving interference-free results from dynamic tests on half-models in transonic wind tunnels. NPL Aero Report 1293 (1969)
21	S.B. Berndt	Theory of wall interference in transonic wind tunnels. Symposium Trans-Sonicum (ed. Oswatitsch) Springer-Verlag, Berlin, p.288 (1964)
22	H.H. Pearcey	Some effects of wind tunnel interference observed in tests on two dimensional aero-foils at high subsonic and transonic speeds. AGARD Report 296 (1959)
23	J. Lukasiwicz	Effects of boundary layer and geometry on the characteristics of perforated walls for transonic wind tunnels. Aero Space Engineering, Vol.20, No.4 (1964)
24	B.H. Goethert	Transonic wind tunnel testing. Pergamon Press, p.269 (1961)
25	J.A. Kirk	Design and operational problems of the transonic jet-driven wind tunnel. Journ. Roy. Aero. Soc., Vol.62, January 1958
26	J.E. Robertson	Measurements of the pressure fluctuations in the test section of the 1 ft transonic tunnel in the frequency range from 5 to 1250 c/s. AEDC-TDR-62-109, May 1962
27	H.L. Chevalier H.E. Todd	Measurement of the pressure fluctuations in the test section of the 16ft transonic circuit in the frequency range from 5 to 1000 c/s. AEDC-TN-61-51, May 1961

REFERENCES (Contd.)

<u>No.</u>	<u>Author(s)</u>	<u>Title, etc.</u>
28	J.R. Boone G.F. McCanless	Application of the techniques for evaluating the acoustic sources of background noise in wind tunnel facilities. TR NAS 8-20336, March 1969
29	N.J. Martin K. Holzhaueh	Analysis of factors influencing the stability characteristics of symmetric twin-intake air-induction systems. NACA TN 2049, March 1950
30	R.J. Karabinus B.W. Sanders	Measurements of fluctuating pressures in an 8ft x 6ft supersonic wind tunnel for Mach number range of 0.56 to 2.07. NASA TMX 2009, May 1970
31	G.F. McCanless	Additional correction of 4% Saturn V protuberance test data. US Chrysler Corporation (Space Division). Technical Report HSM-R1-71, January 1971

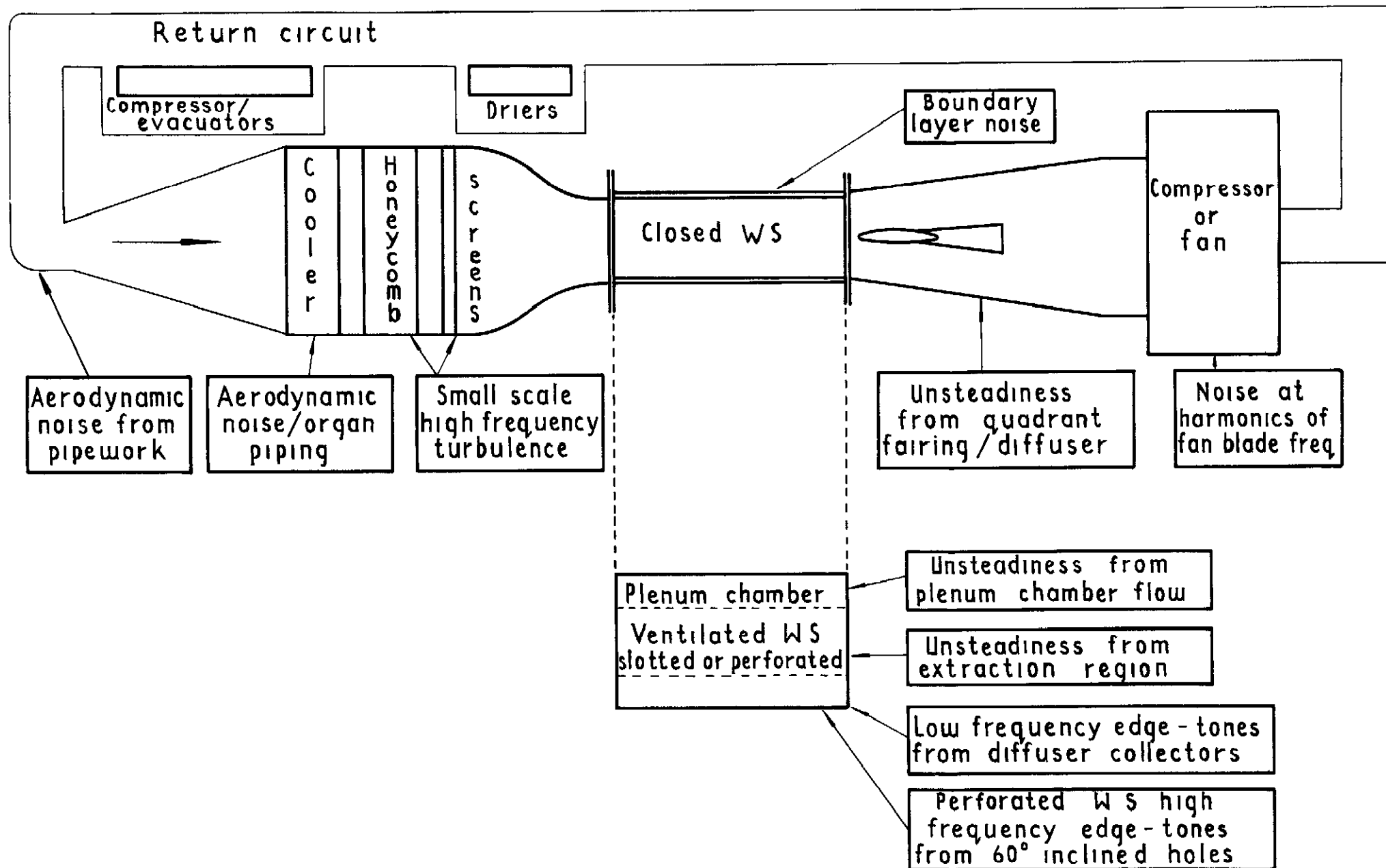


Fig.12 Sources of unsteadiness in transonic tunnels

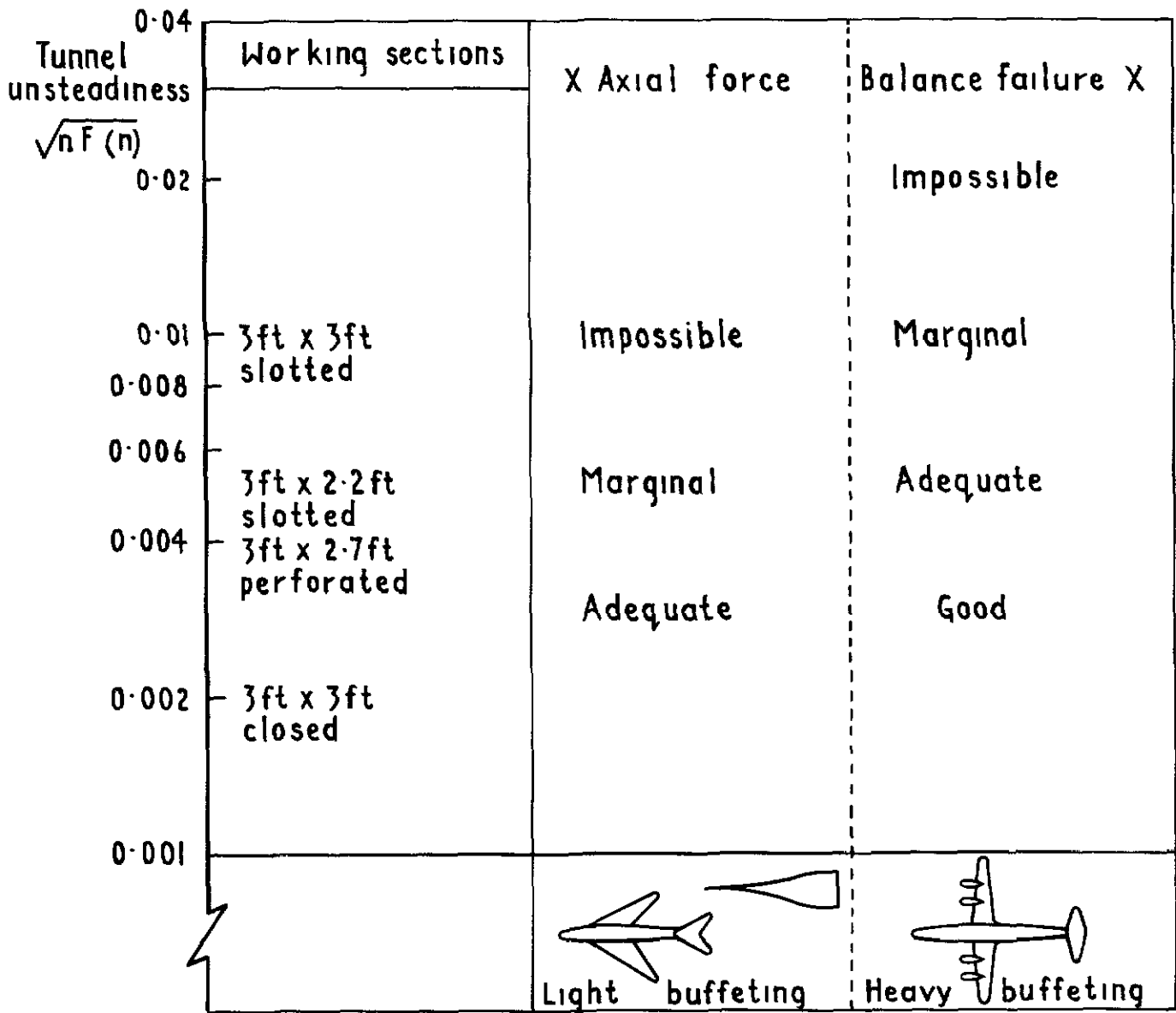


Fig. 7 Tunnel unsteadiness criteria for buffeting tests

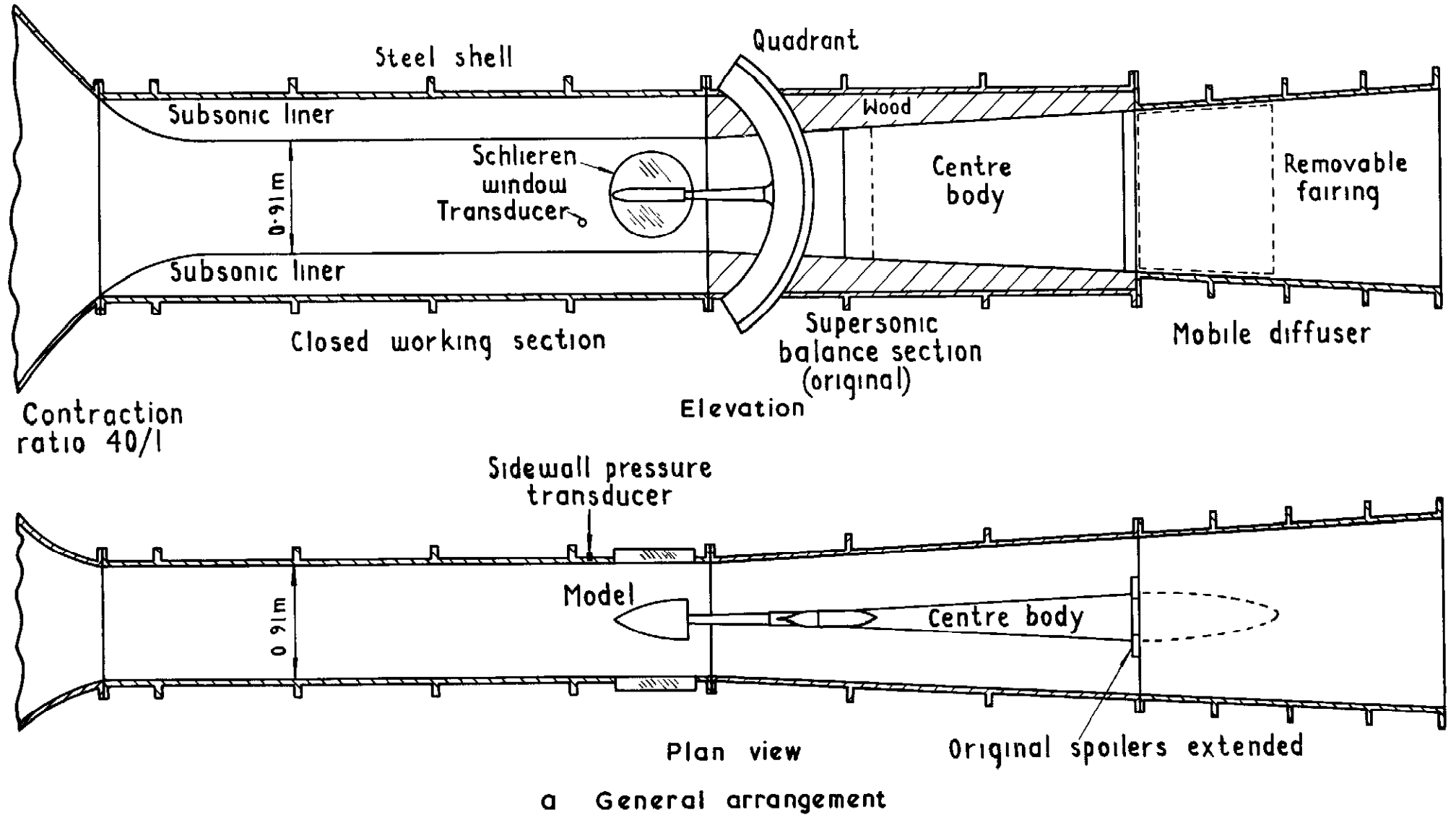
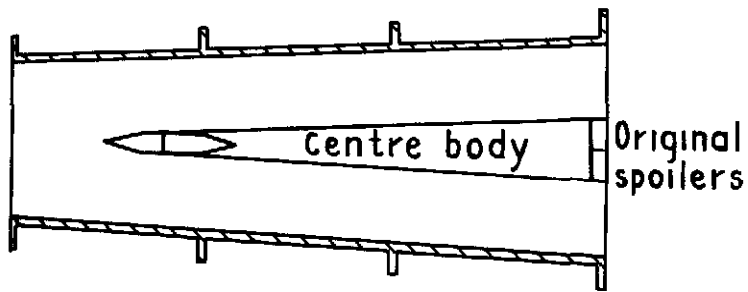
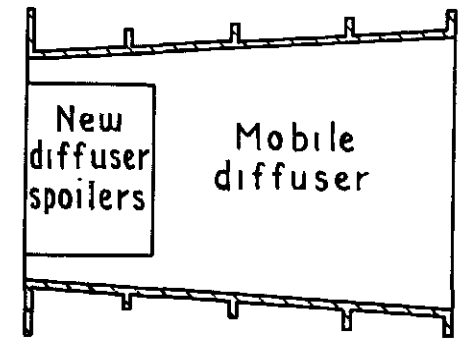
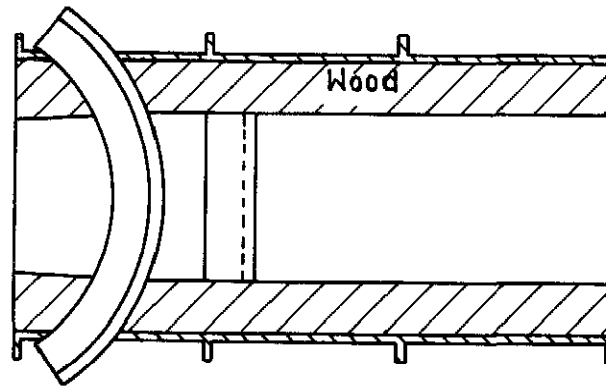
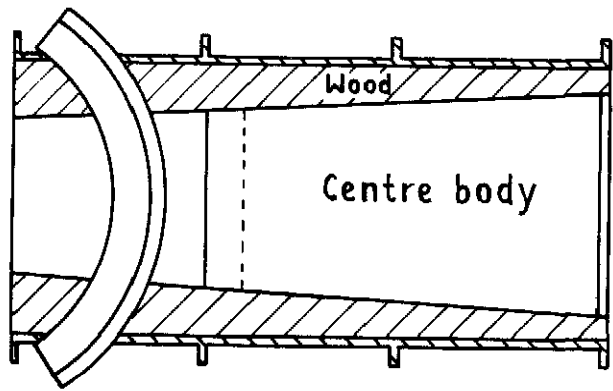
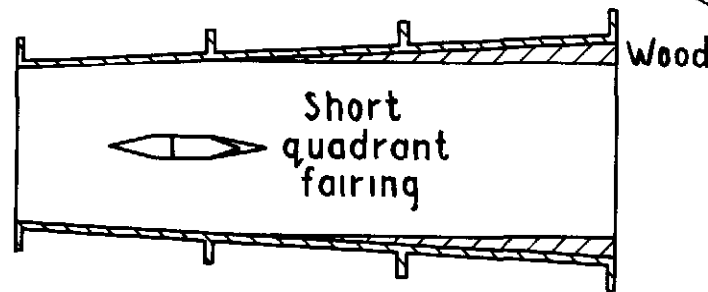


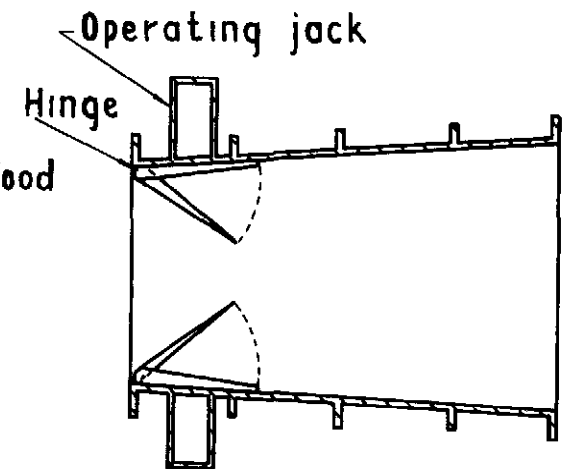
Fig 3 3ft x 3ft tunnel - closed working section



Original



Revised



Mobile diffuser

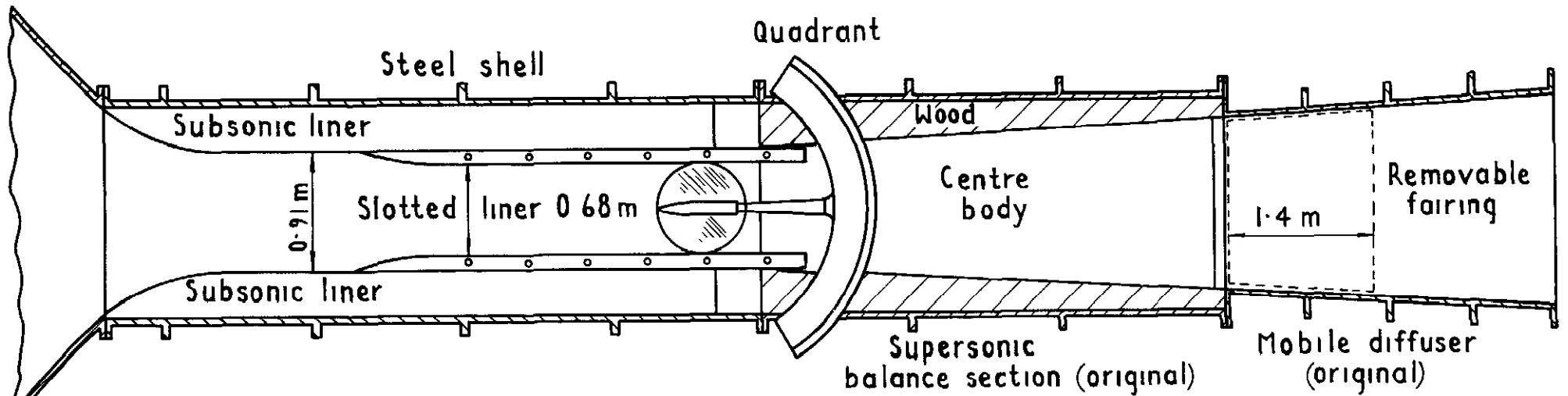
b Balance section for closed working section

c New spoilers

Fig.3 contd 3ft x 3ft tunnel-closed working section

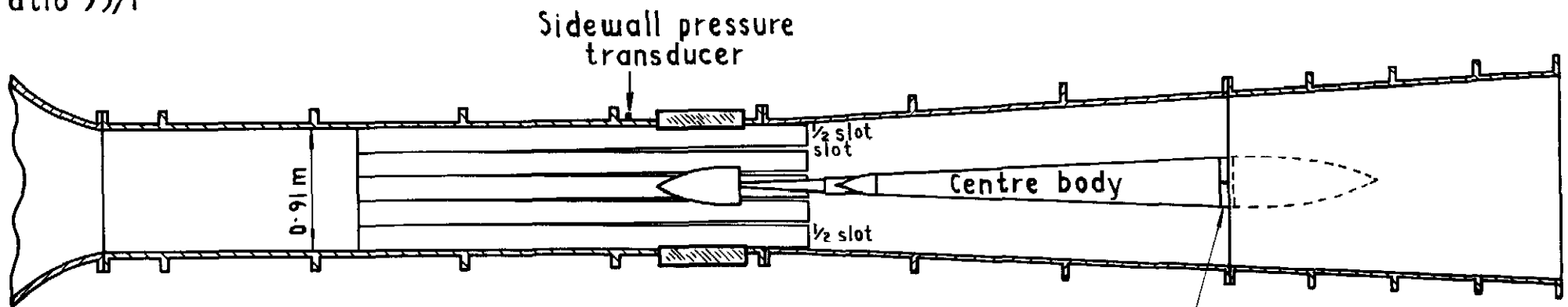


Open area ratio	3ft 8%	4m 16%
	8 complete slots	
	4 1/2 slots	



a Elevation

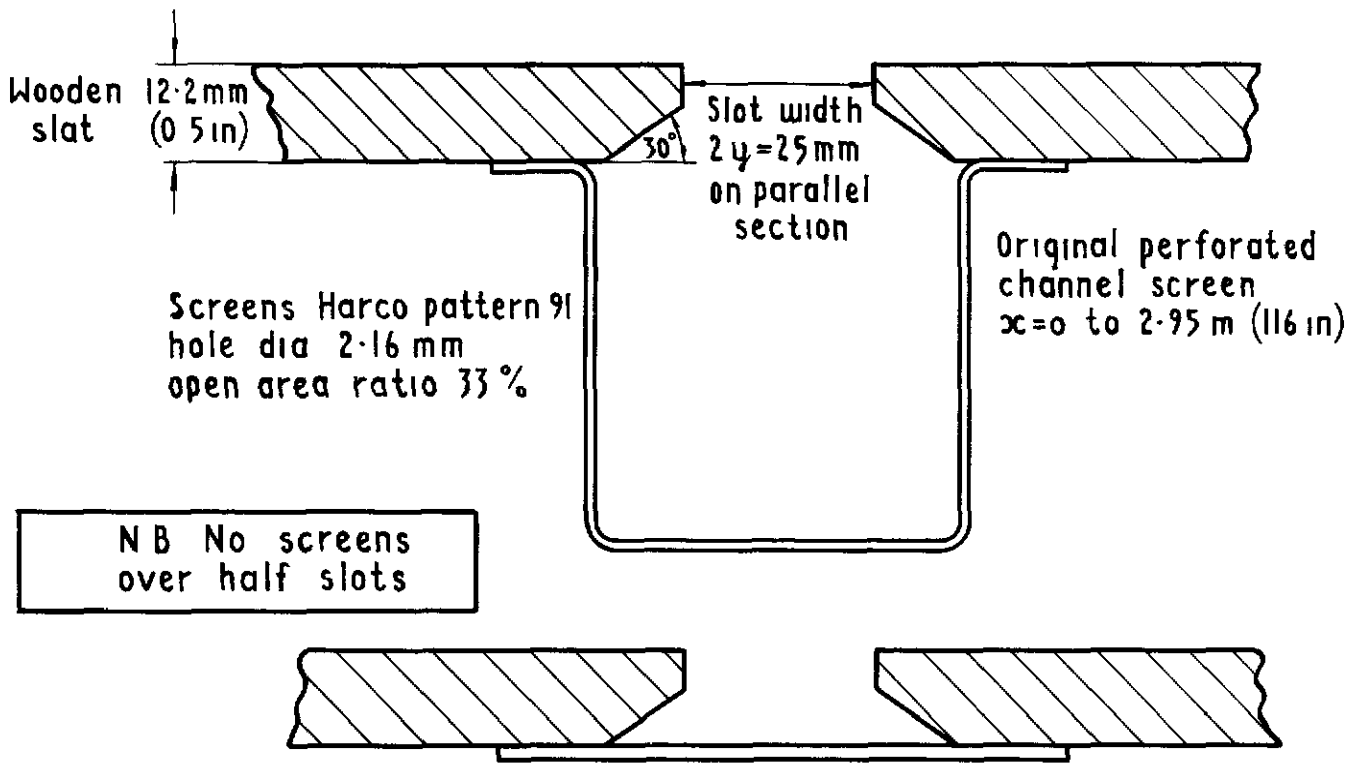
Contraction ratio 55/1



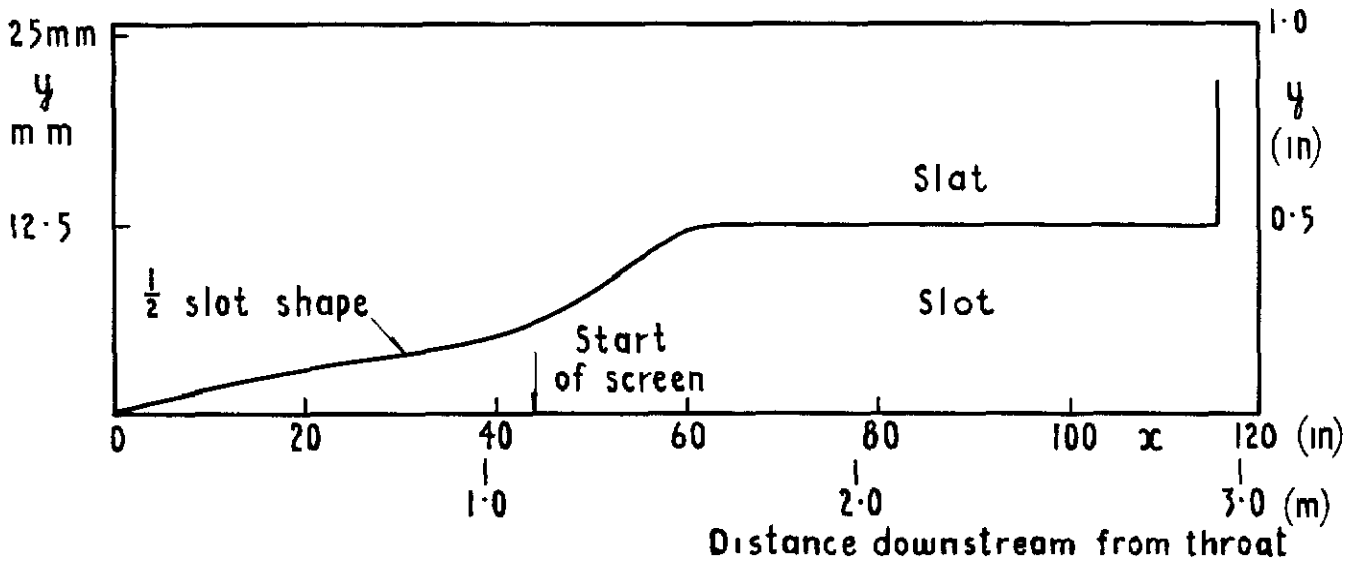
b Plan view

Original spoilers retracted

Fig.4 3ft x 3ft tunnel-top and bottom slotted working section



c Section across complete slot



d Slot and screen geometry

Fig.4 contd 3ft x 3ft tunnel-  
top and bottom slotted working section

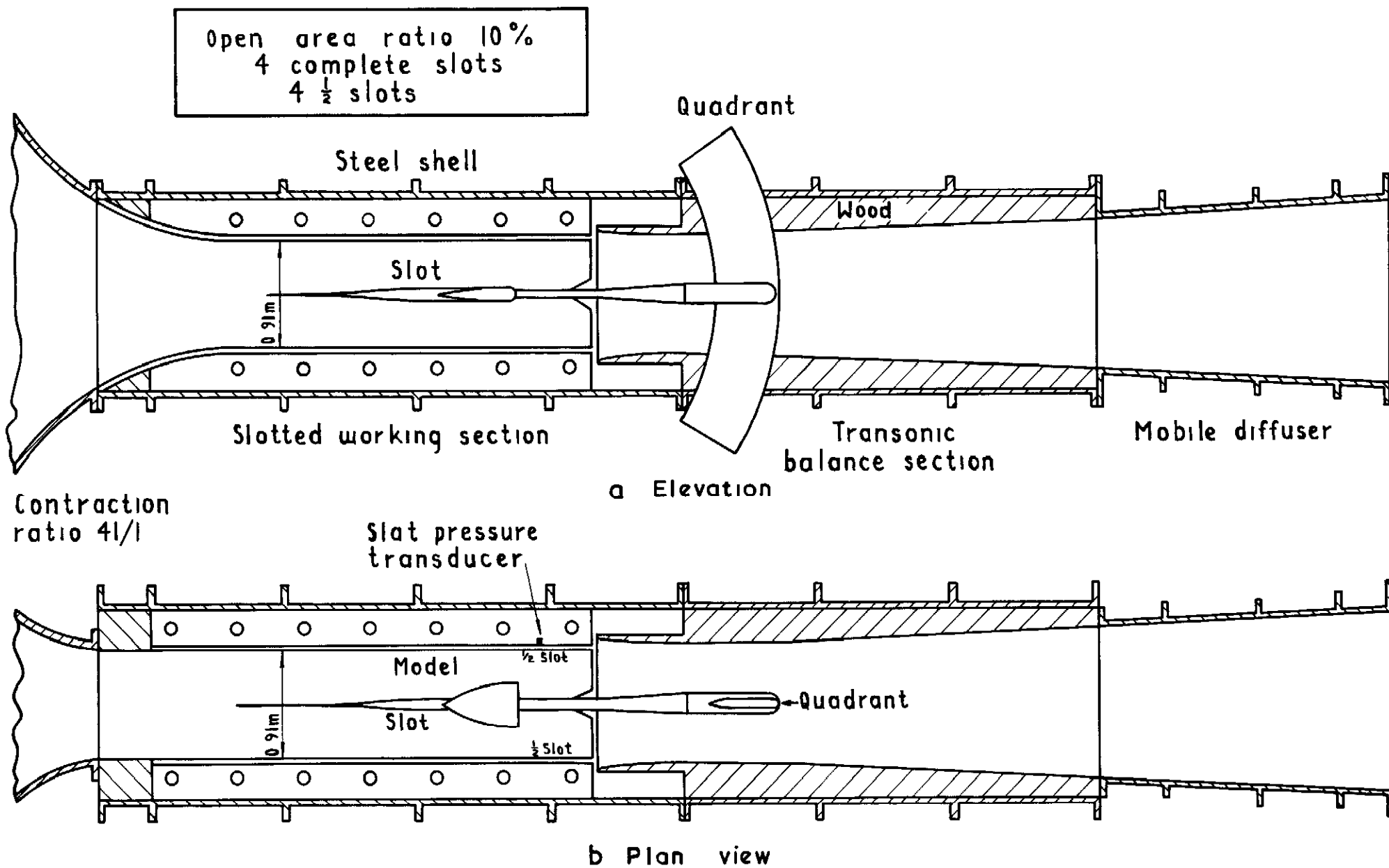
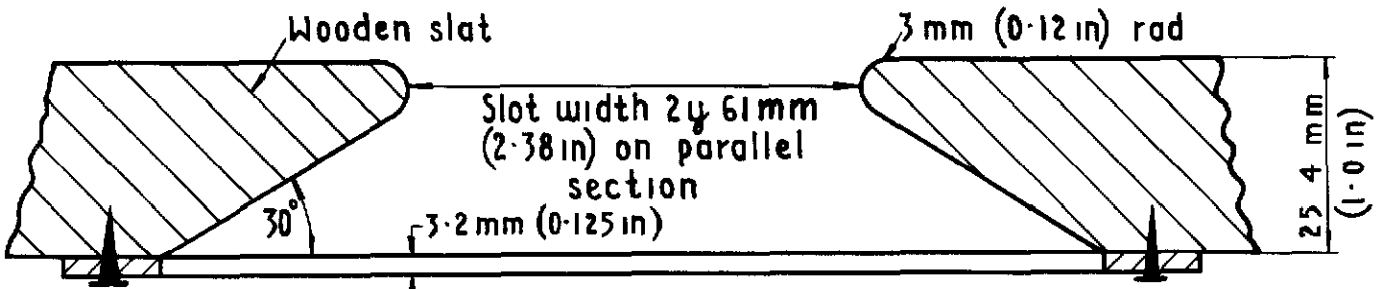


Fig 5 3ft x 3ft tunnel - slotted working section

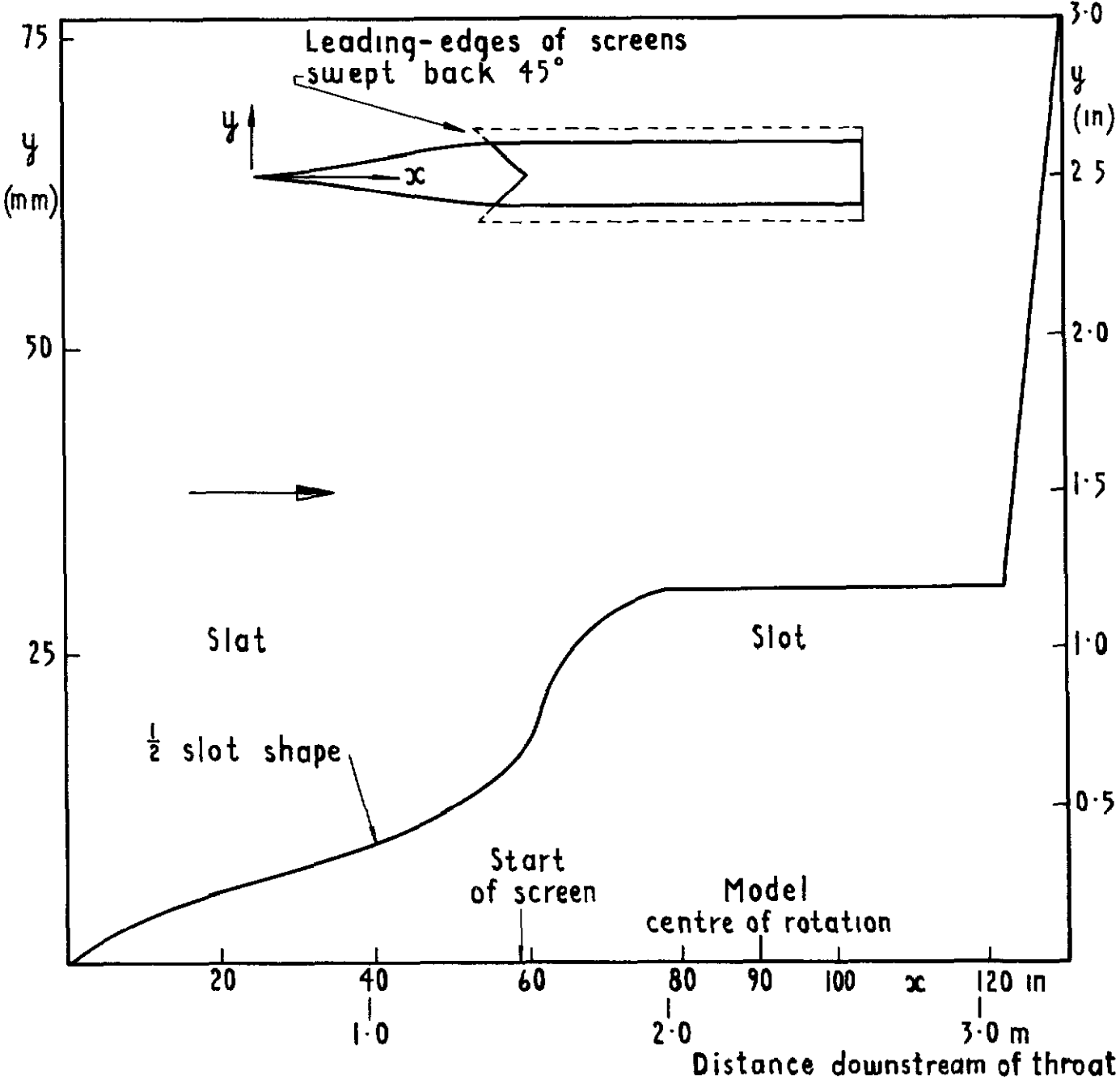


0.30m (12 in) deep Plenum chamber

Perforated flat screen added  
 Harco pattern 208  
 Hole dia 6.3 mm (0.25 in)  
 Open area ratio 50%

NB Screens over half slots

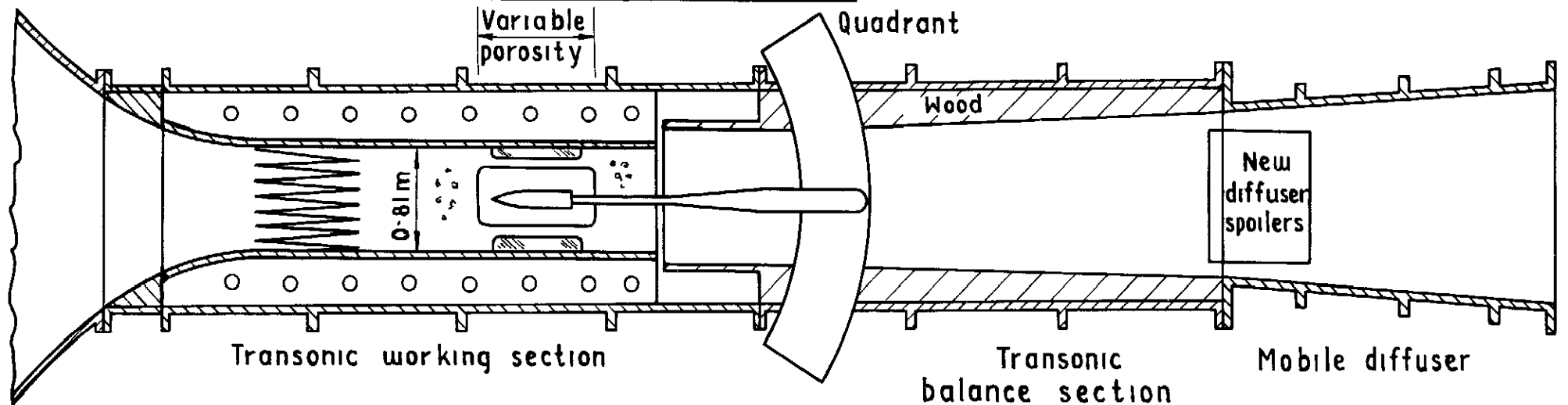
c Section across complete slot



d Slot and screen geometry

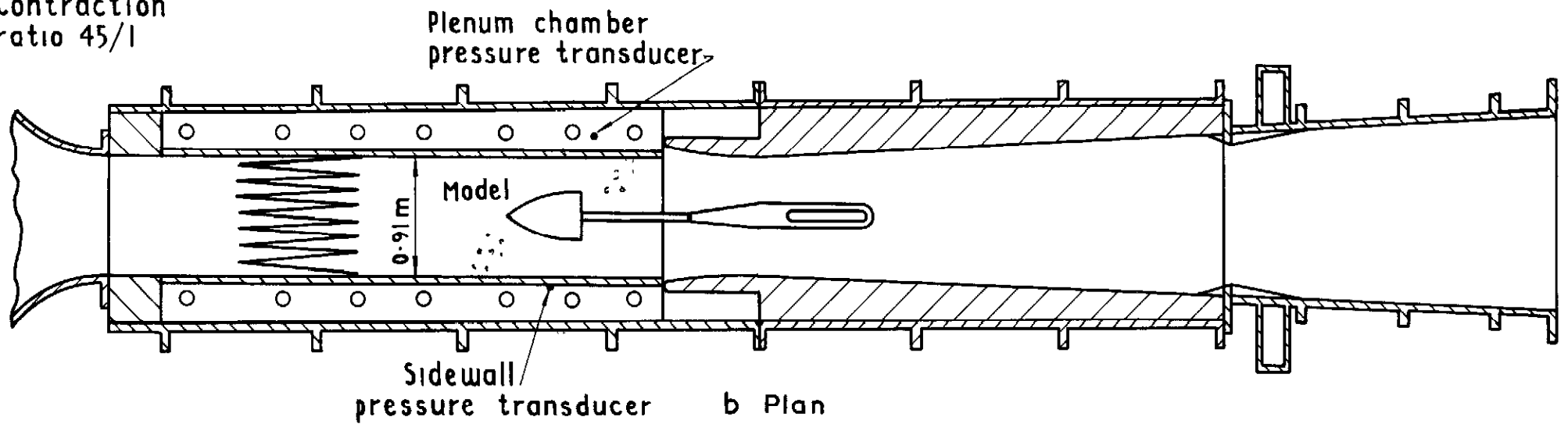
Fig.5 contd 3ft x 3ft tunnel slotted working section

Open area ratio 6%  
 Hole diameter=plate thickness= 9.55mm (0.375 in)  
 Holes 60° to normal



a Elevation

Contraction  
 ratio 45/1



b Plan

Fig.6 3ft x 3ft tunnel-perforated working section

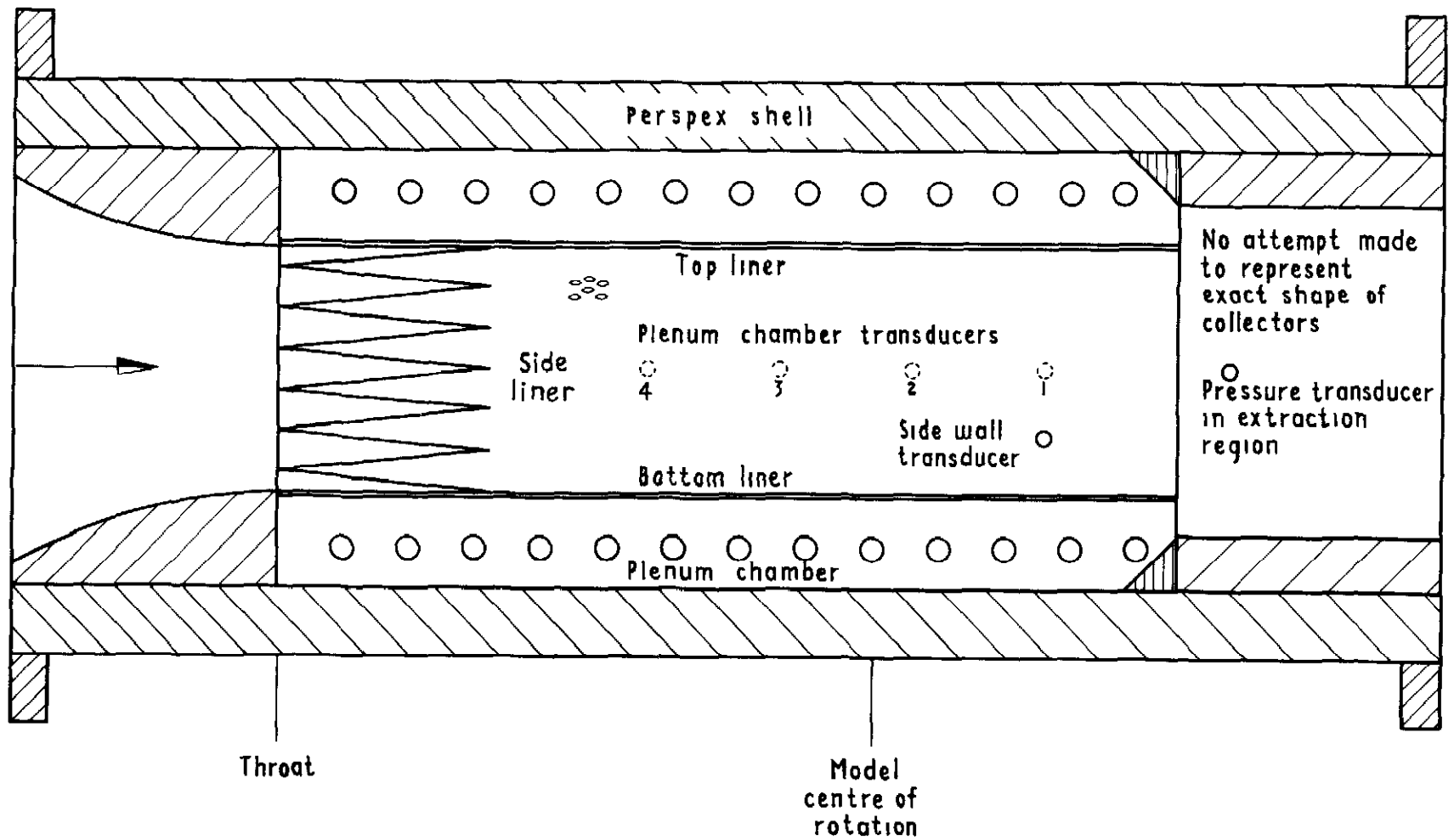


Fig.7 4in x 4 in tunnel-perforated working section

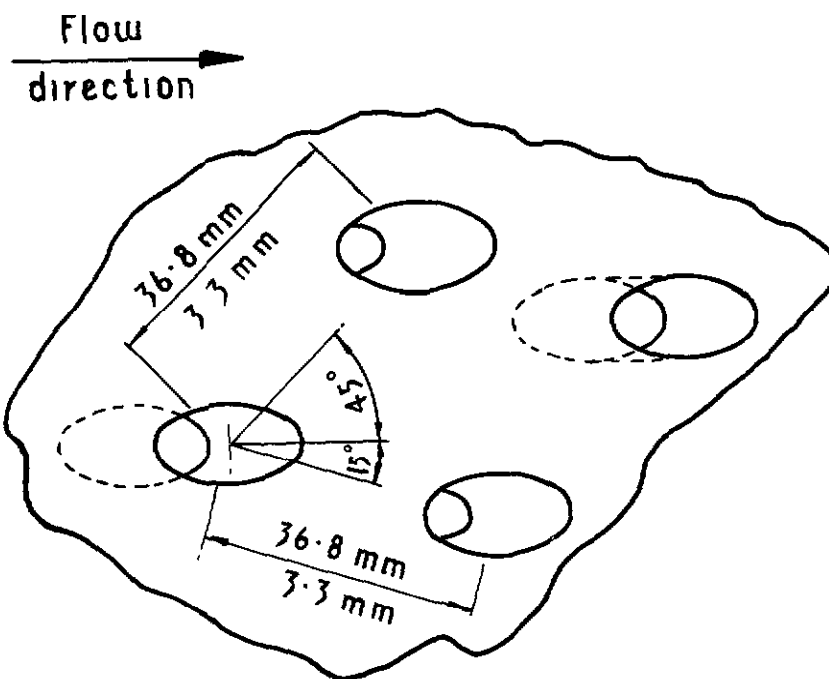
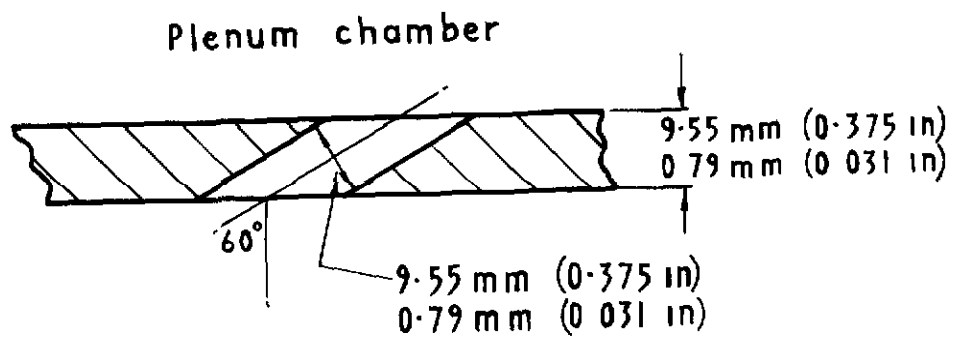
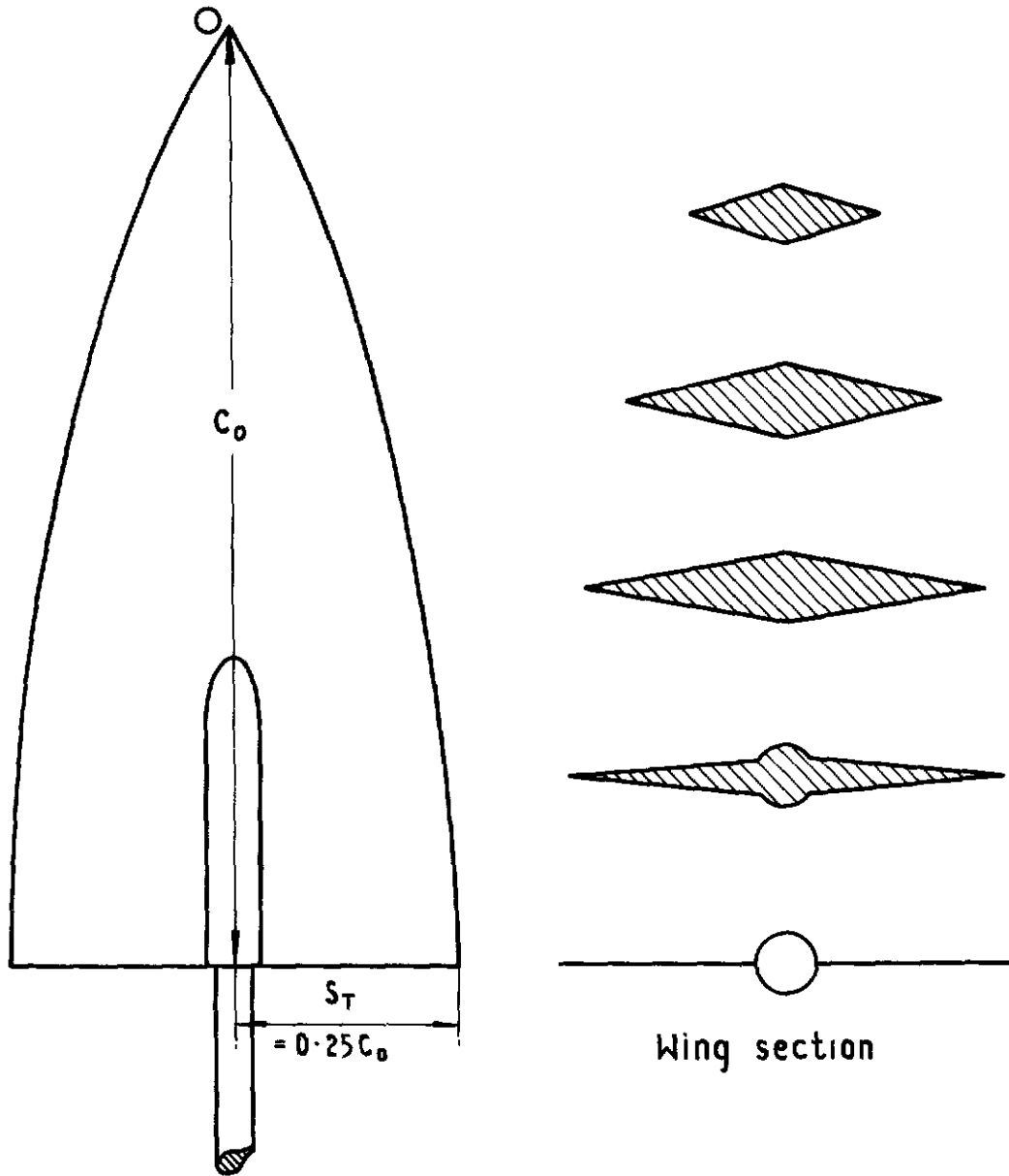



Fig.8 Geometry of perforated walls  
3ft x 3ft and 4in x 4in tunnels



Sting with internal  
strain gauge balance  
Natural frequency of vibration in  
the axial force direction 140 Hz

Fig 9 Slender wing



$M=0.80$  Air flow 

Working section

Diffuser side wall

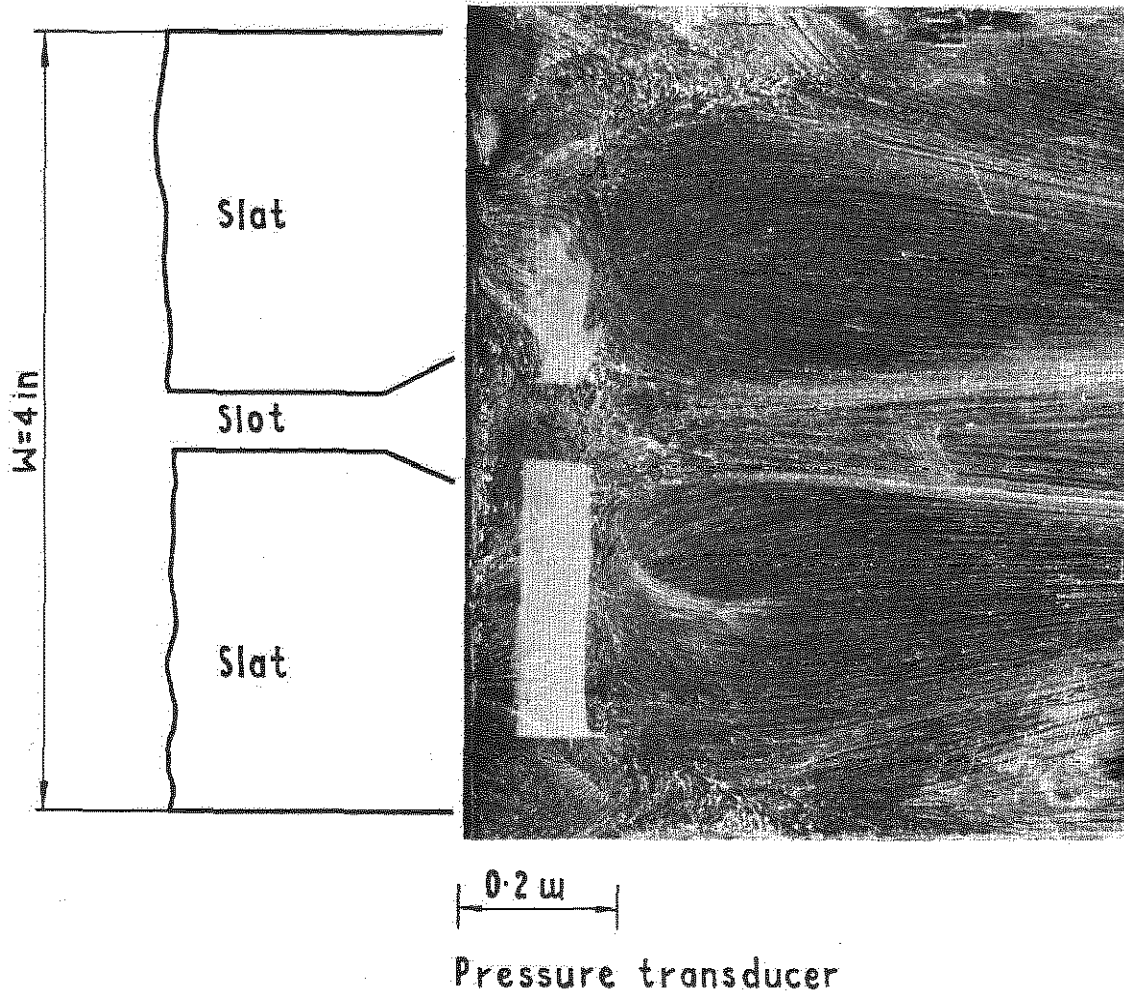
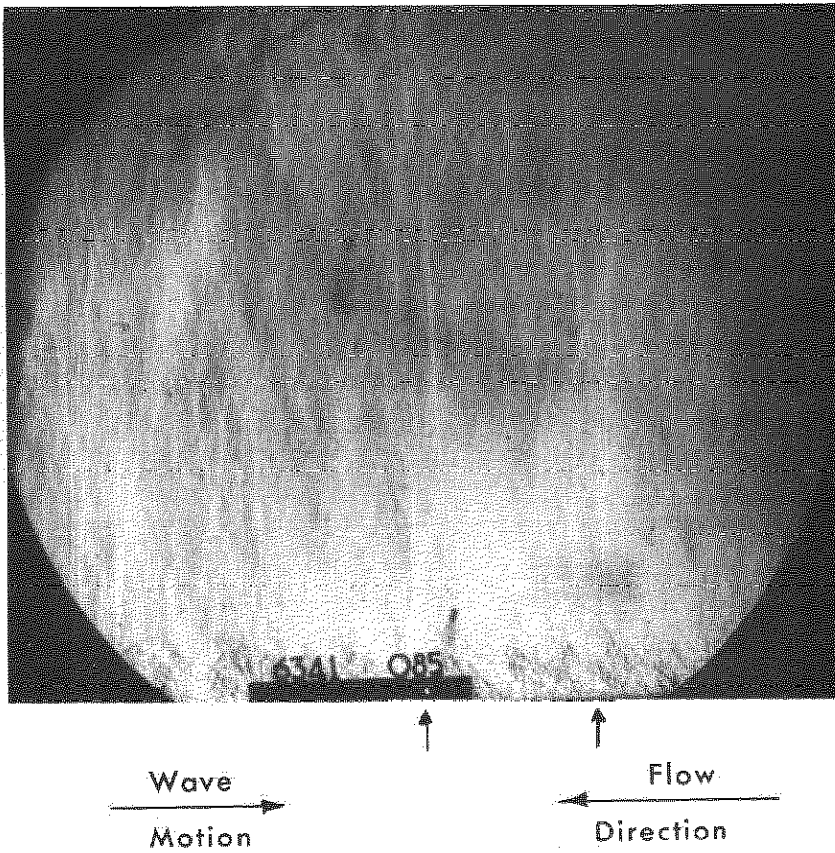


Fig 10 Oil flow photograph showing the extraction region for the 4 in x 4 in tunnel

(a)  $M=0.85$



(b)  $M=1.00$

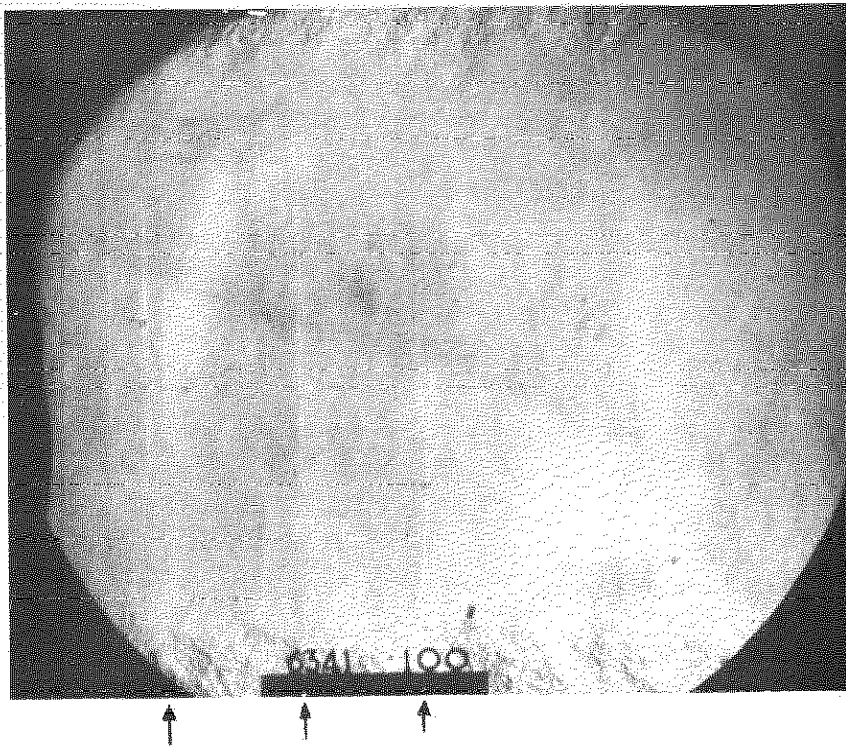


Fig.11. 3ftx3ft Tunnel spark Schlieren photographs in top and bottom slotted section showing normal waves moving upstream

08  
14  
3  
42  
52  
08  
1.2  
1.6  
1.8

NEG.NO.C7341

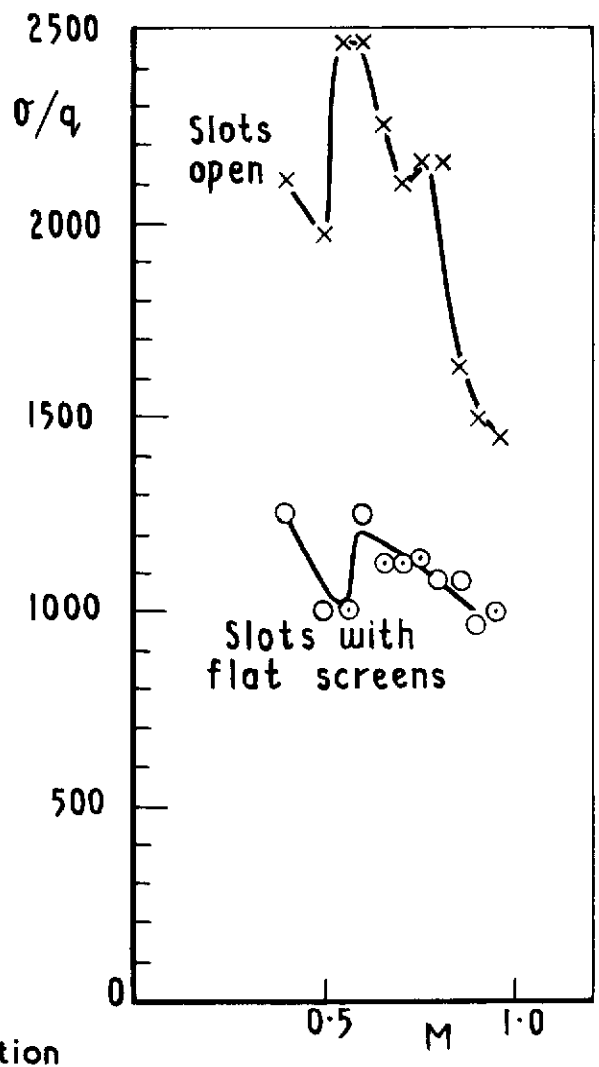
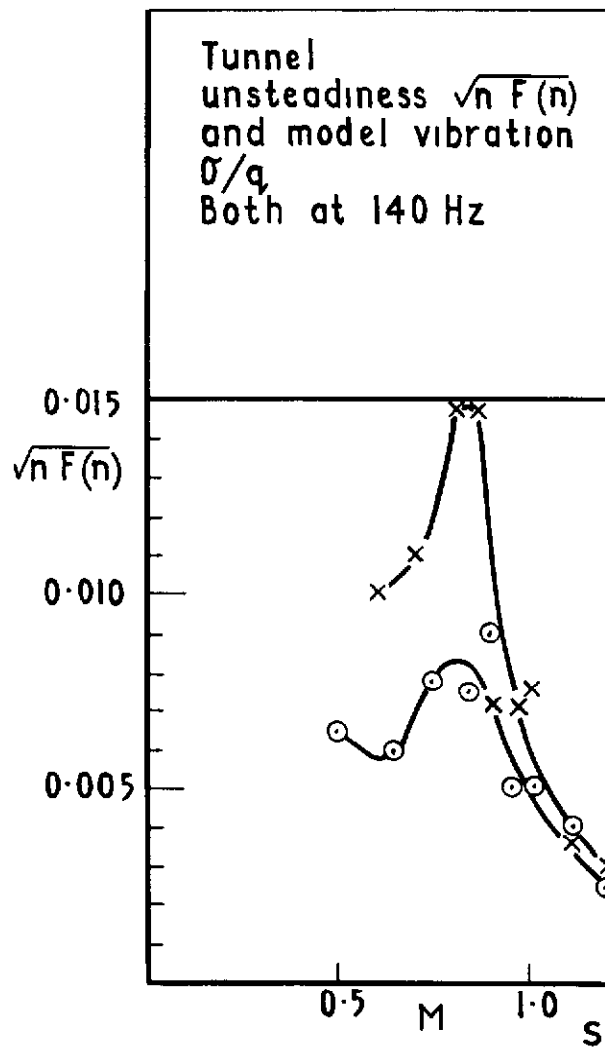
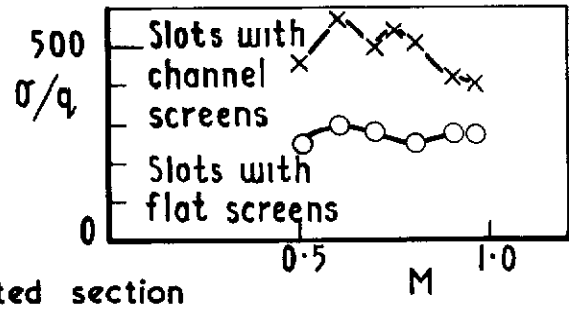
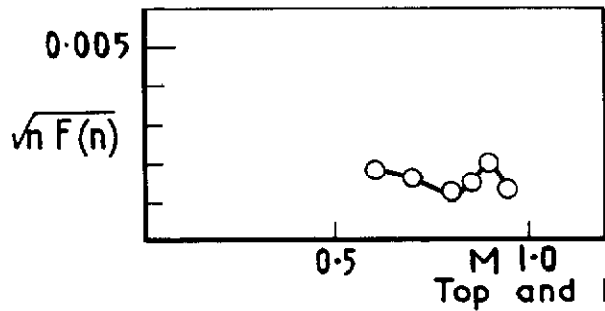
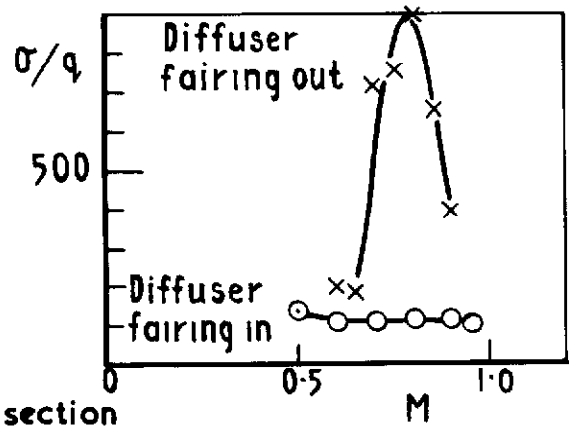
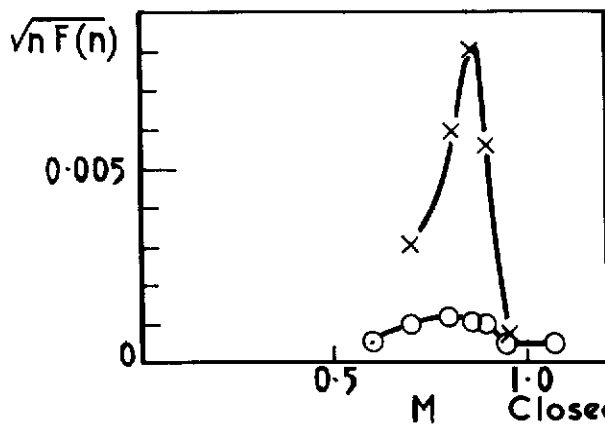


Fig.12 3ft x 3ft tunnel-comparison of unsteadiness and model vibration in different working sections

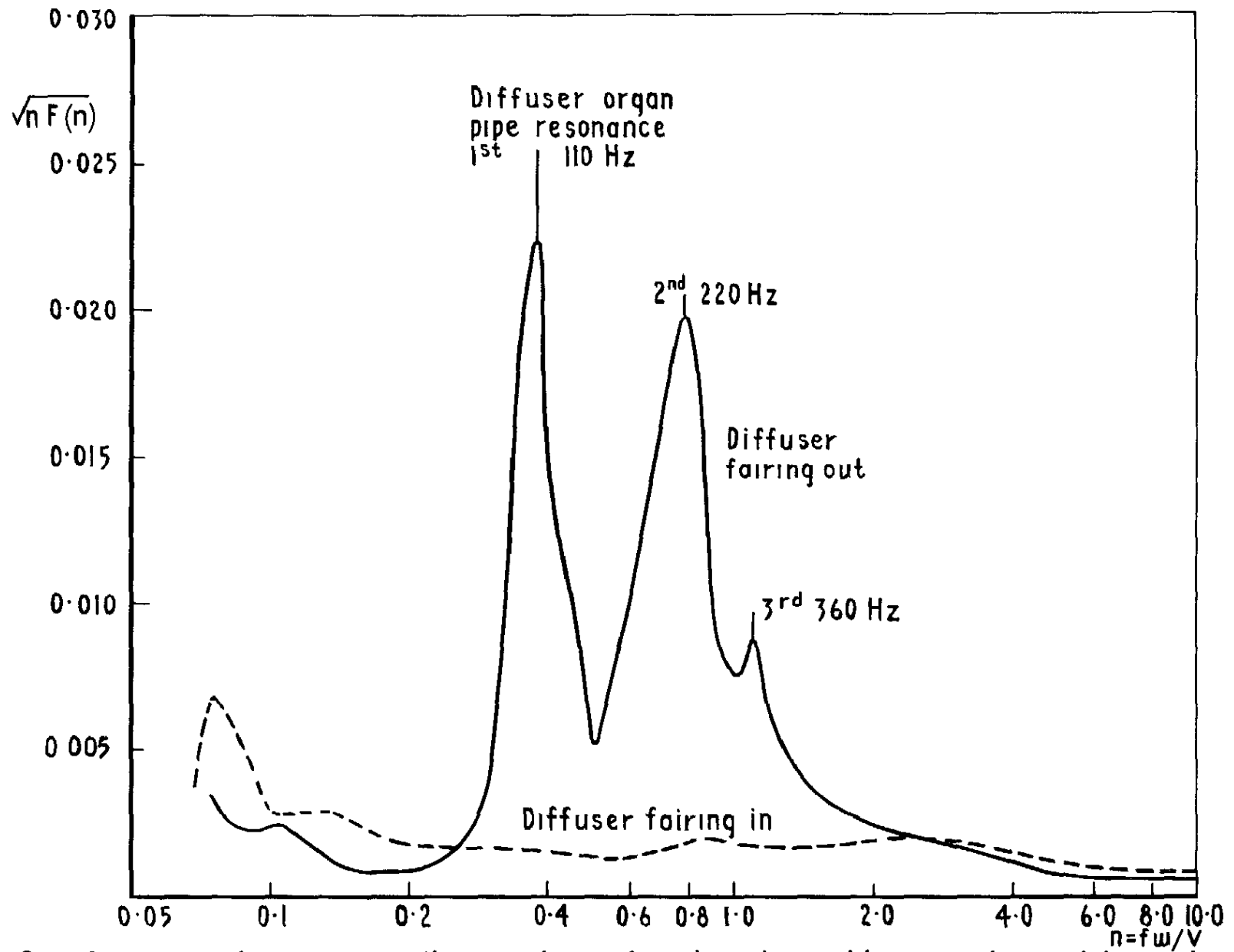


Fig.13 3ft x 3ft tunnel - pressure fluctuations in closed working section with and without diffuser fairing  $M = 0.80$

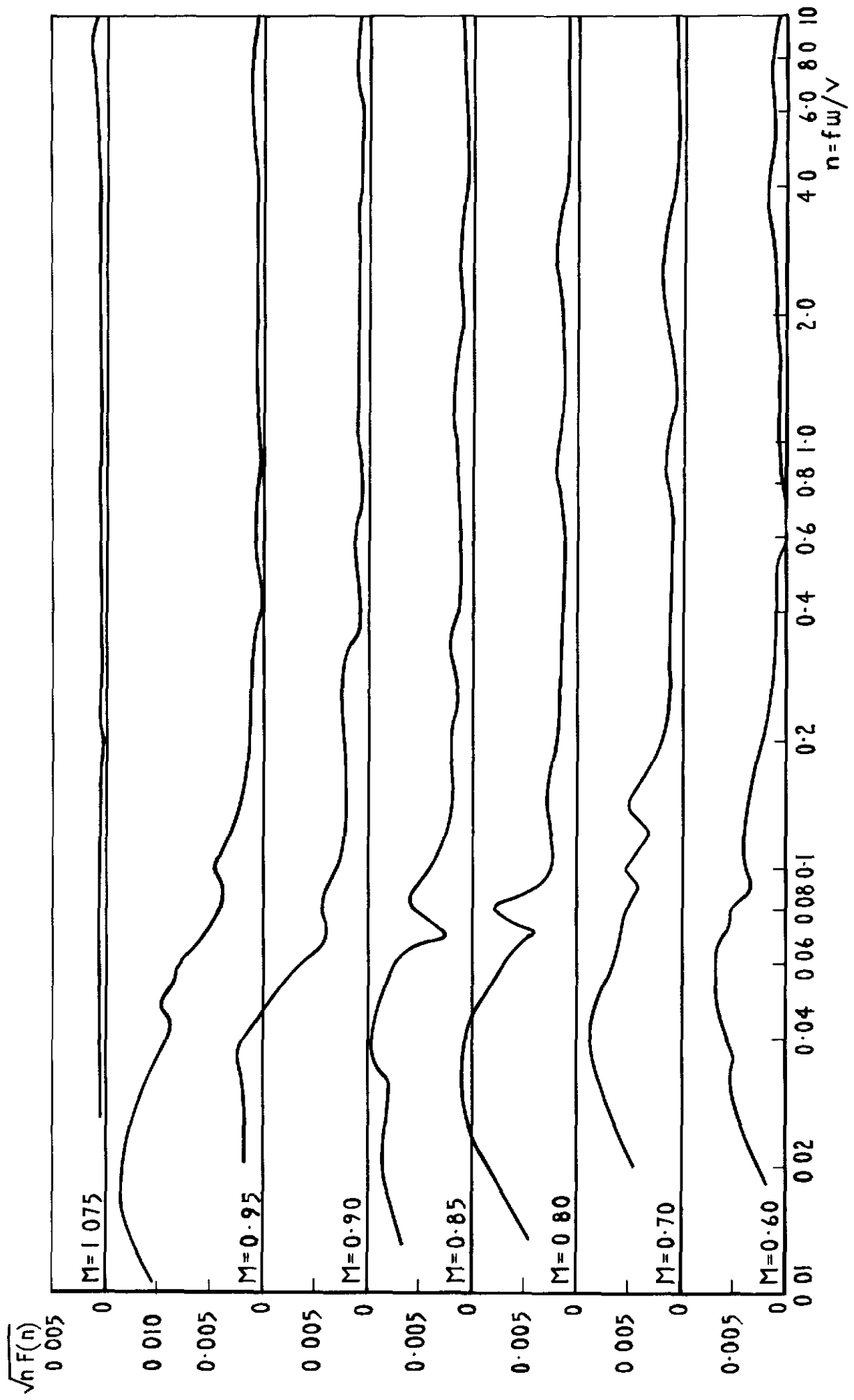


Fig 14 3ft x 3ft tunnel - pressure fluctuations in closed working section - diffuser fairing in

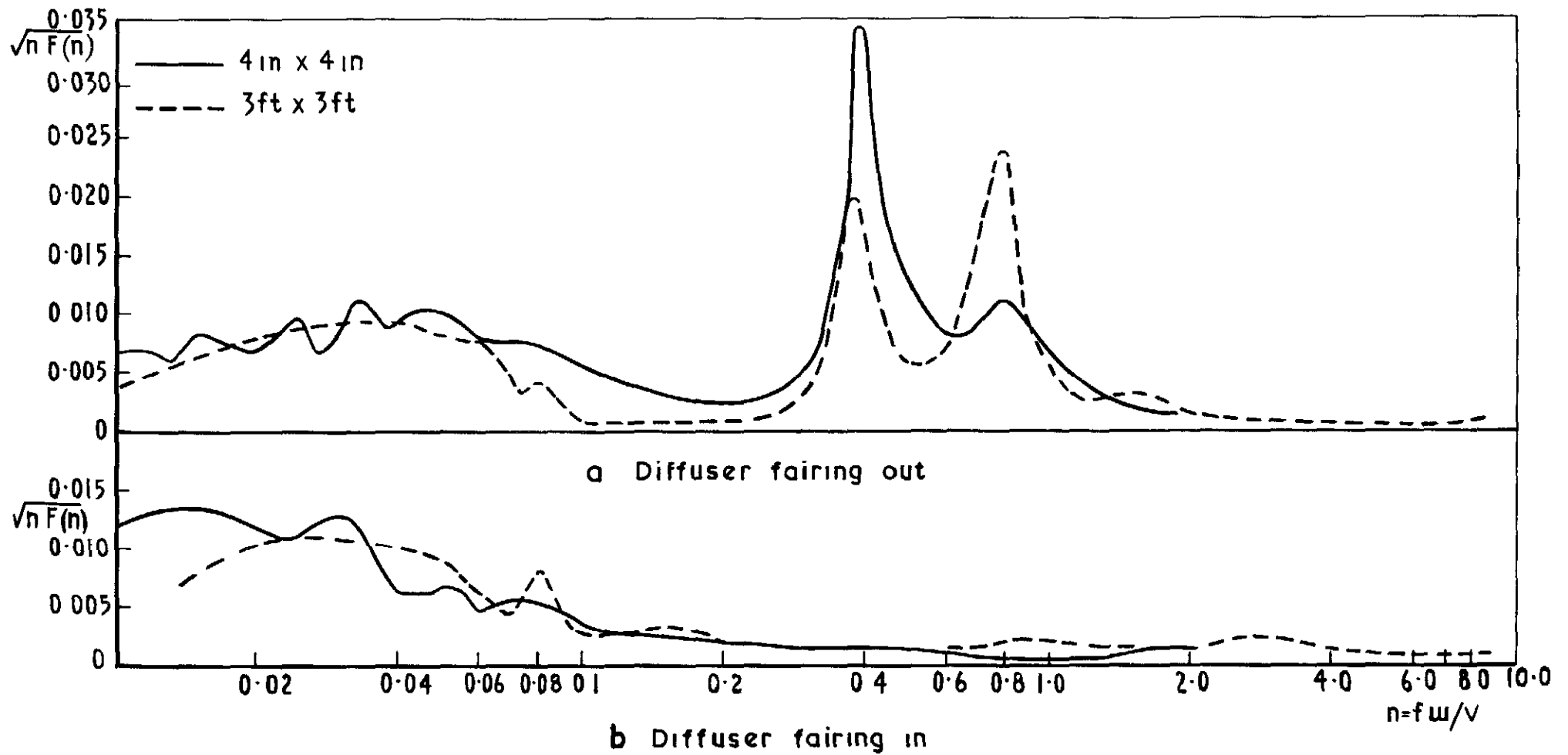


Fig.15 Comparison of pressure fluctuations in closed working sections of 3ft x 3ft and 4 in x 4 in tunnels  $M=0.80$

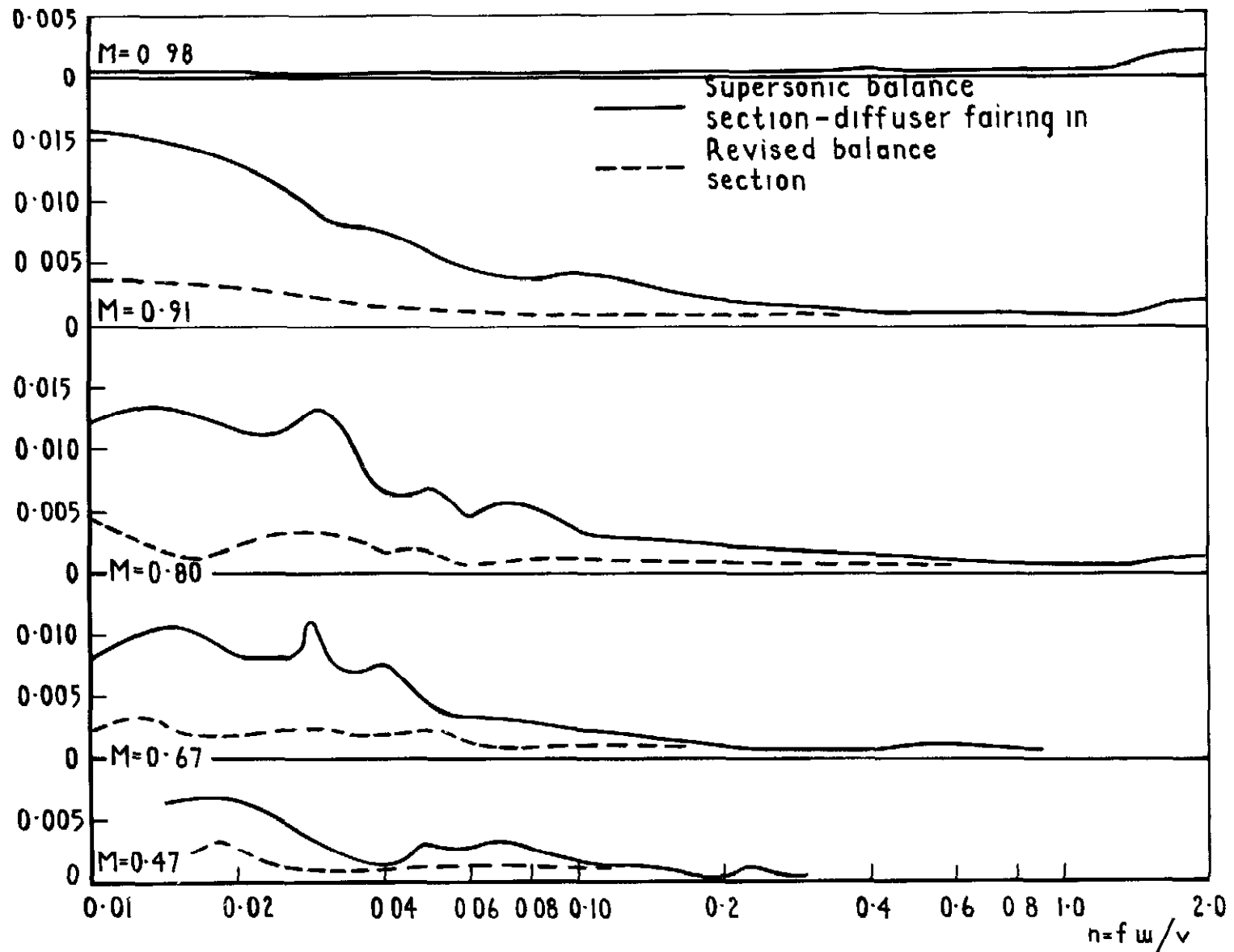


Fig 16 4in x 4in tunnel- pressure fluctuations in closed working section with original and revised balance sections

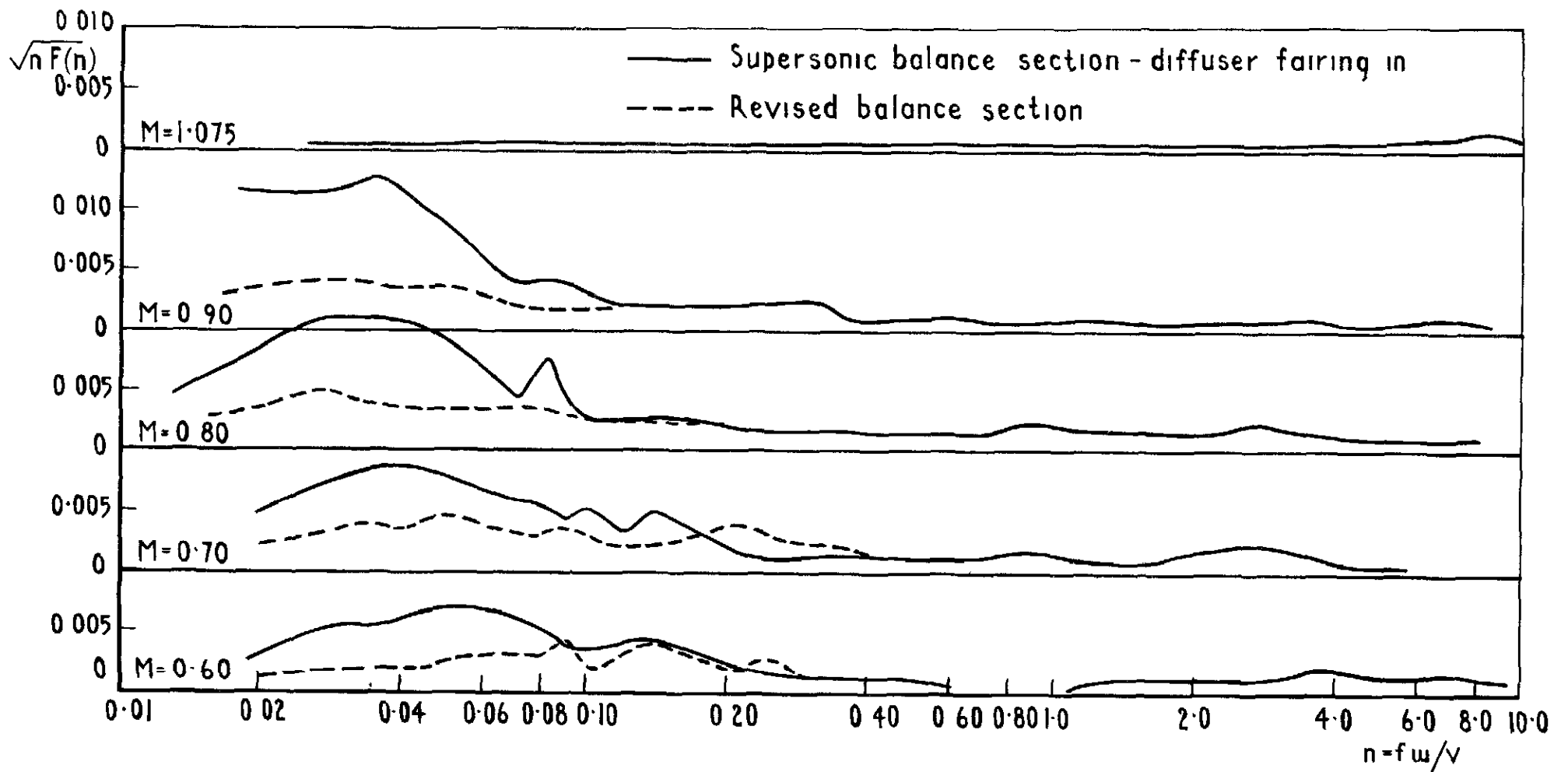


Fig.17 3ft x 3ft tunnel - pressure fluctuations in closed working section with original and revised balance sections



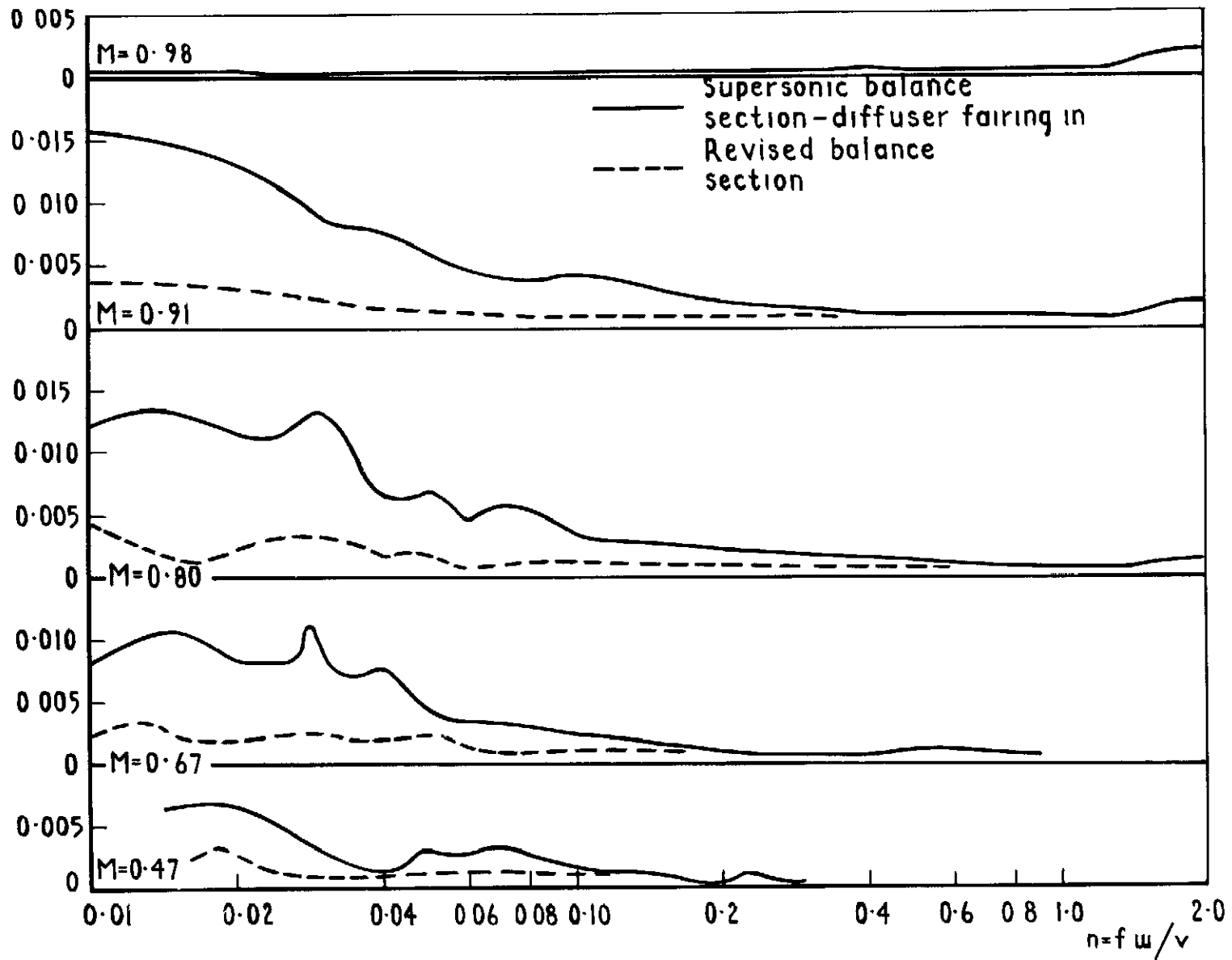


Fig.16 4in x 4in tunnel- pressure fluctuations in closed working section with original and revised balance sections

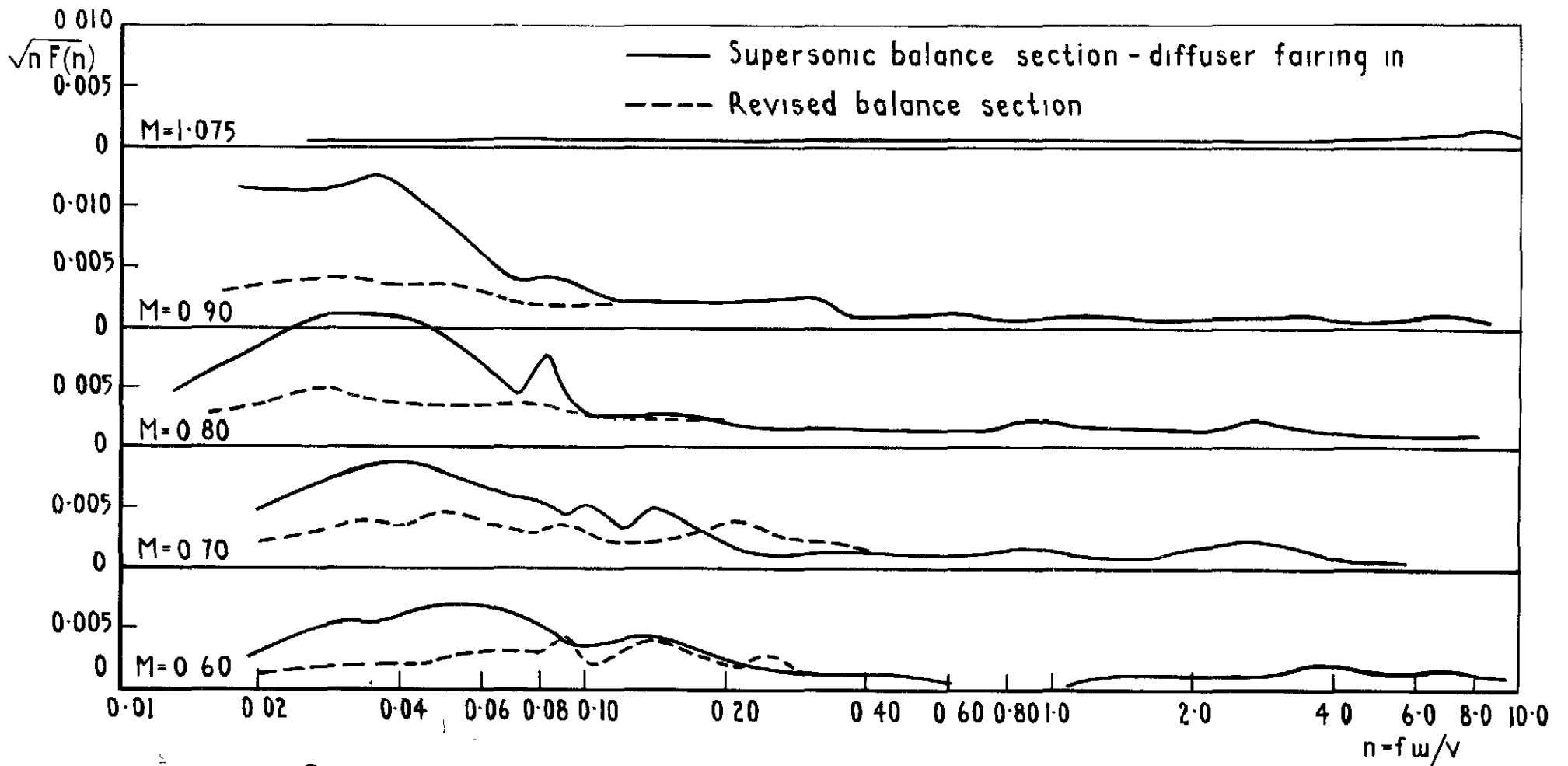


Fig.17 3ft x 3ft tunnel - pressure fluctuations in closed working section with original and revised balance sections

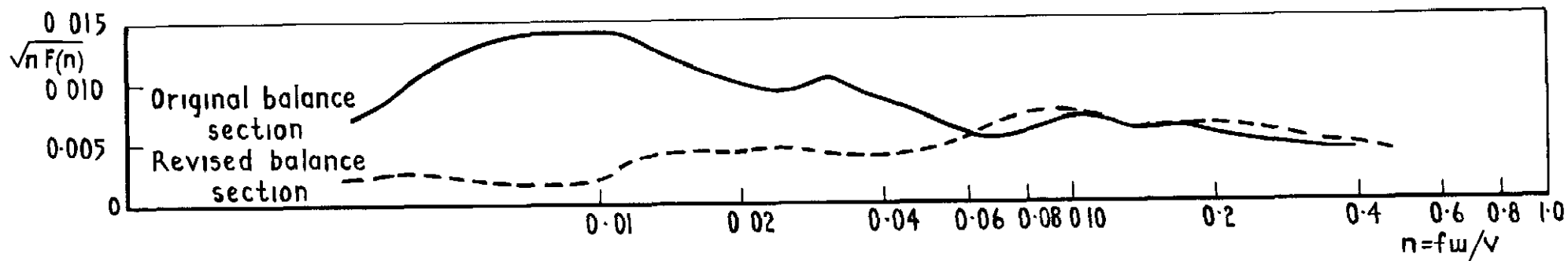


Fig 18 4in x 4in tunnel-pressure fluctuations on quadrant  $M = 2.0$

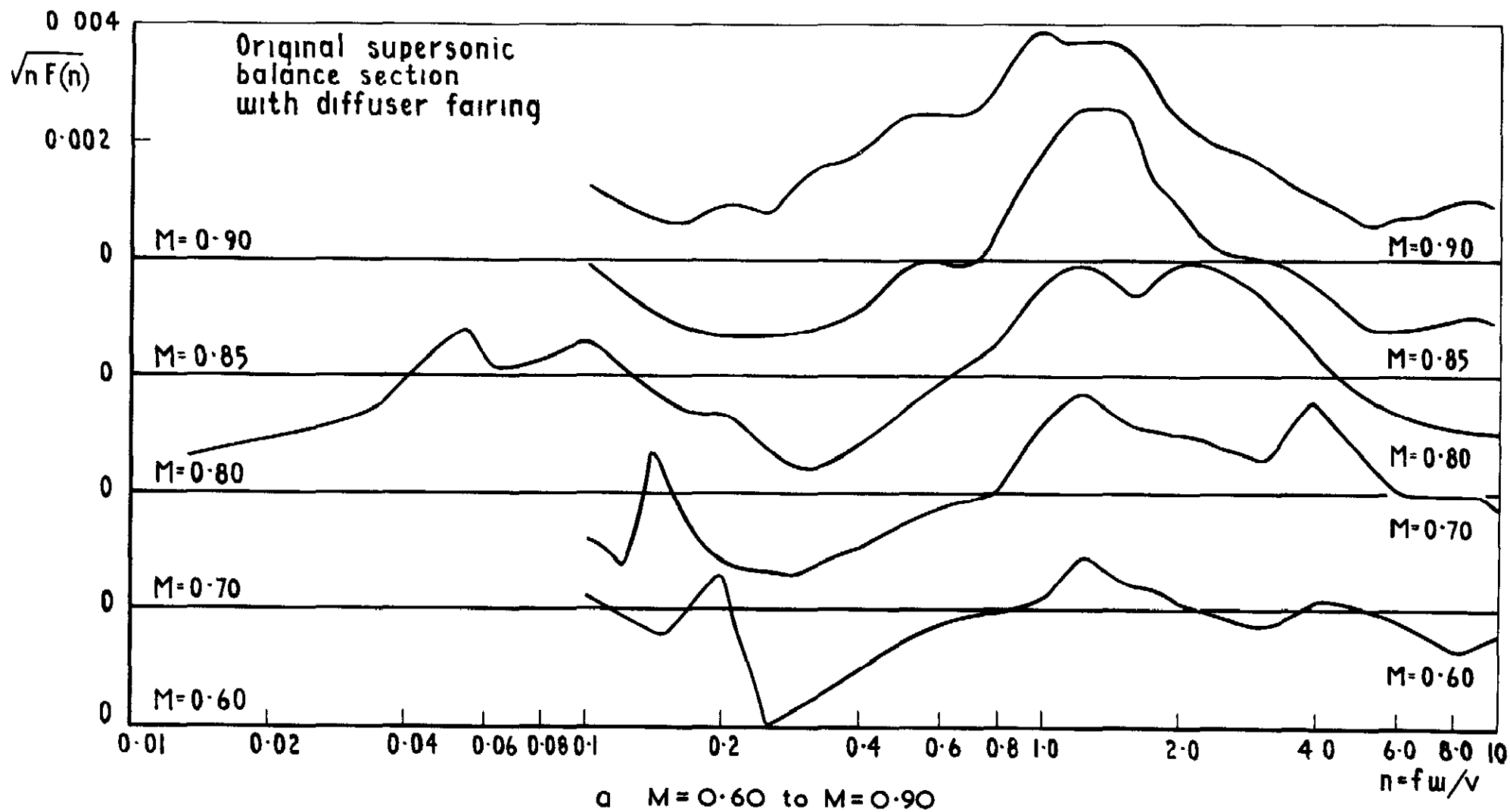


Fig 19 3ft x 3ft tunnel - pressure fluctuations in top and bottom slotted section (flat screens)

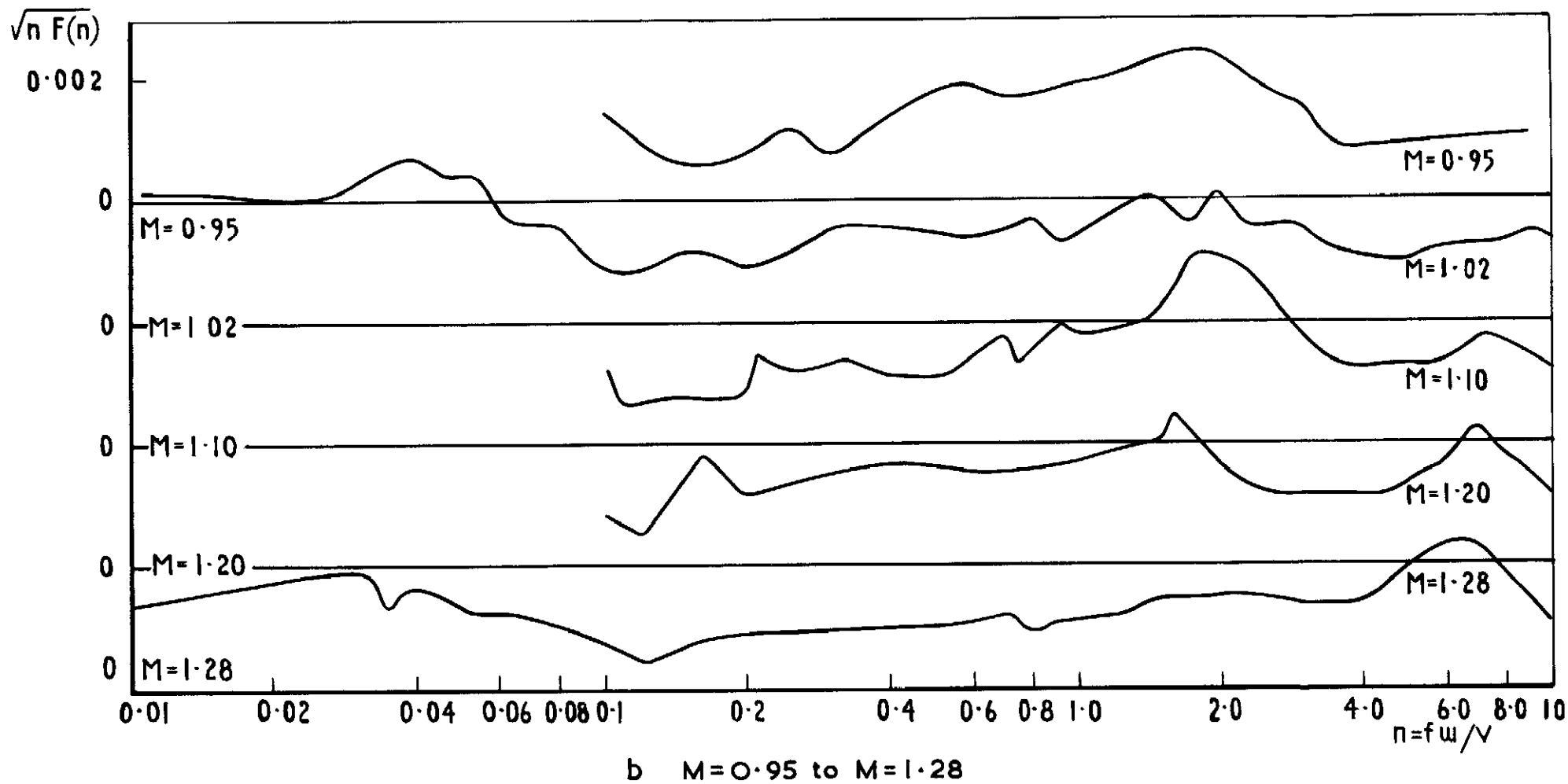


Fig 19contd 3ft 3ft tunnel- pressure fluctuations in top and bottom slotted section (flat screens)

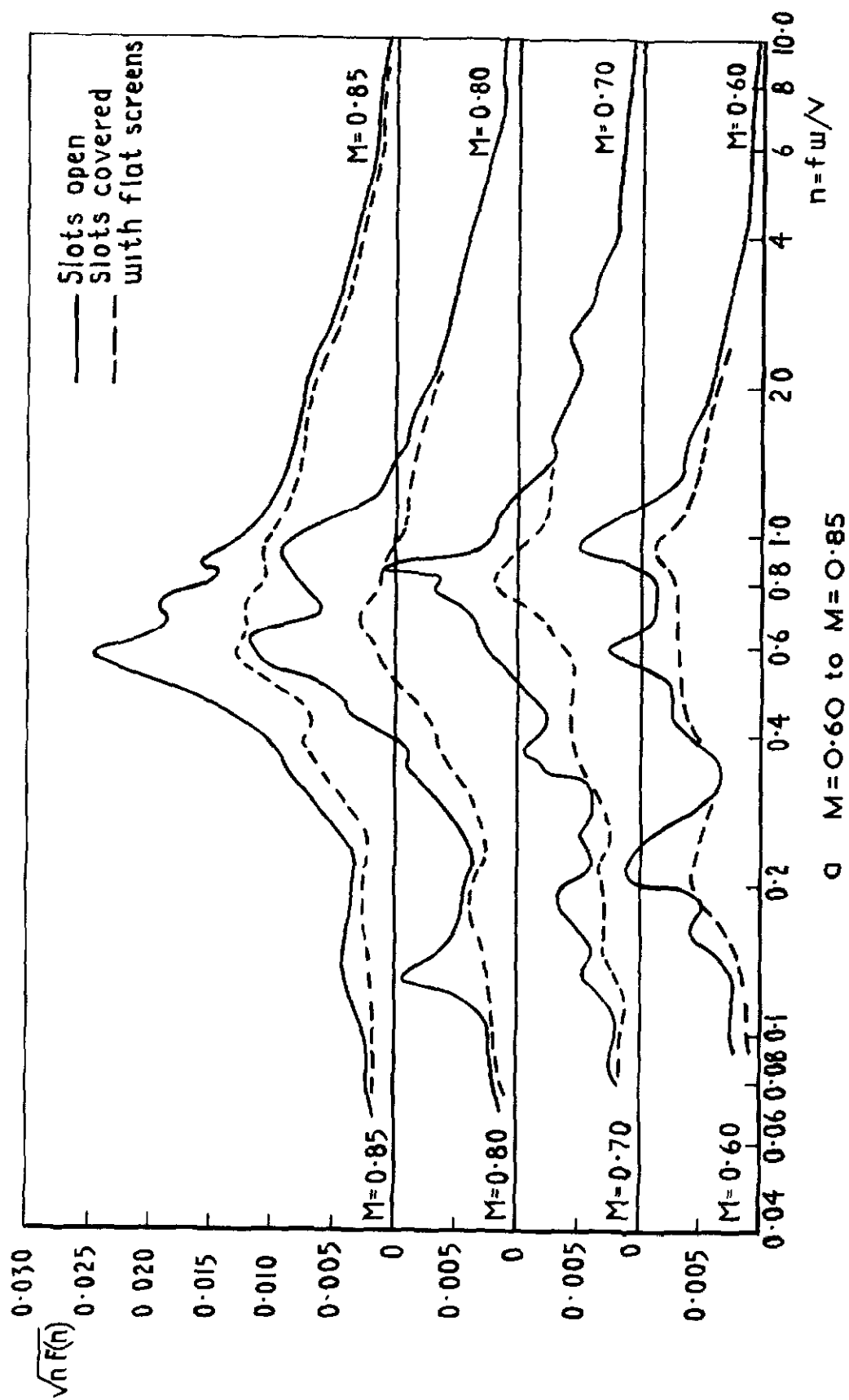


Fig 20 3ft x 3ft tunnel - comparison of pressure fluctuations in slotted working section

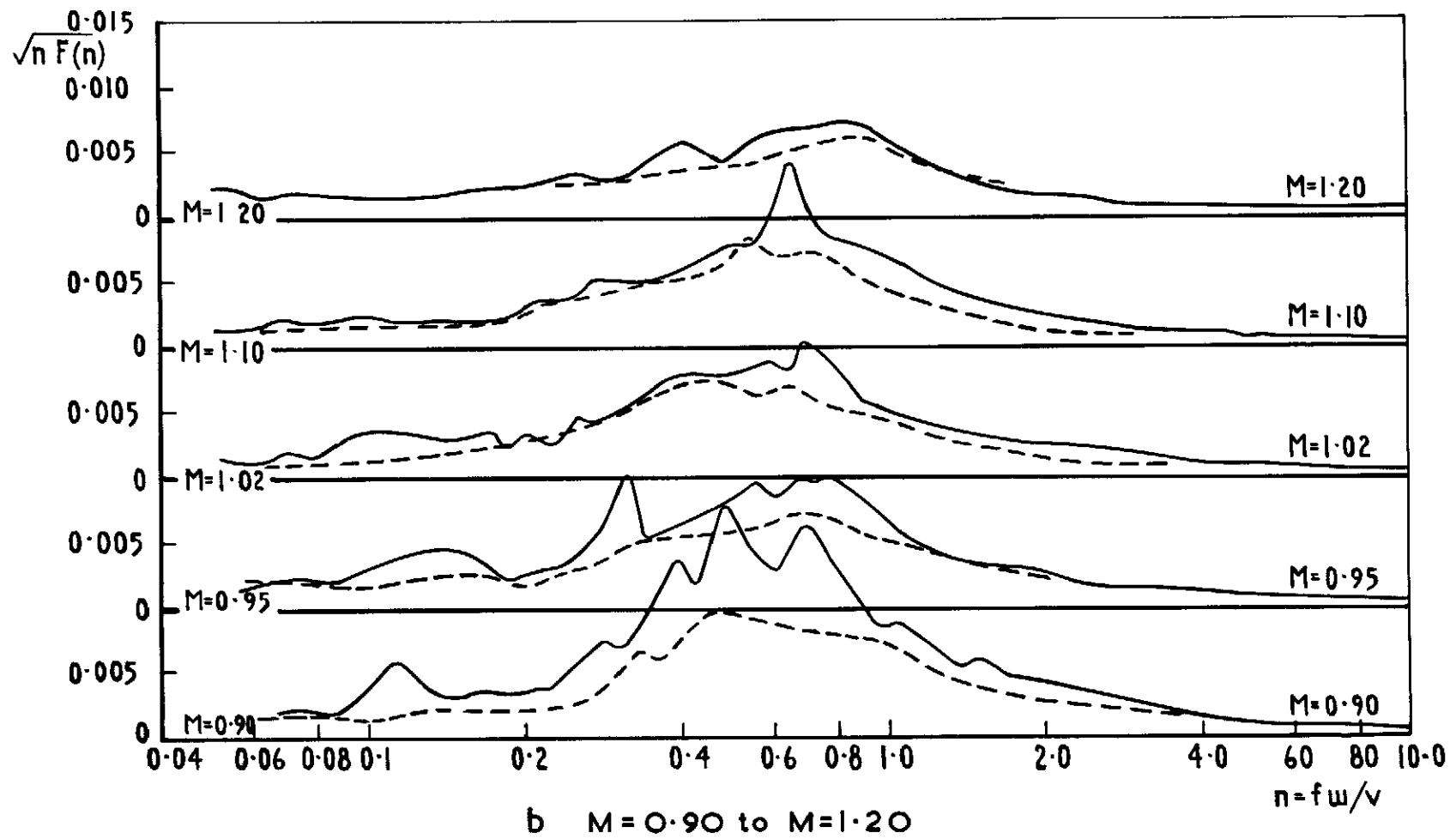


Fig. 20 contd 3ft x 3ft tunnel comparison of pressure fluctuations in slotted working section

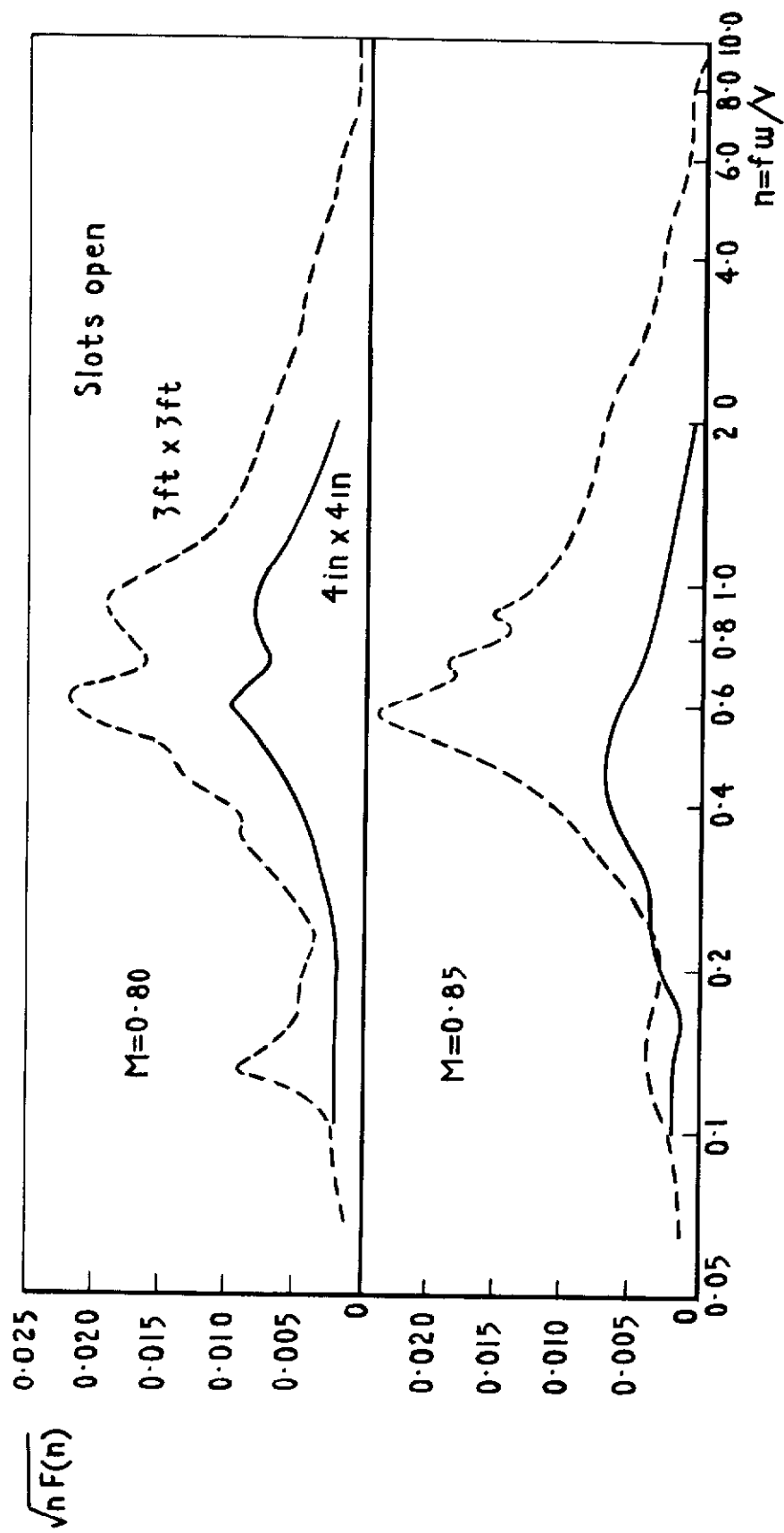
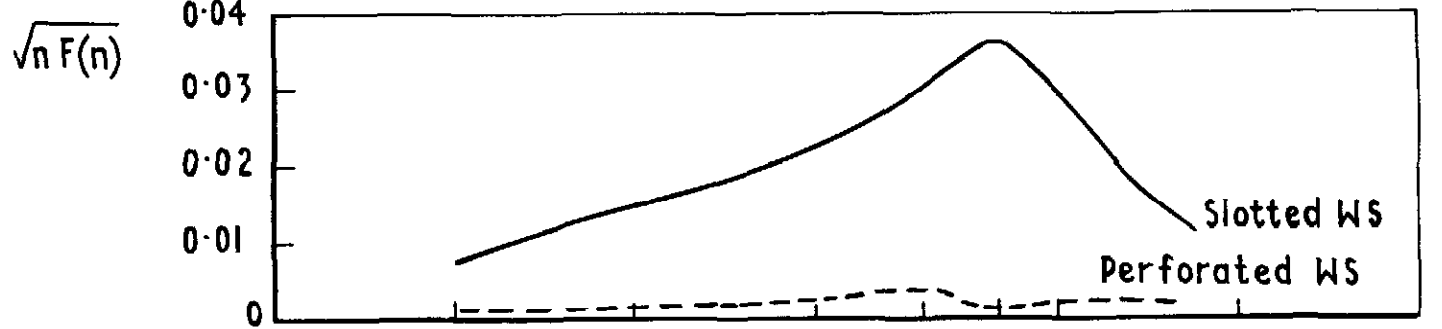
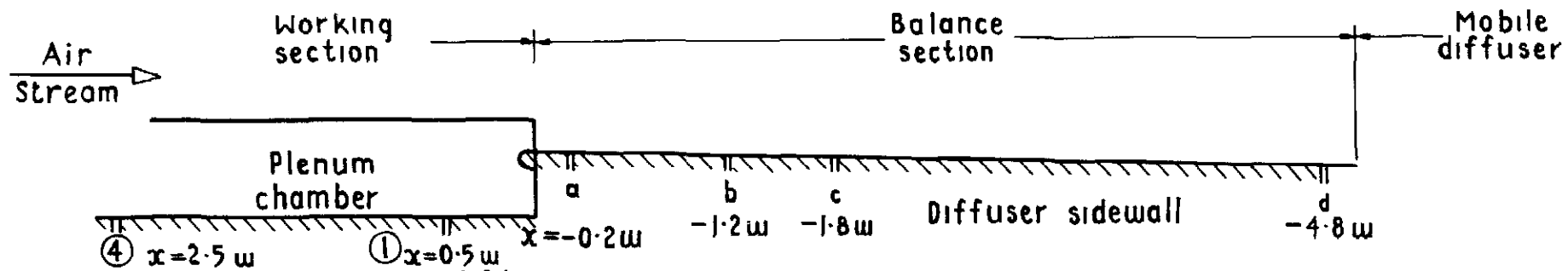


Fig 21 Comparison of pressure fluctuations in slotted working sections of 3ft x 3ft and 4in x 4in tunnels

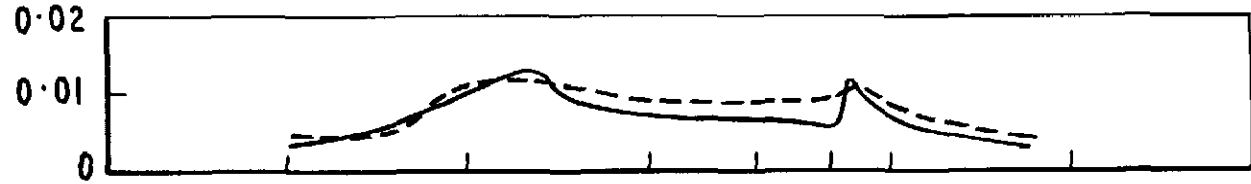




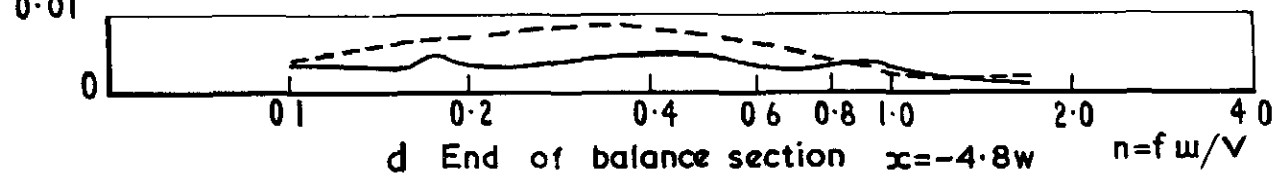
a Extraction region  $x = -0.2w$



b Front flange of balance section  $x = -1.2w$



c Centre line of quadrant  $x = -1.8w$



d End of balance section  $x = -4.8w$   $n = fw/V$

Fig.22 a-d 4in x 4in tunnel-diffuser pressure fluctuations with slotted and perforated working sections  $M = 0.80$

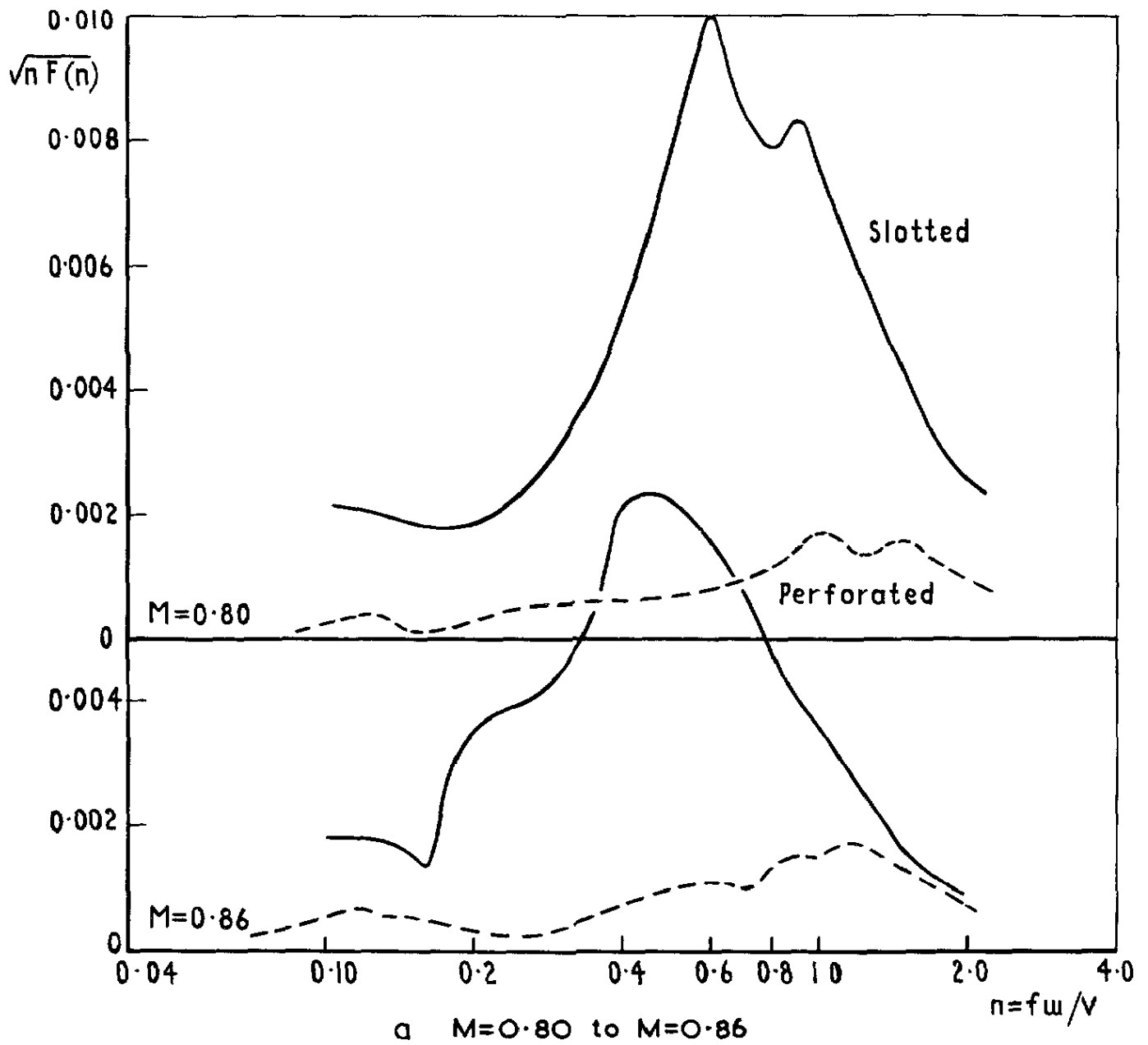


Fig 23 4 in x 4 in tunnel - comparison of pressure fluctuations in slotted and perforated sections

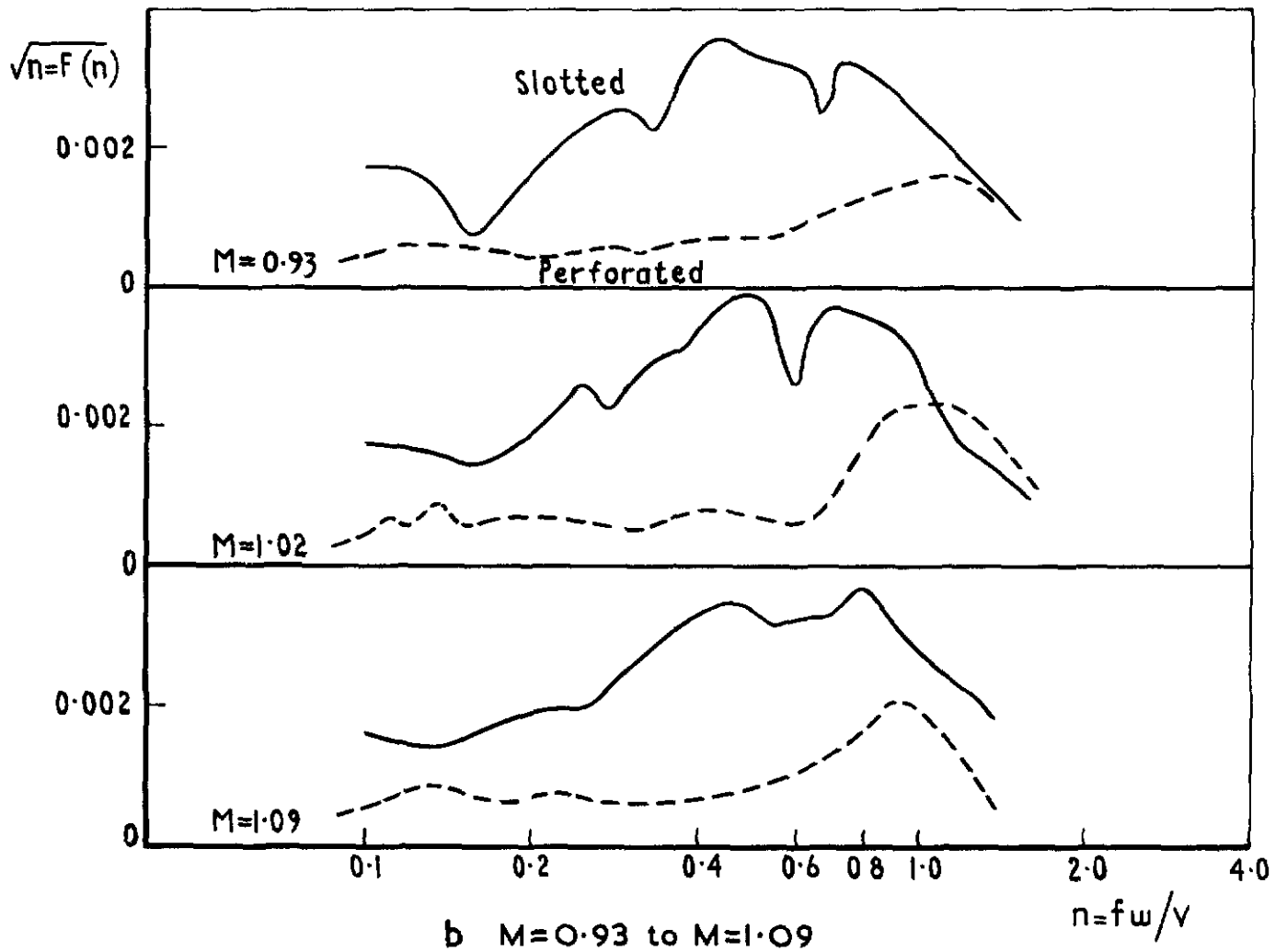


Fig.23 contd 4in x 4in tunnel-comparison of pressure fluctuations in slotted and perforated sections

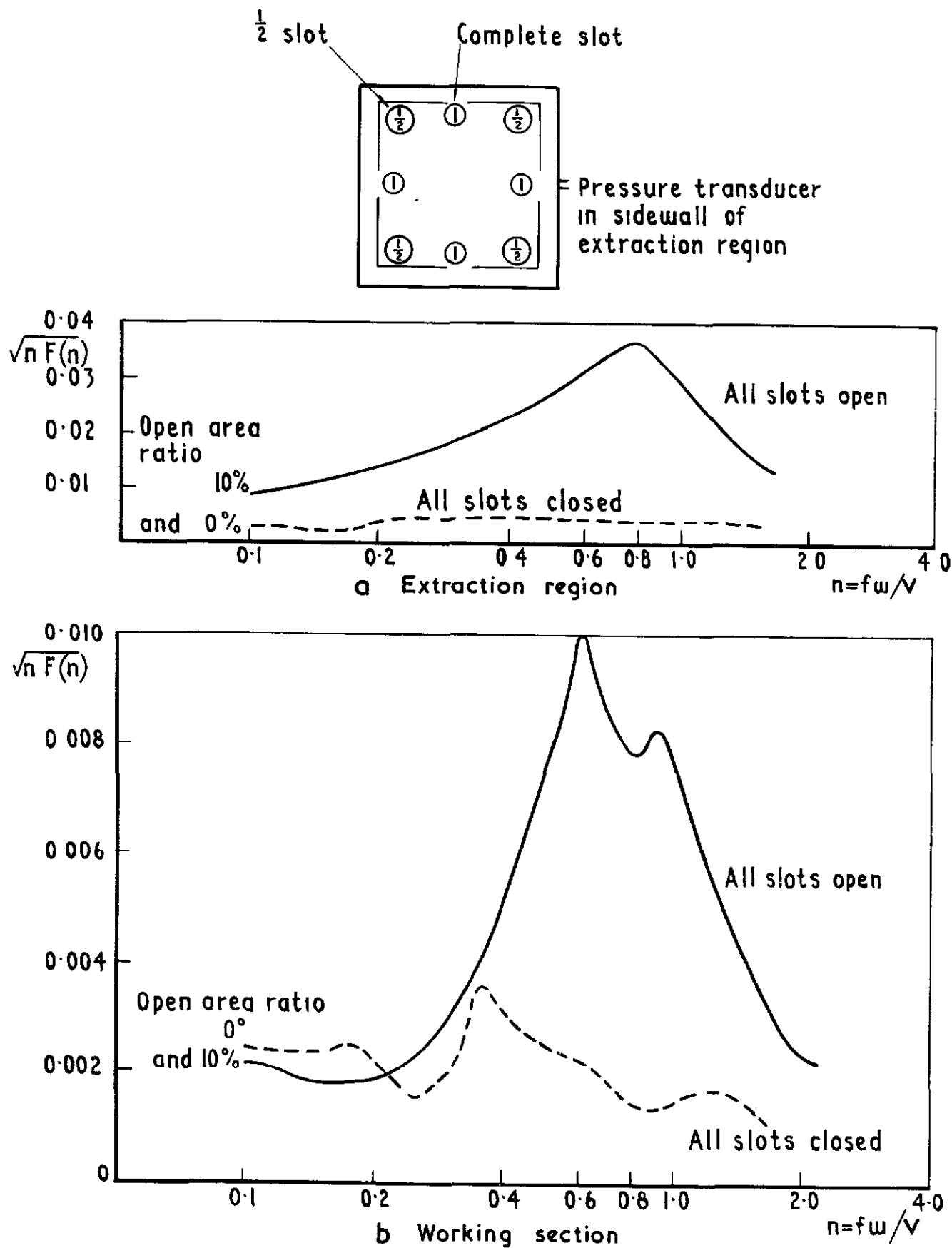
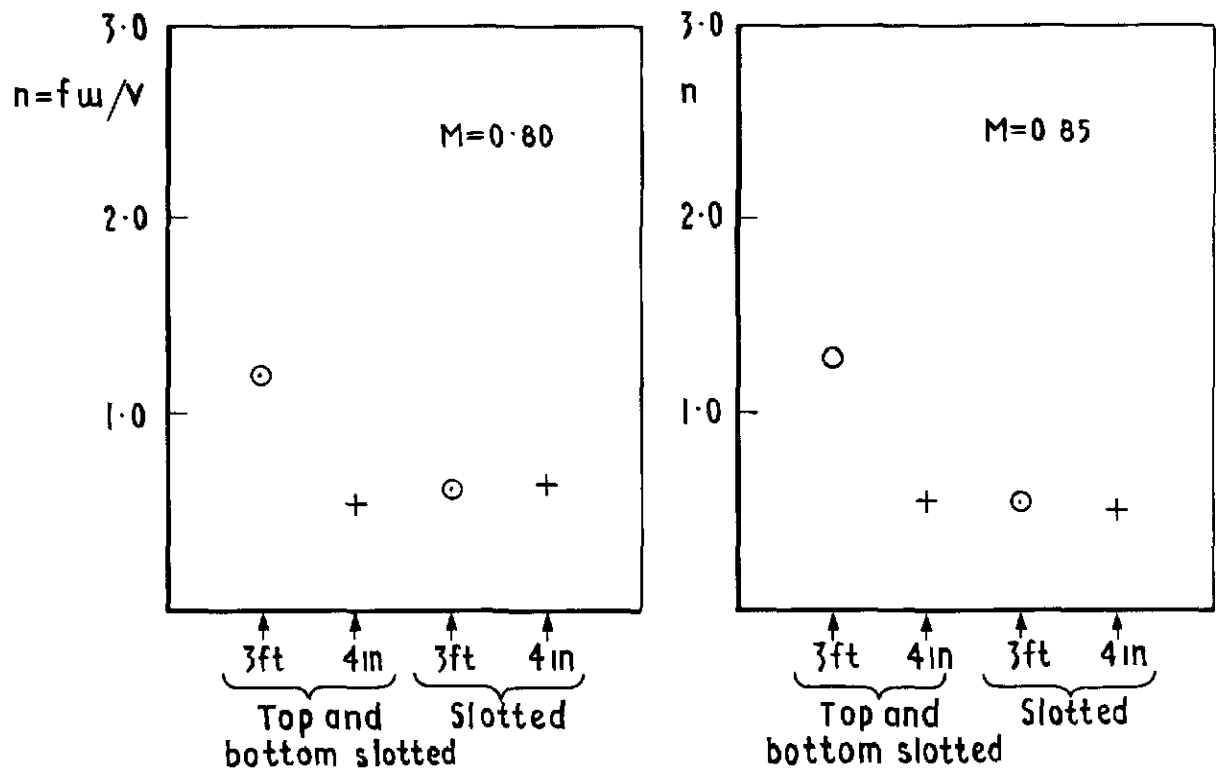
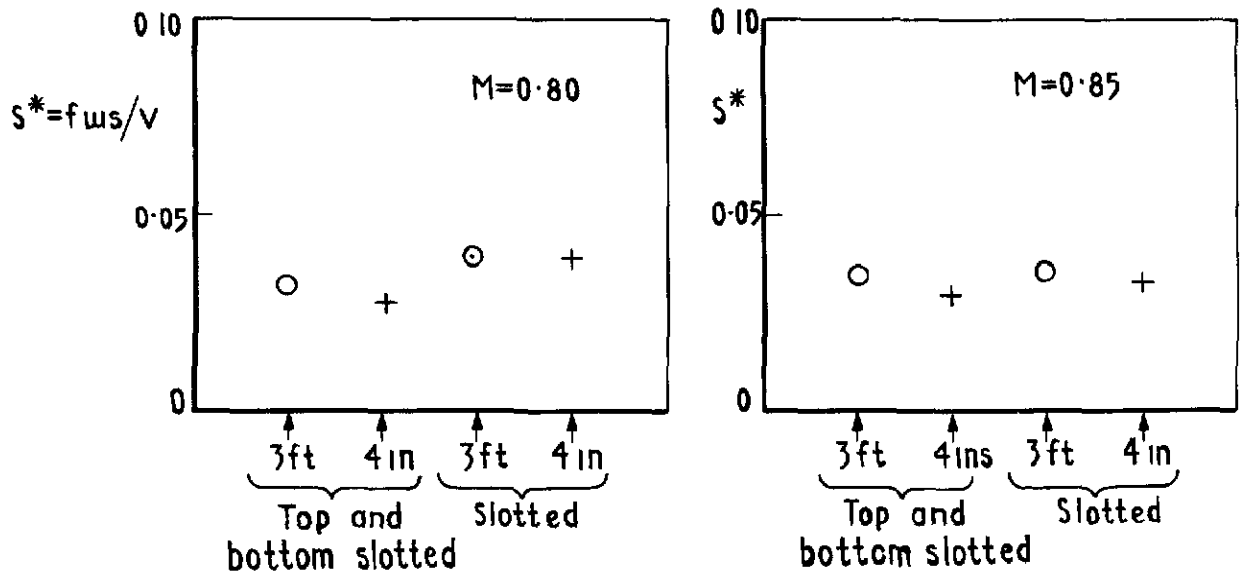


Fig 24a & b 4in x 4in tunnel - origin of pressure fluctuations in slotted section  $M = 0.80$



a n based on tunnel width w



b S\* based on slot width w<sub>s</sub>

Fig 25a & b Frequency of peak excitation in slotted working sections

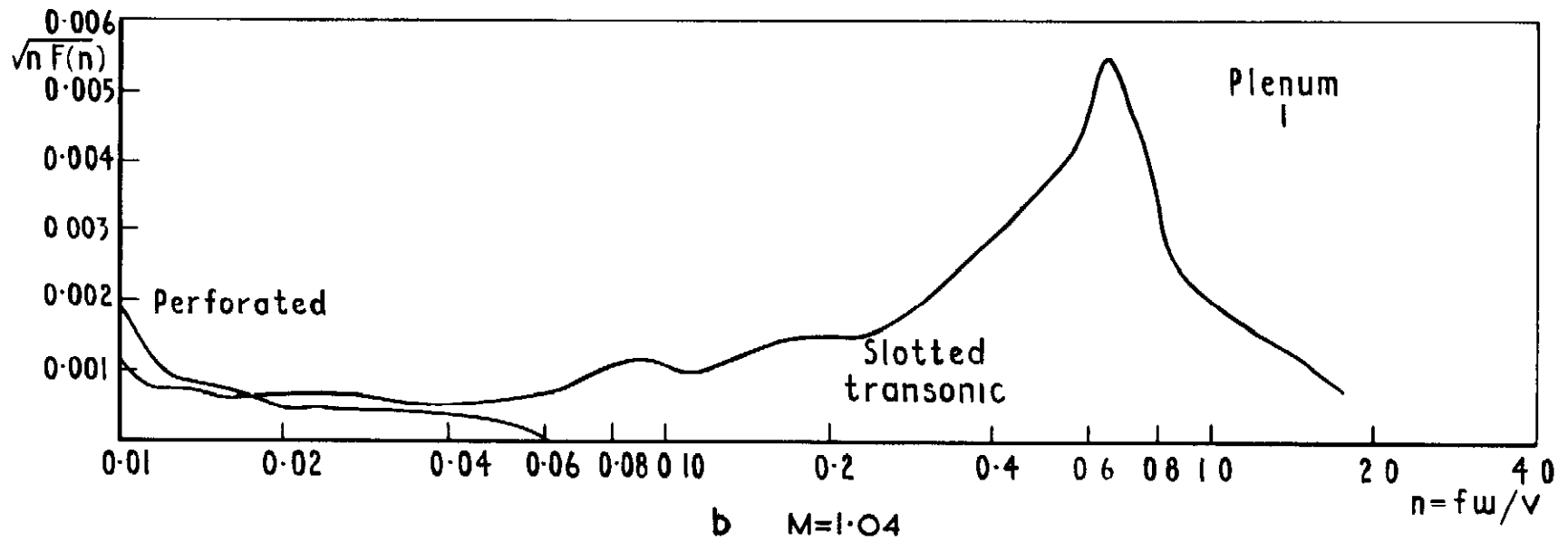
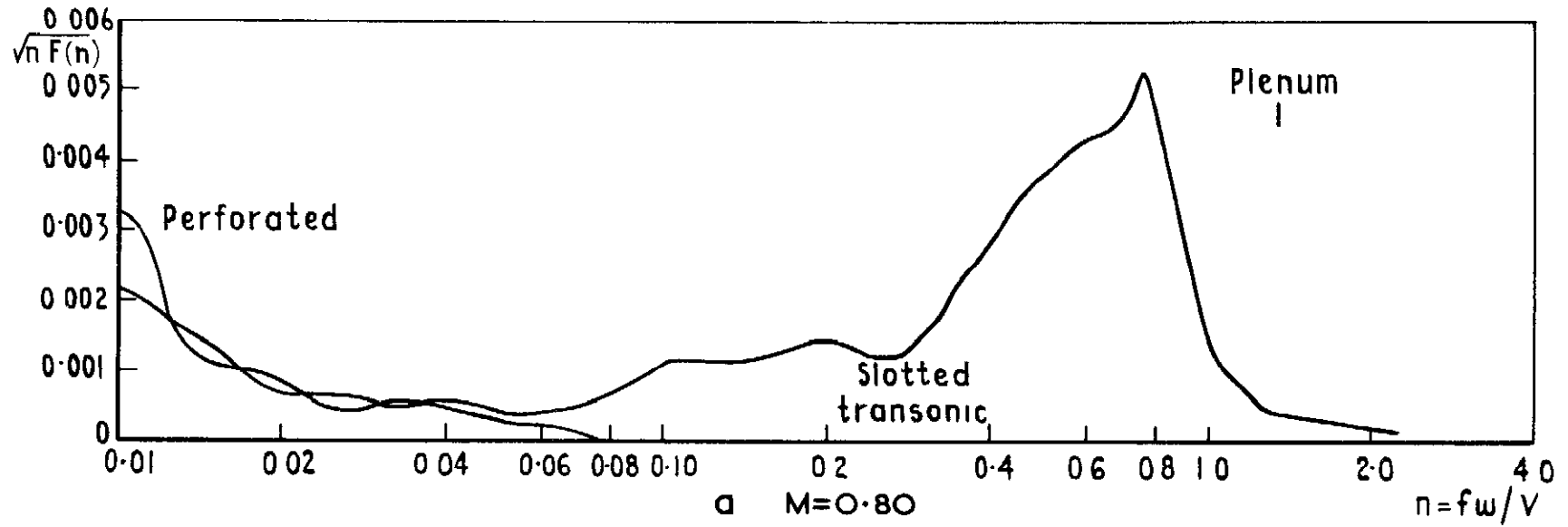


Fig.26 4in x 4in tunnel - pressure fluctuations in plenum chamber

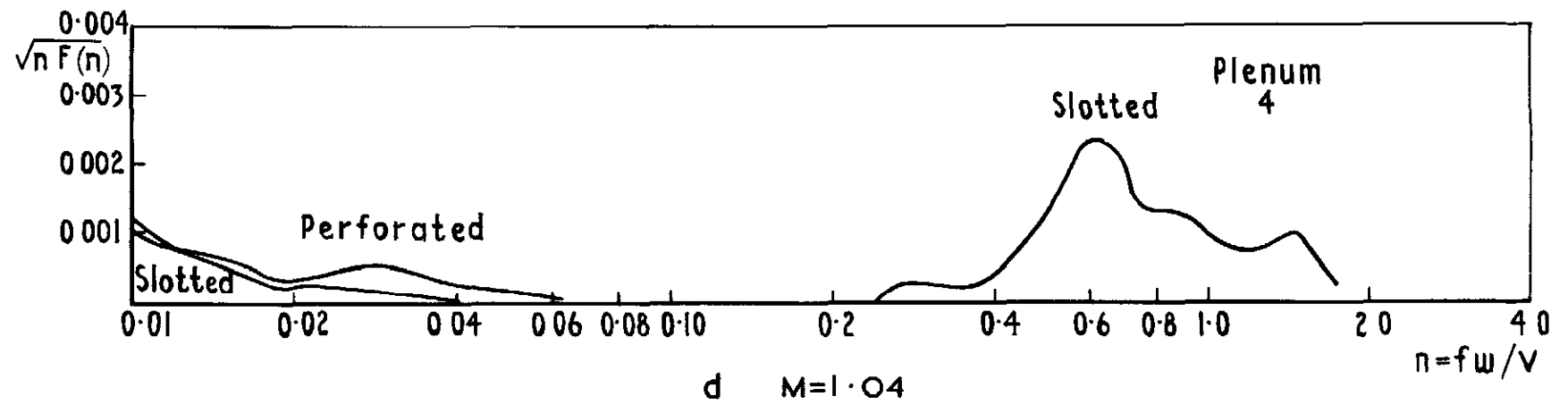
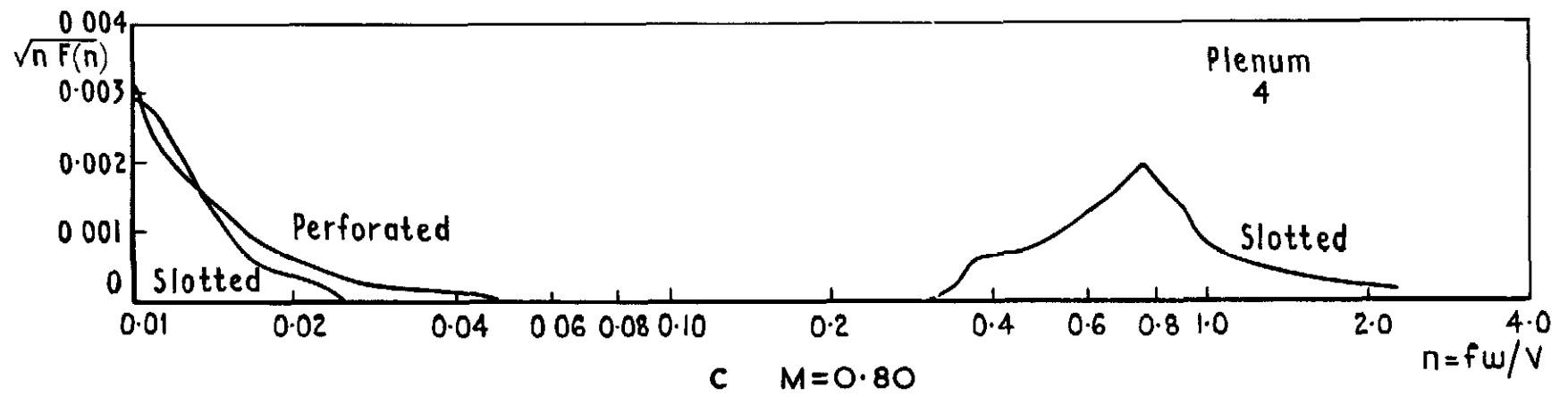


Fig.26 contd 4in x 4in tunnel - pressure fluctuations in plenum chamber

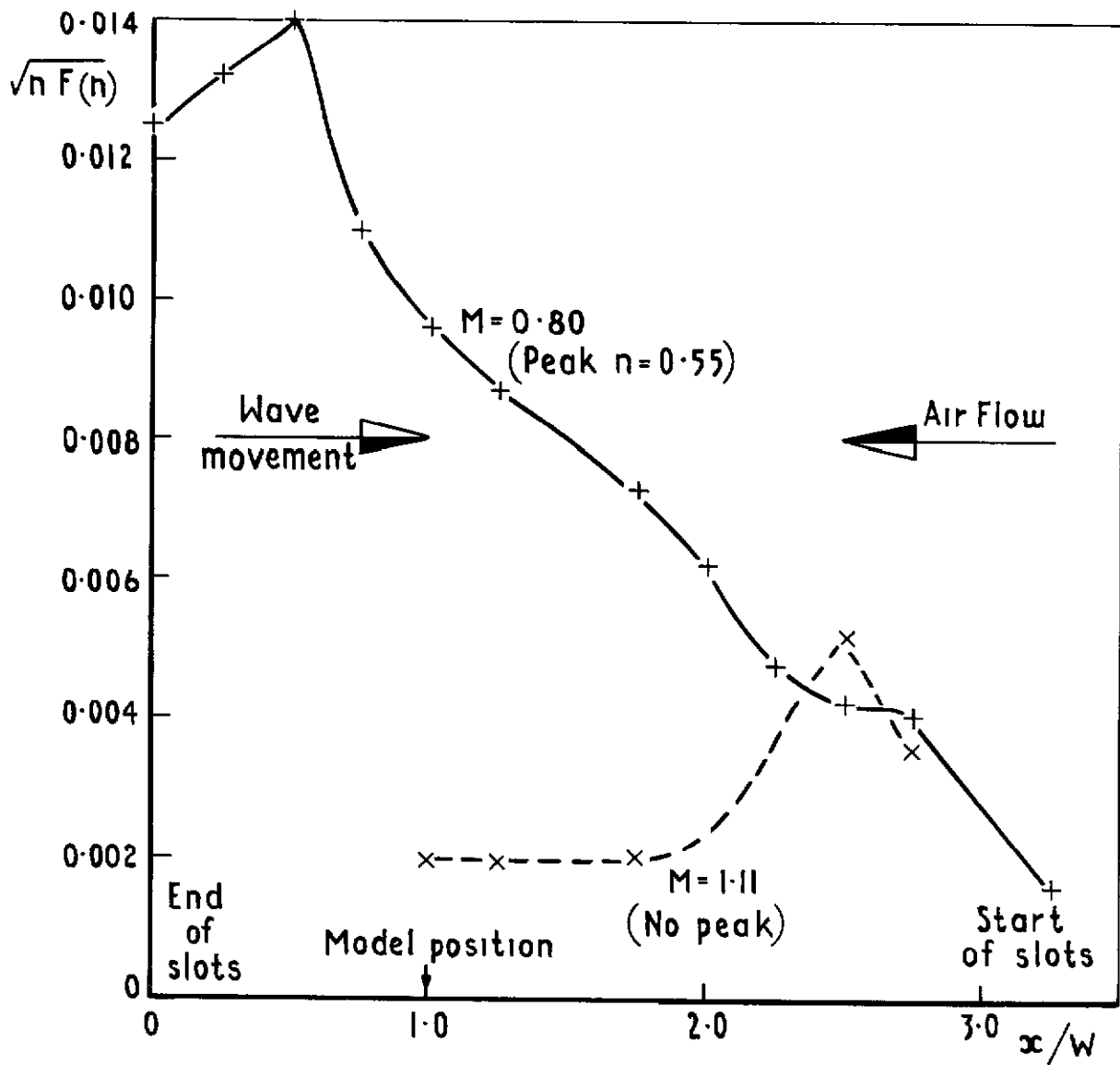


Fig 27 4in x 4in tunnel—attenuation of working section pressure fluctuations



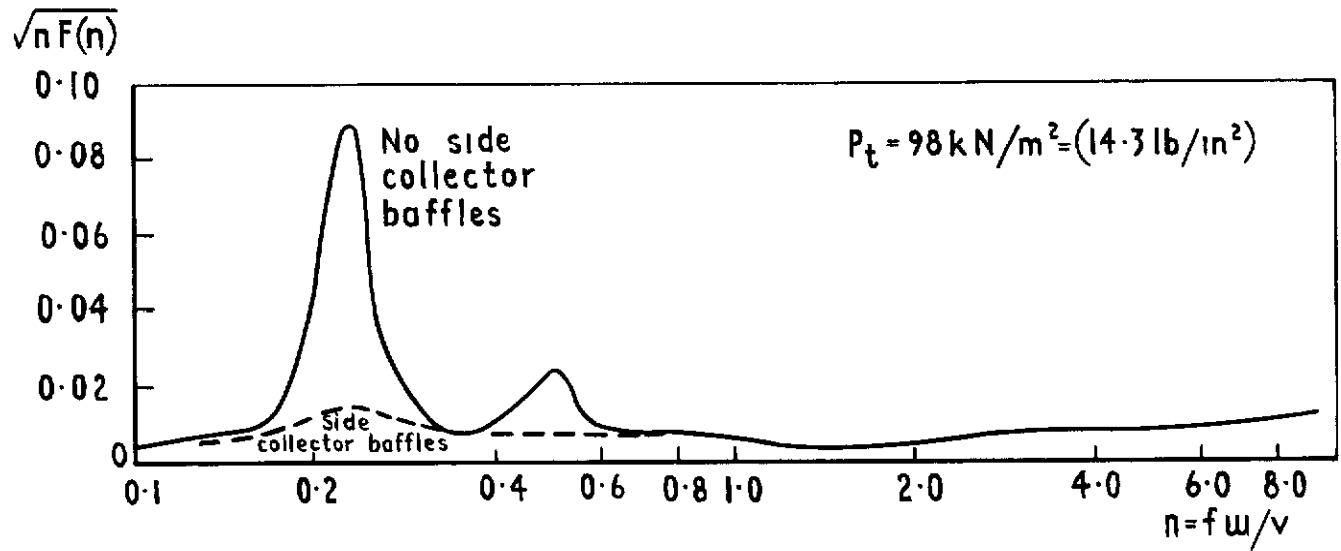
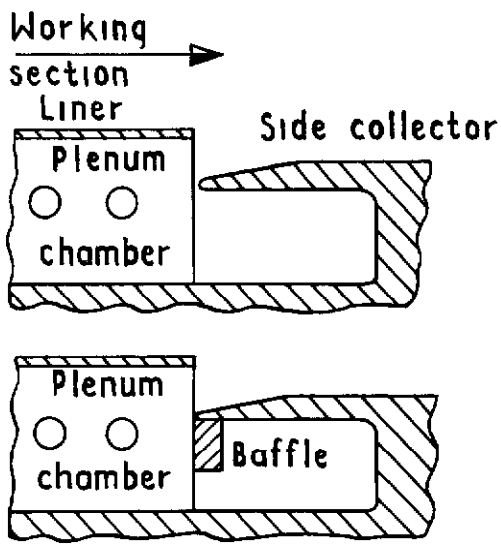


Fig 28 3ftx3ft perforated tunnel-effect of side collector baffles on edge-tones  $M=0.60$

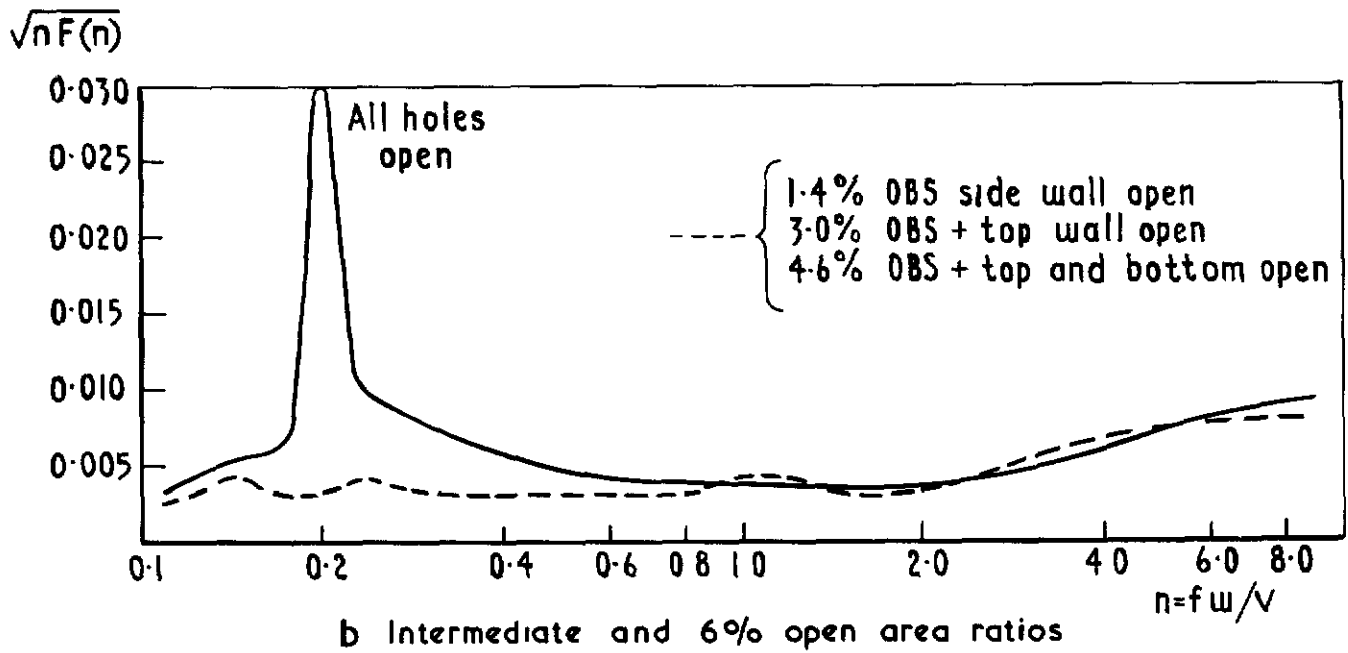
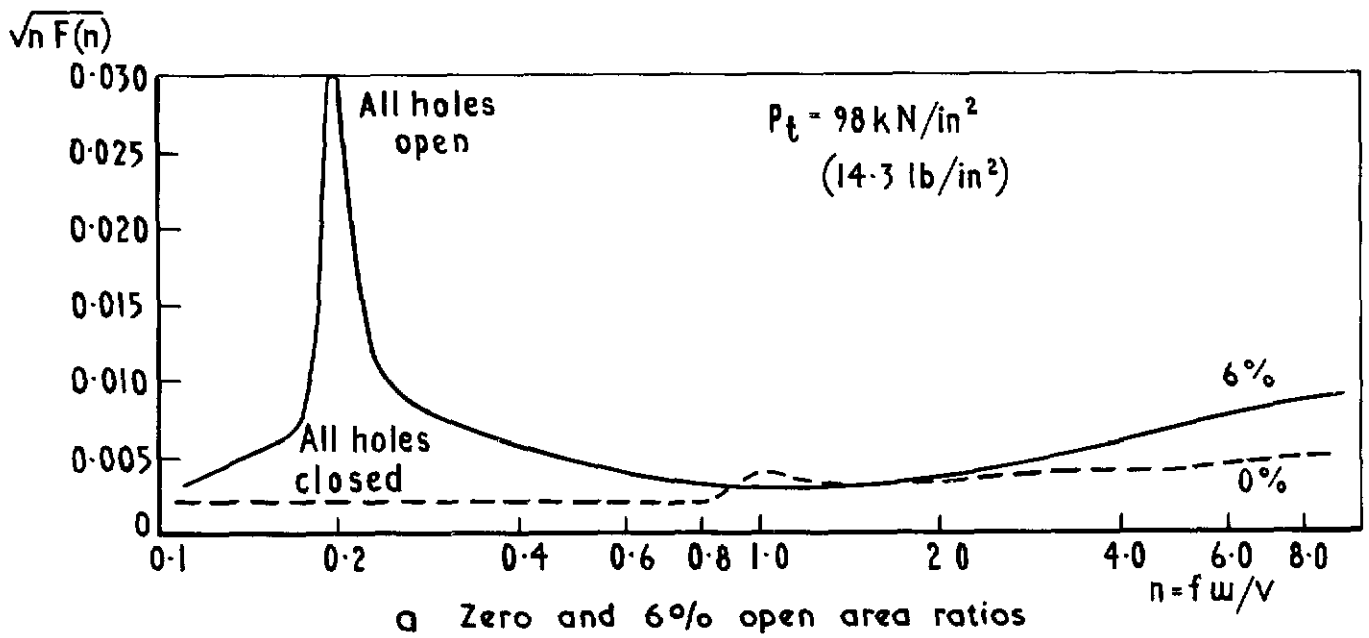


Fig 29a&b 3ft x 3ft perforated tunnel - effect of sealing holes on edge-tones  $M = 0.60$

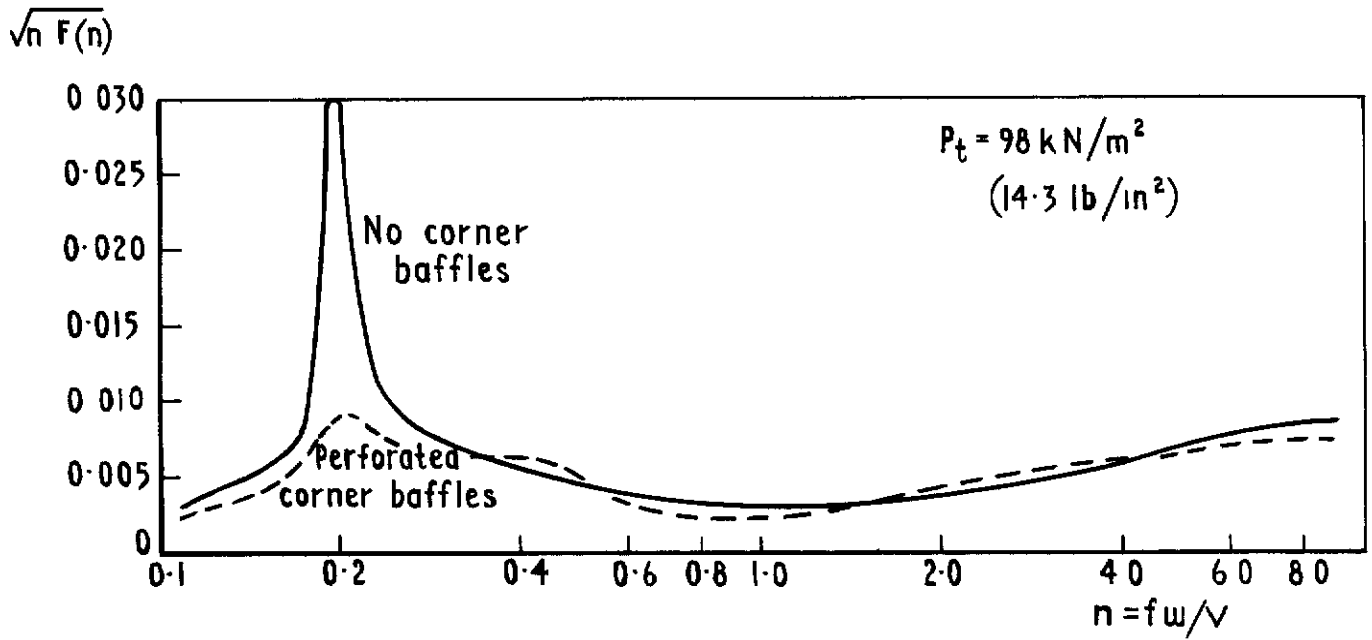


Fig.30 3ft x 3ft perforated tunnel-effect of plenum chamber corner baffles on edge-tones  $M=0.60$

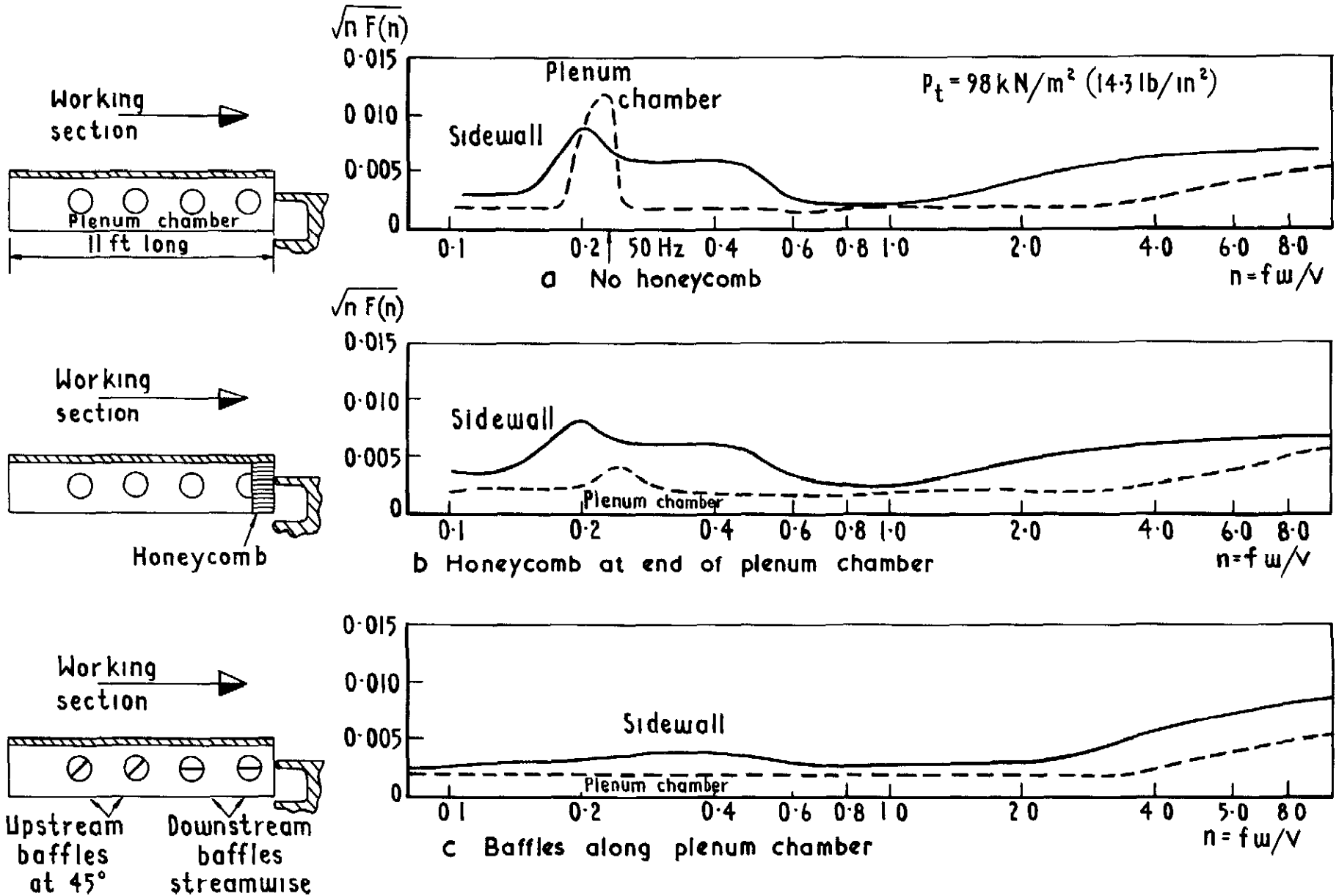


Fig 31a-c 3ftx3ft perforated tunnel-effect of acoustic attenuators in plenum chamber  $M=0.60$

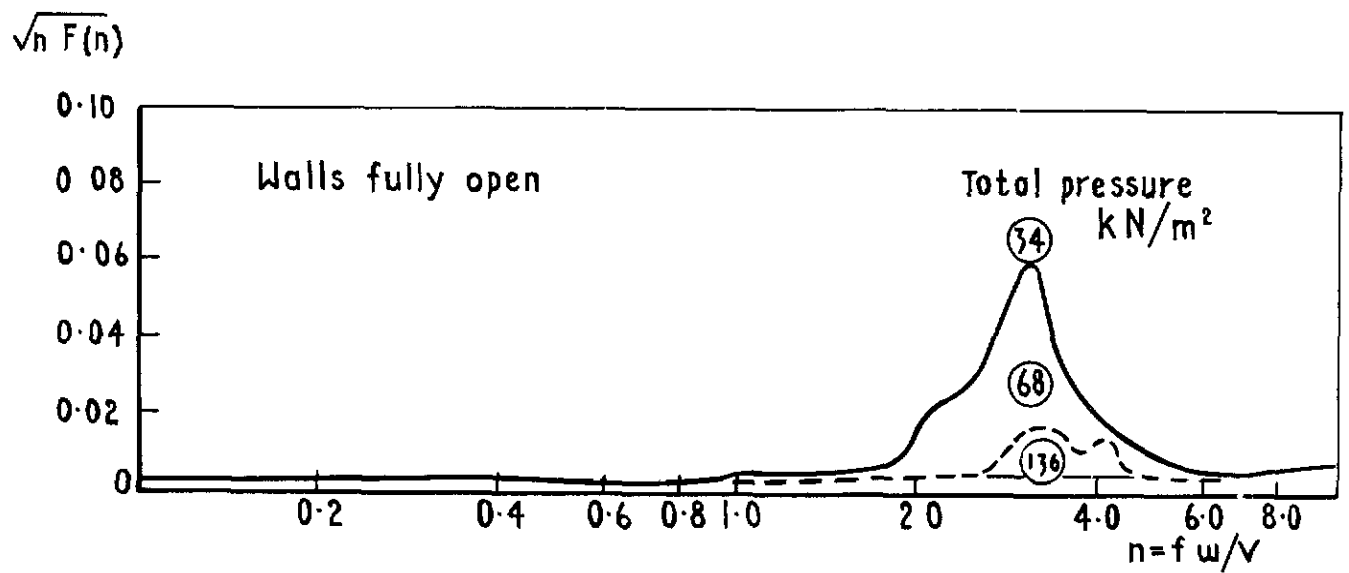
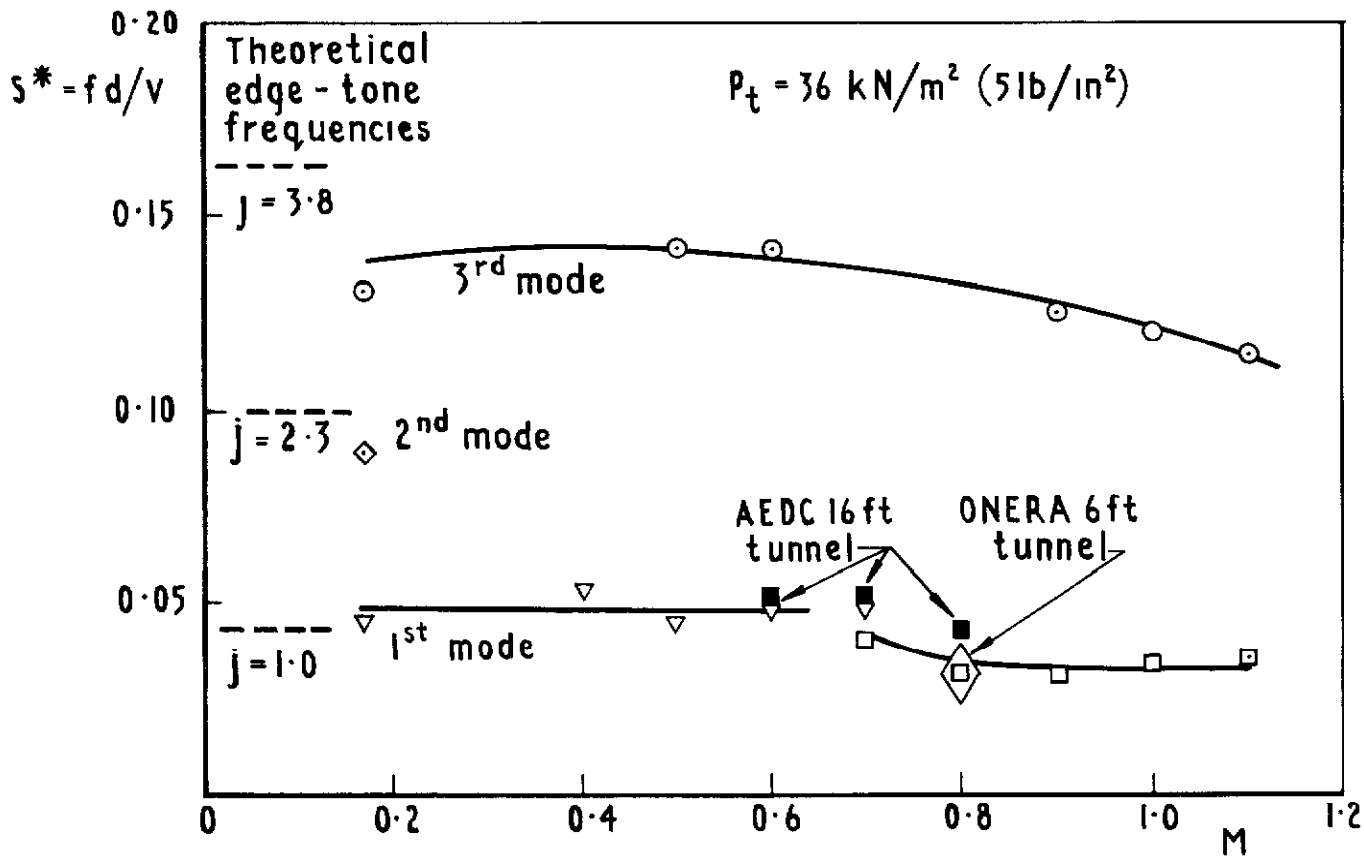
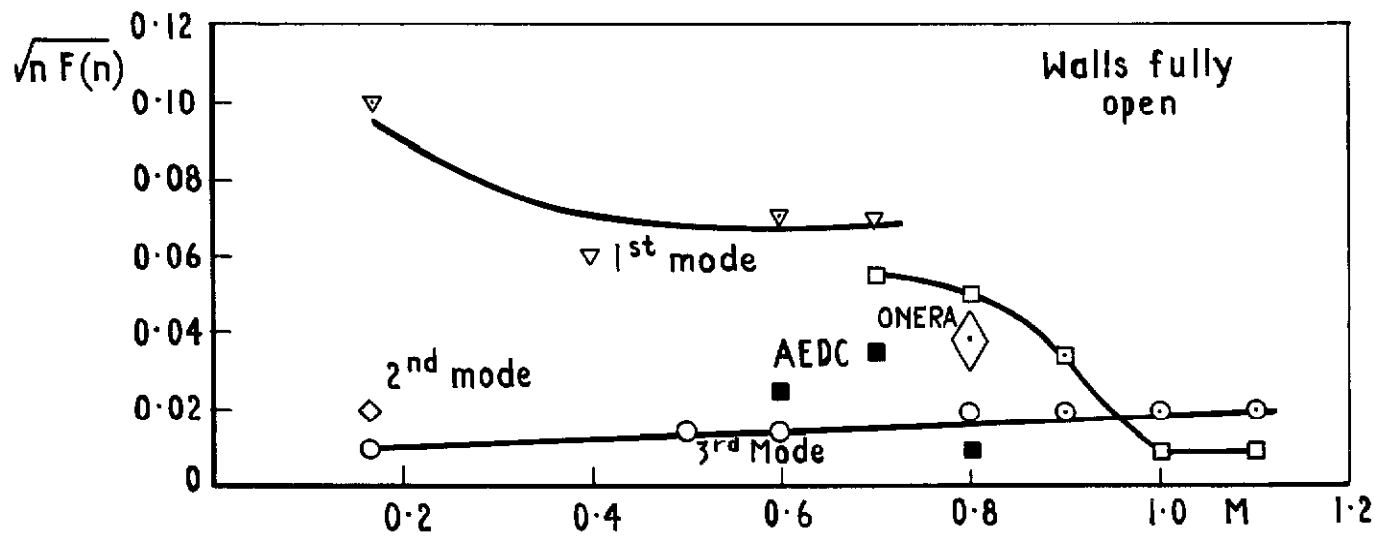


Fig 32 3ftx3ft perforated tunnel - effect of total pressure on pressure fluctuations -  $M=0.80$

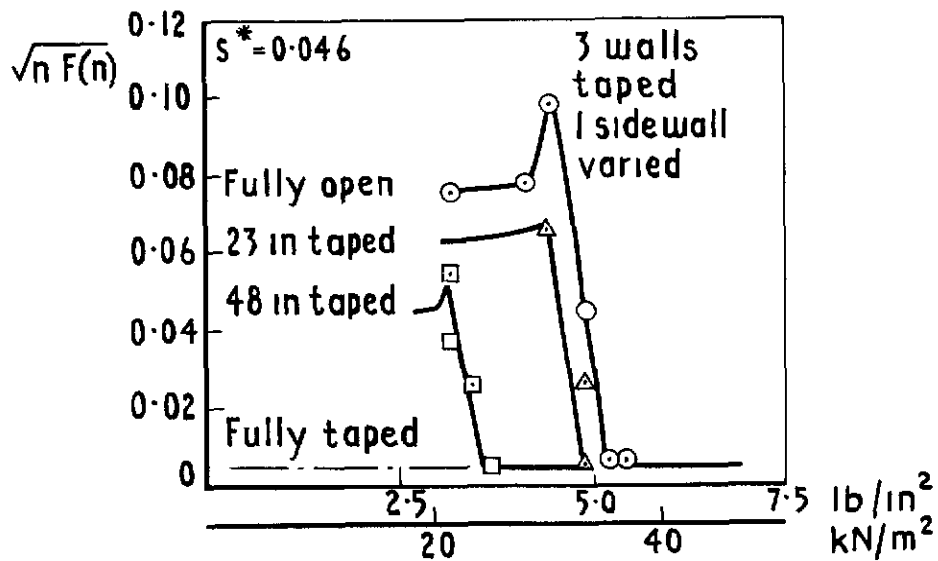


a Variation of Strouhal number with Mach number

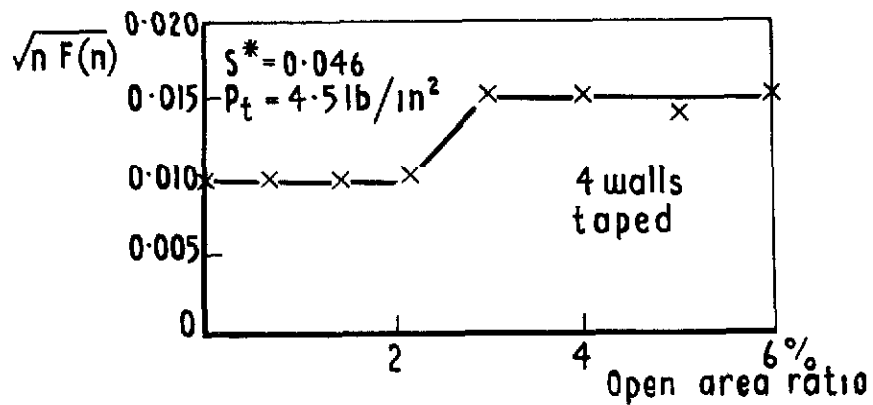


b Variation of pressure fluctuations with Mach number for different modes

Fig.33a & b 3ft x 3ft perforated tunnel-edge-tones generated at low unit Reynolds numbers

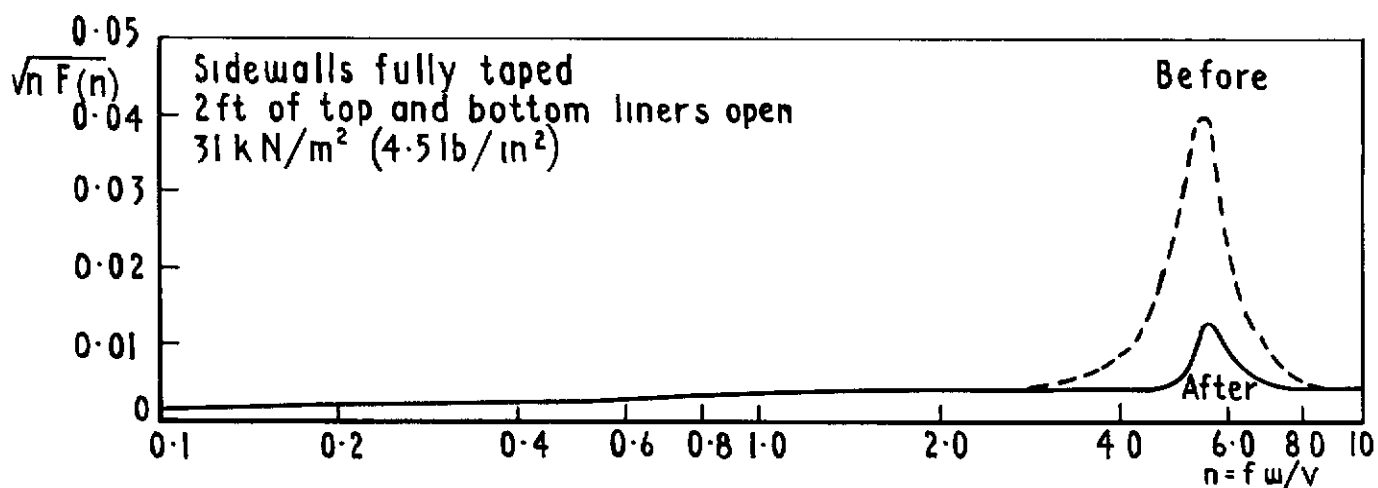


a Variation of pressure fluctuations with total pressure (sidewall partially taped)

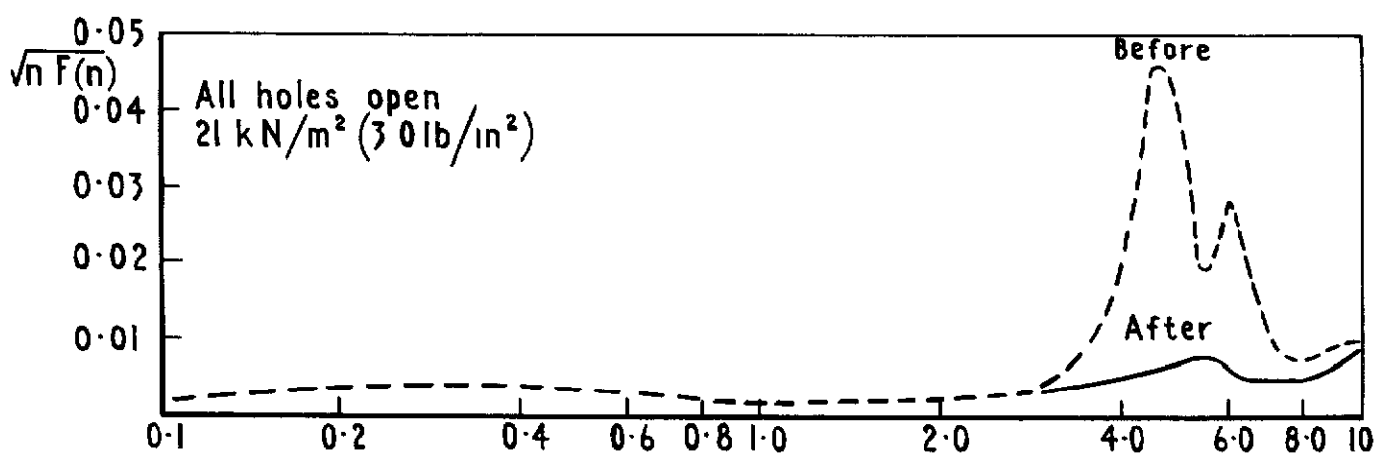


b Variation of pressure fluctuations with open area ratio of variable porosity sidewall plate

Fig 34a&b 3ftx3ft perforated tunnel - reduction of edge-tones  $M=0.60$



a Rear 2ft of top and bottom liner before and after treatment



b All four liners before and after treatment

Fig 35a&b 3ftx3ft perforated tunnel - elimination of edge-tones  $M=0.60$



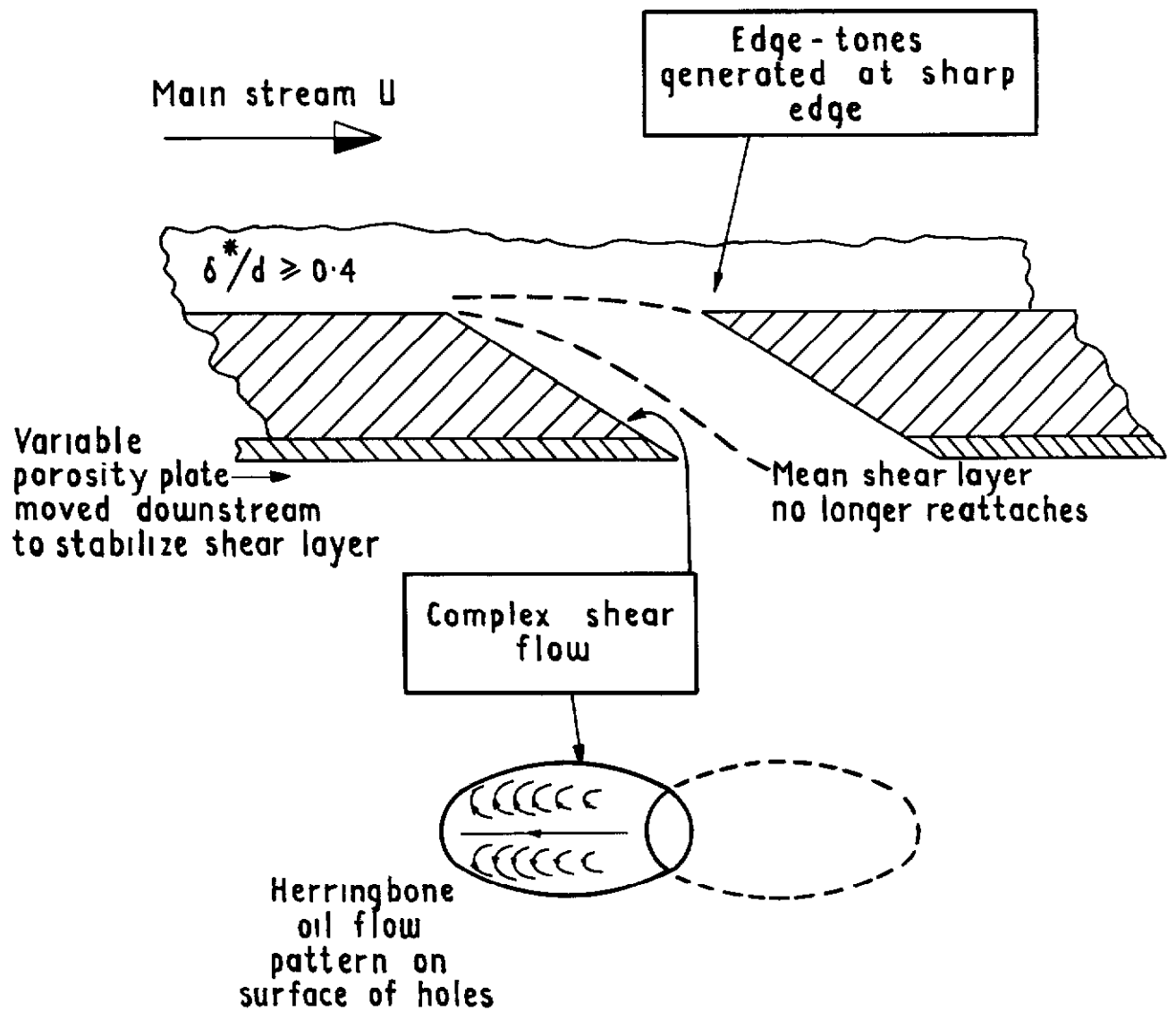


Fig 36 Possible flow model for edge-tone excitation

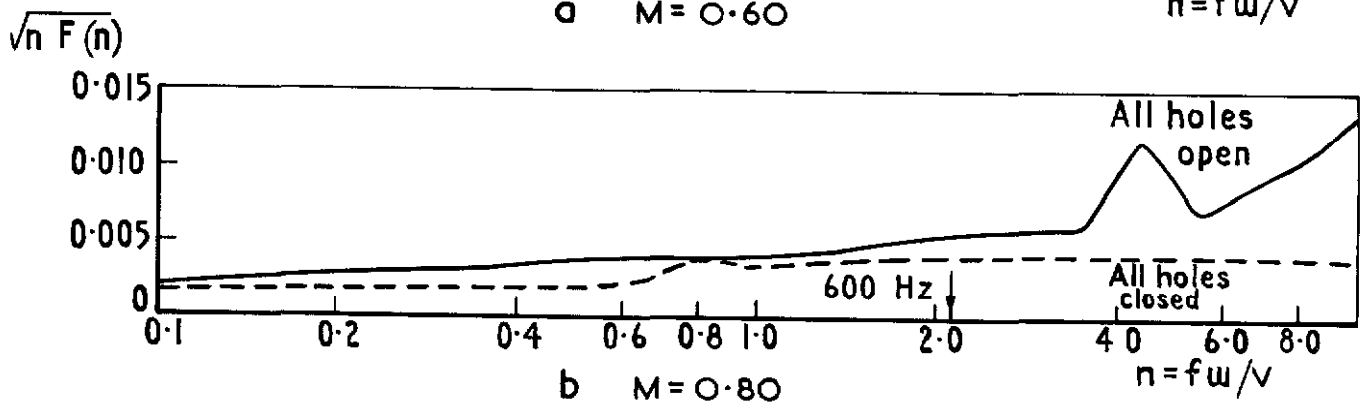
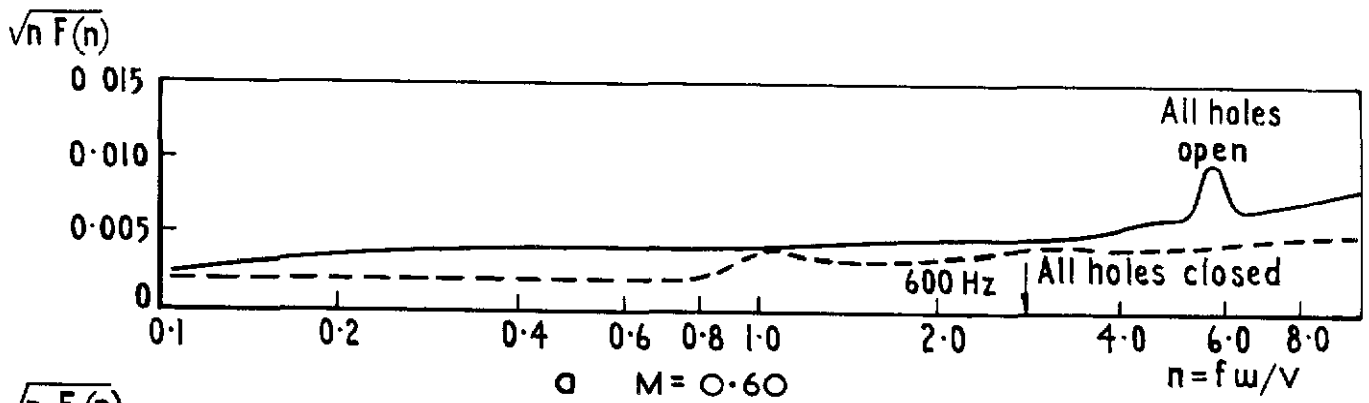


Fig 37a&b 3ft x 3ft tunnel-final comparison of pressure fluctuations measured with perforations open and closed

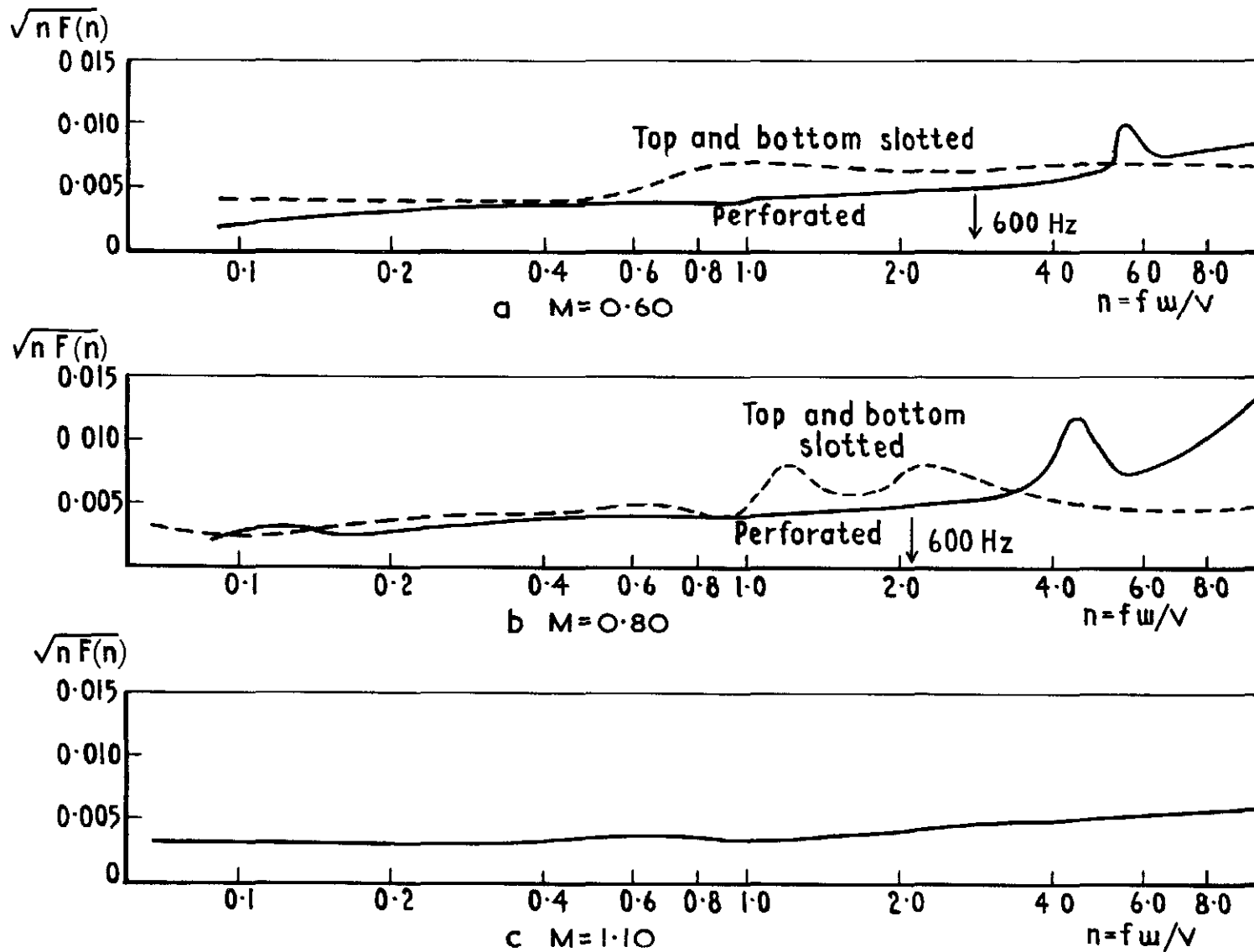


Fig.38a-c 3ftx3ft tunnel-comparison of pressure fluctuations in perforated section and top and bottom slotted section

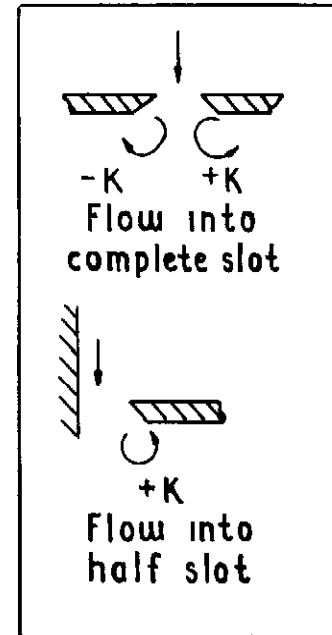
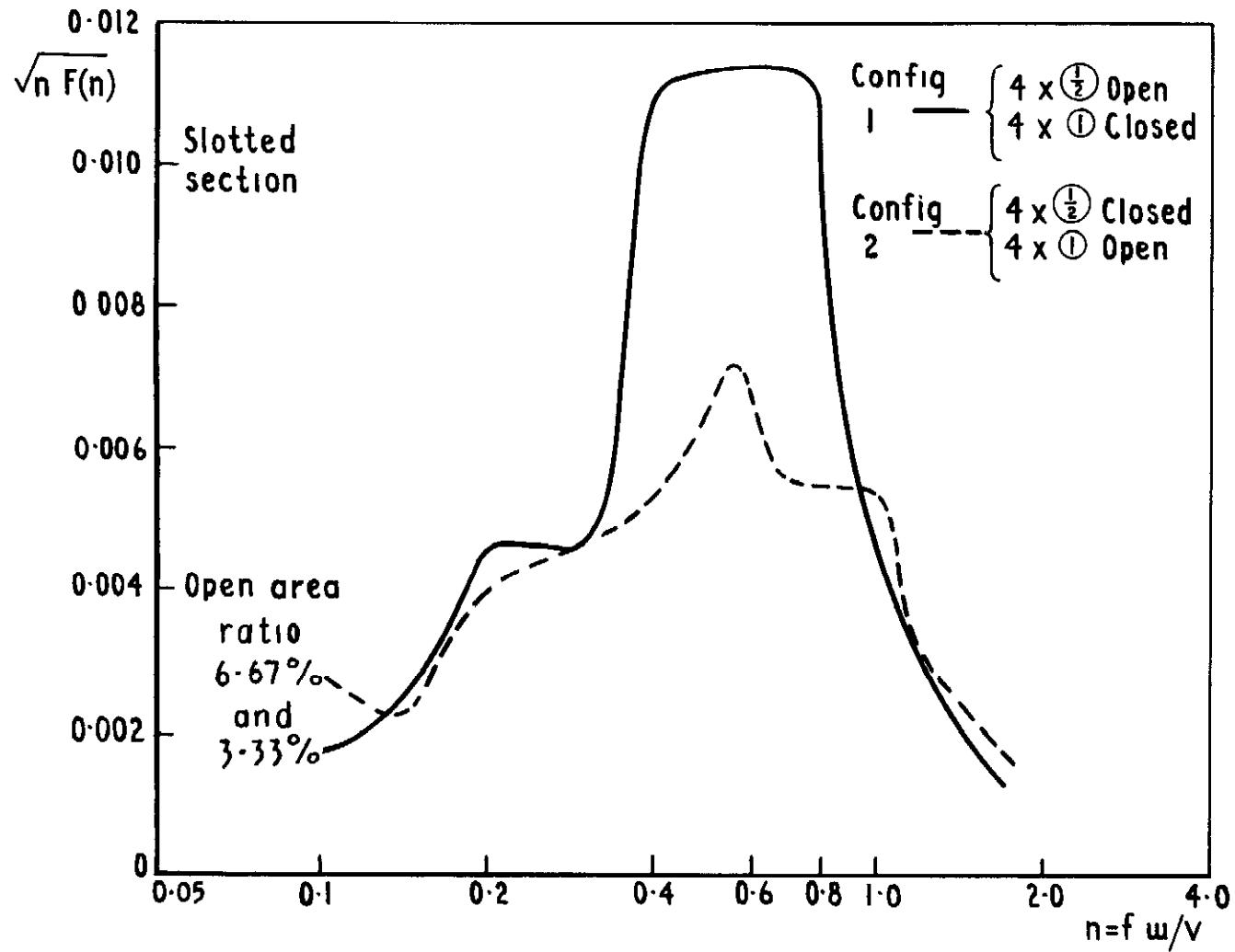


Fig.39 4in x 4in tunnel-adverse effect of half slots  $M=0.80$

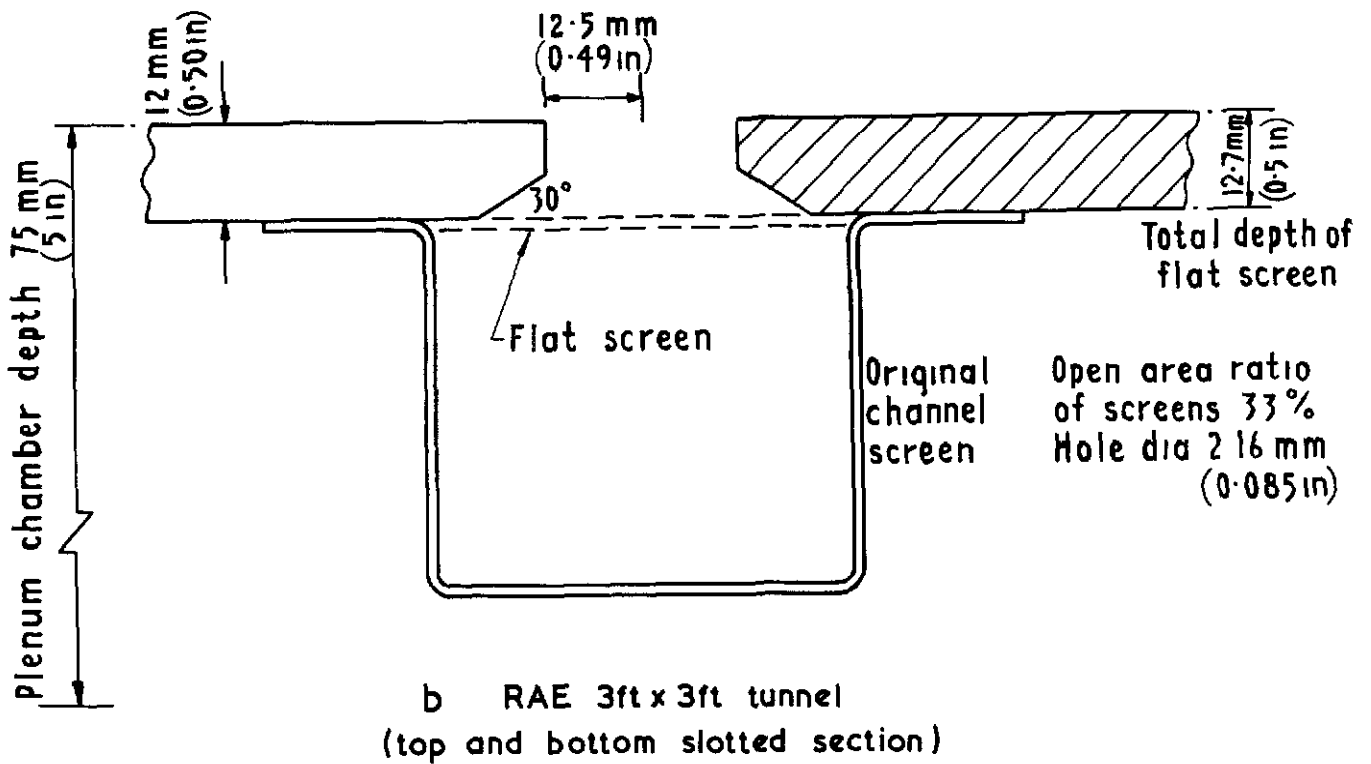
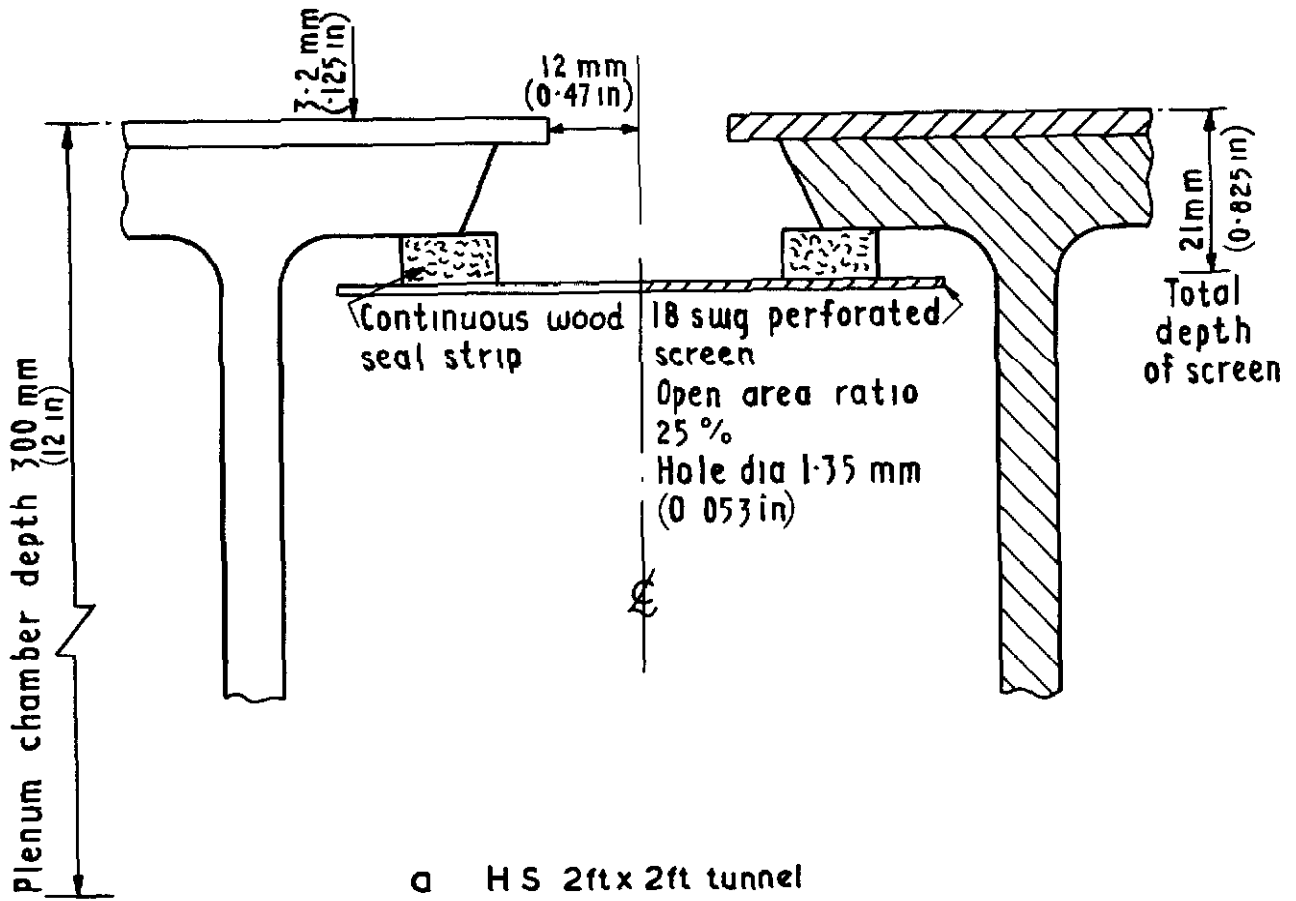


Fig.40a&b Comparison of slots in HS 2ft x 2ft and RAE 3ft x 3ft tunnels

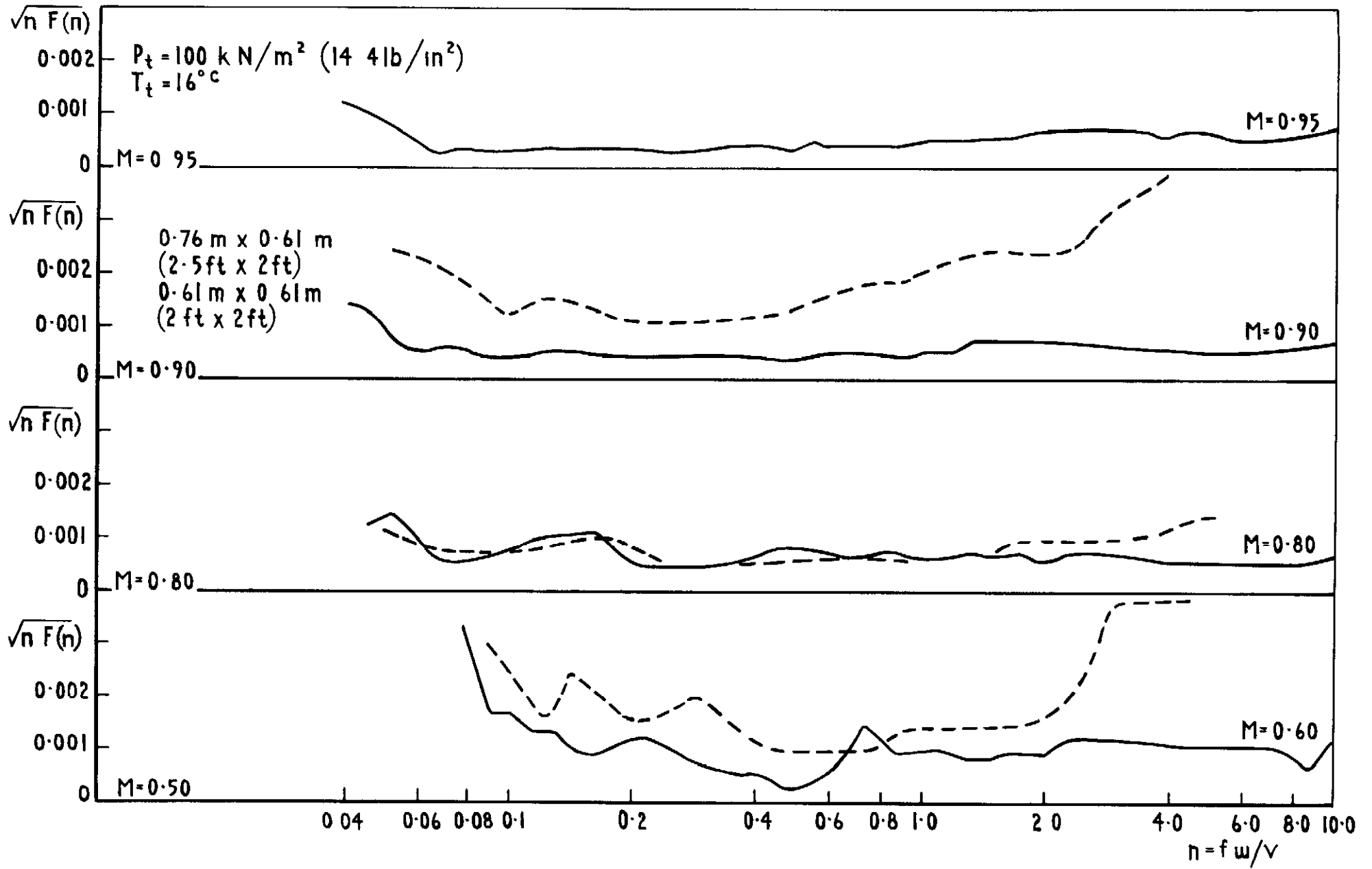


Fig 41 HS 2ft tunnel-working section pressure fluctuations

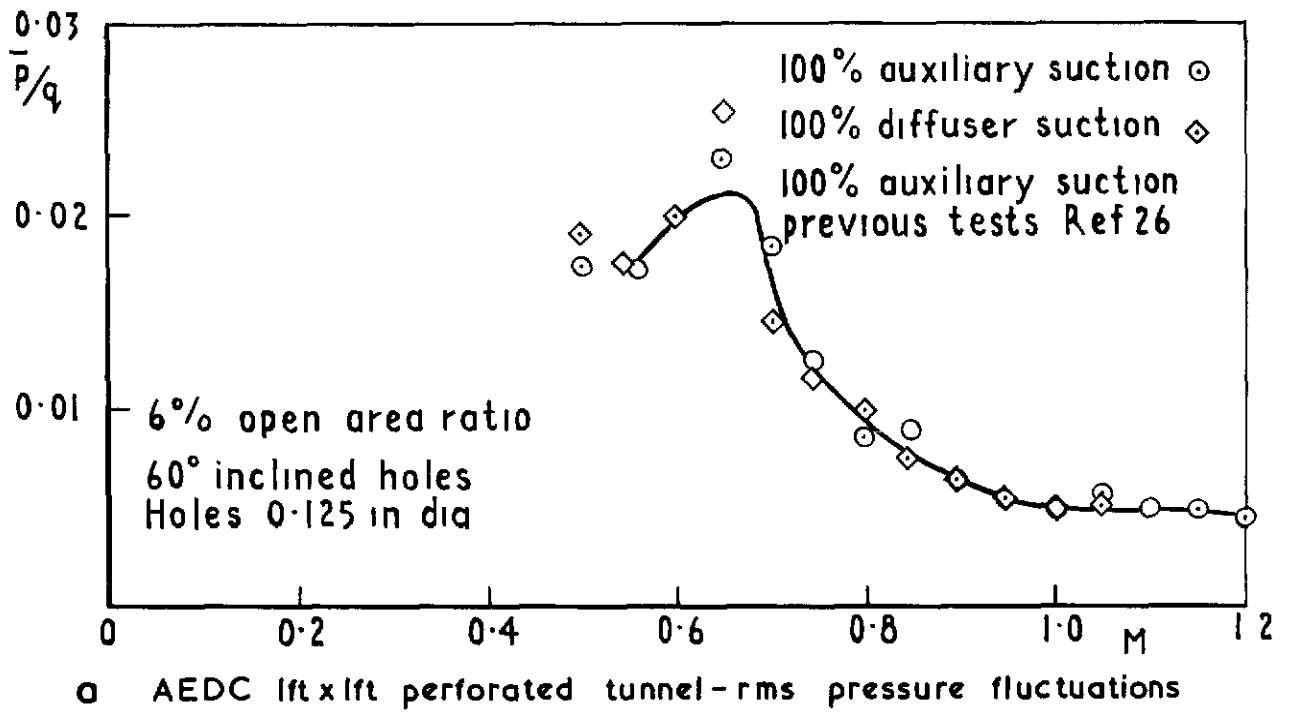


Fig.42 Pressure fluctuations in perforated tunnels with 60° inclined holes

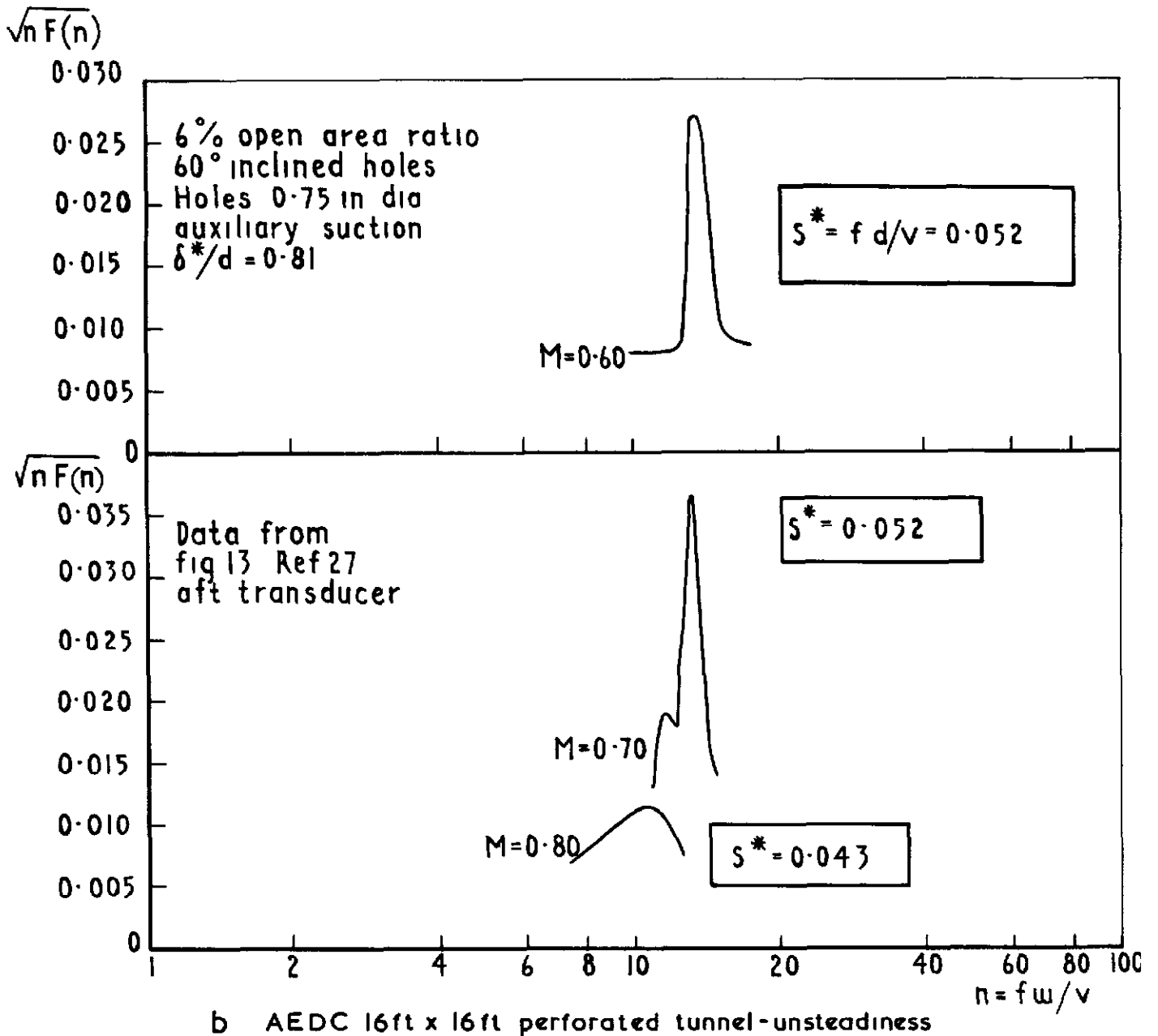


Fig 42contd Pressure fluctuations in perforated tunnels with 60° inclined holes



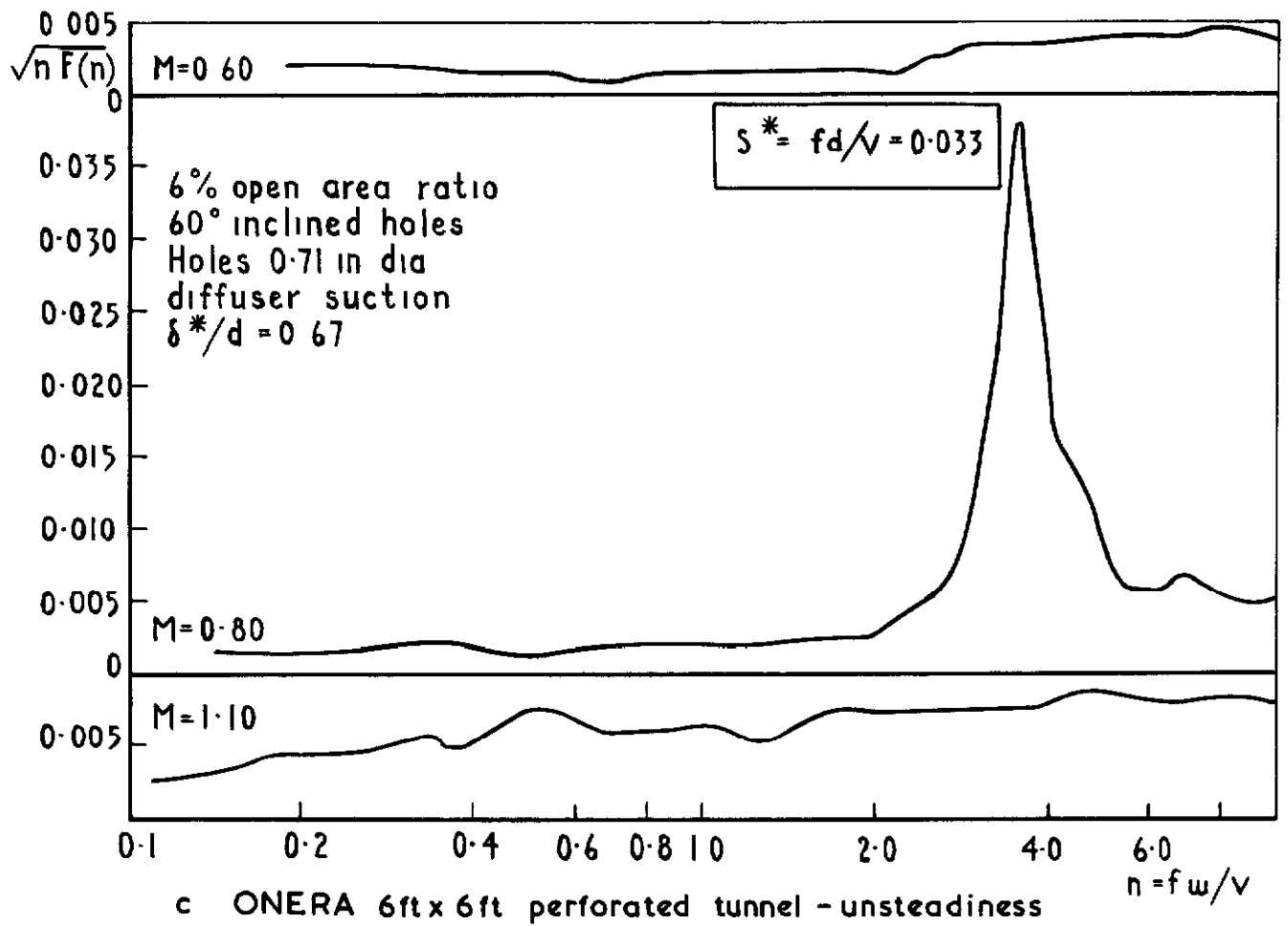


Fig.42 conclud Pressure fluctuations in perforated tunnels with 60° inclined holes

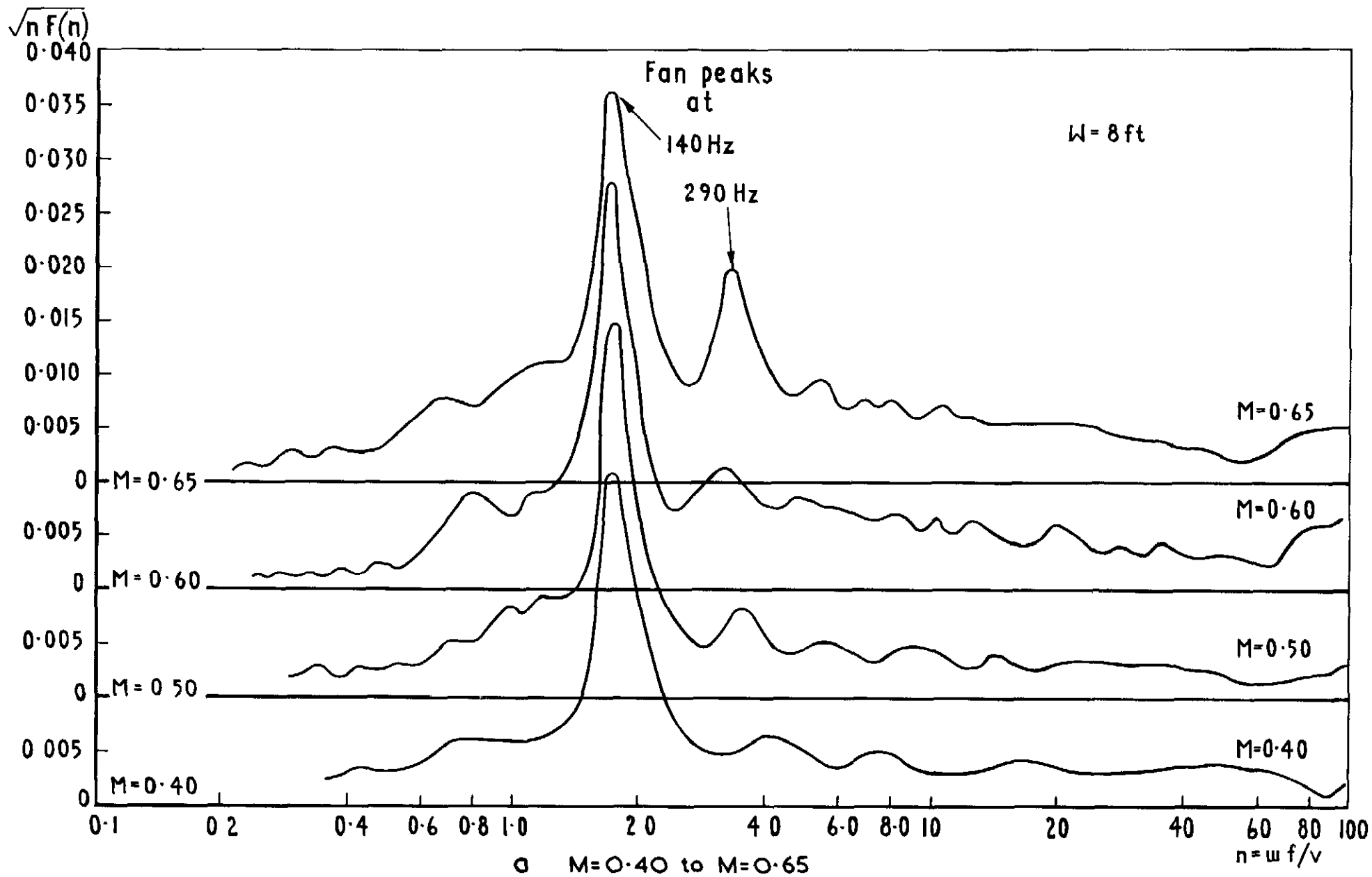


Fig. 43 Unsteadiness in RAE 8ft x 6ft slotted tunnel

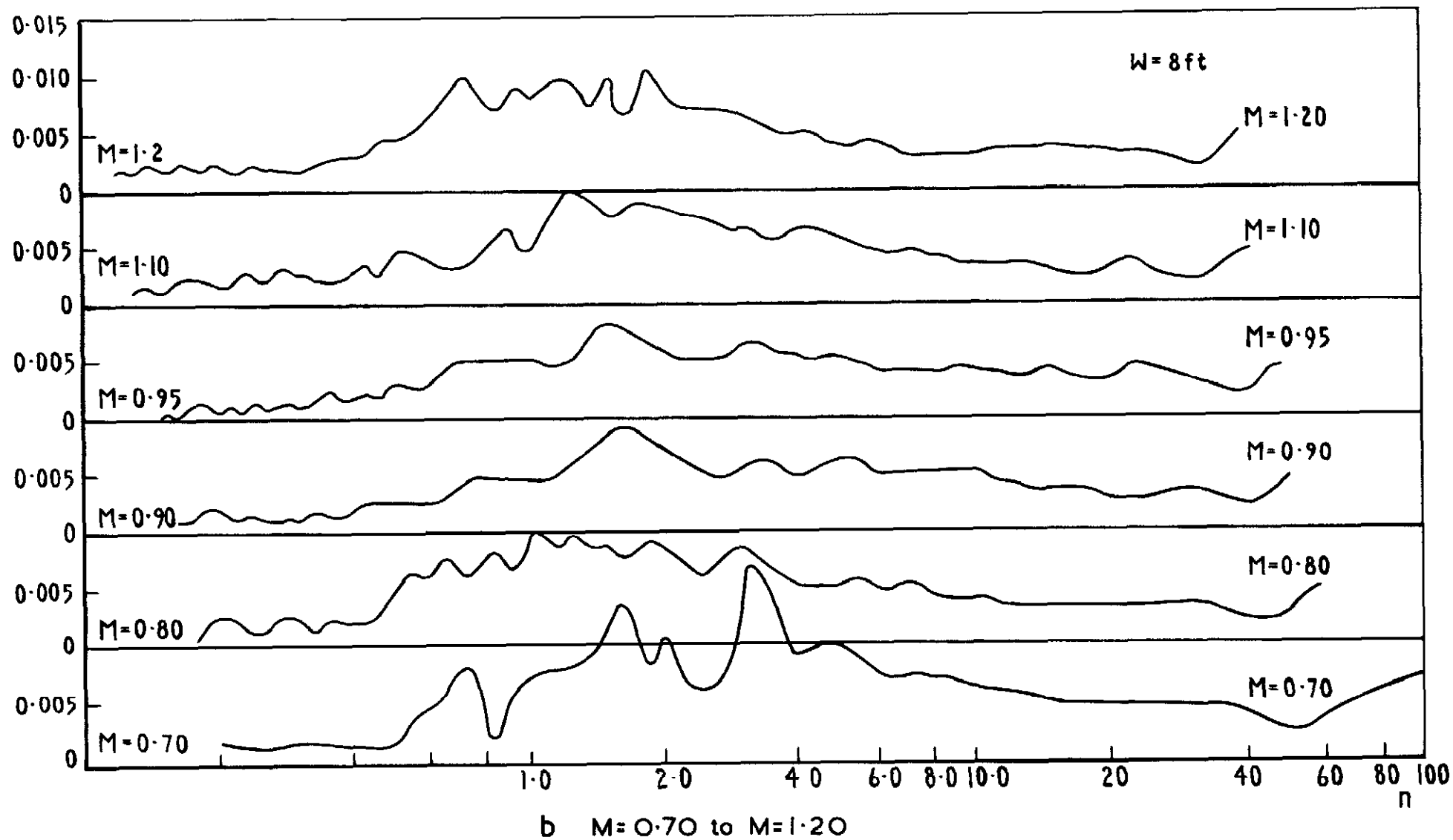


Fig 43 contd Unsteadiness in RAE 8ft x 6ft slotted tunnel

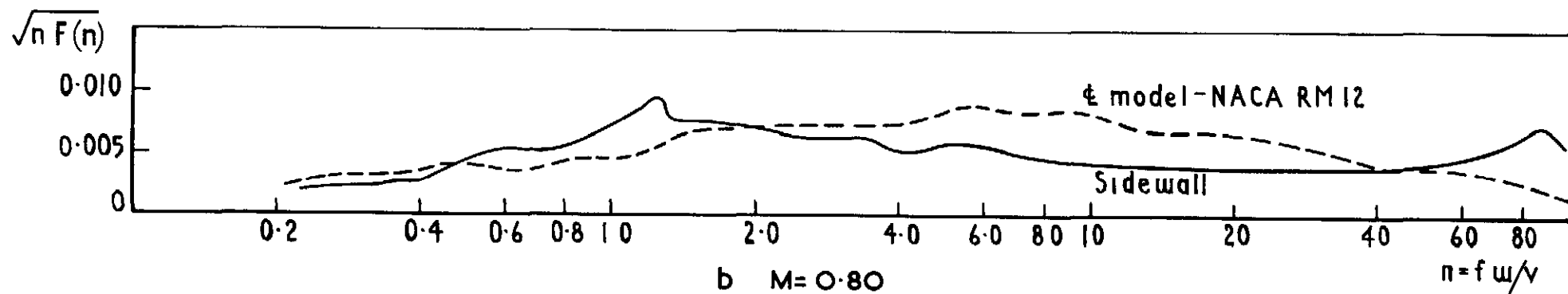
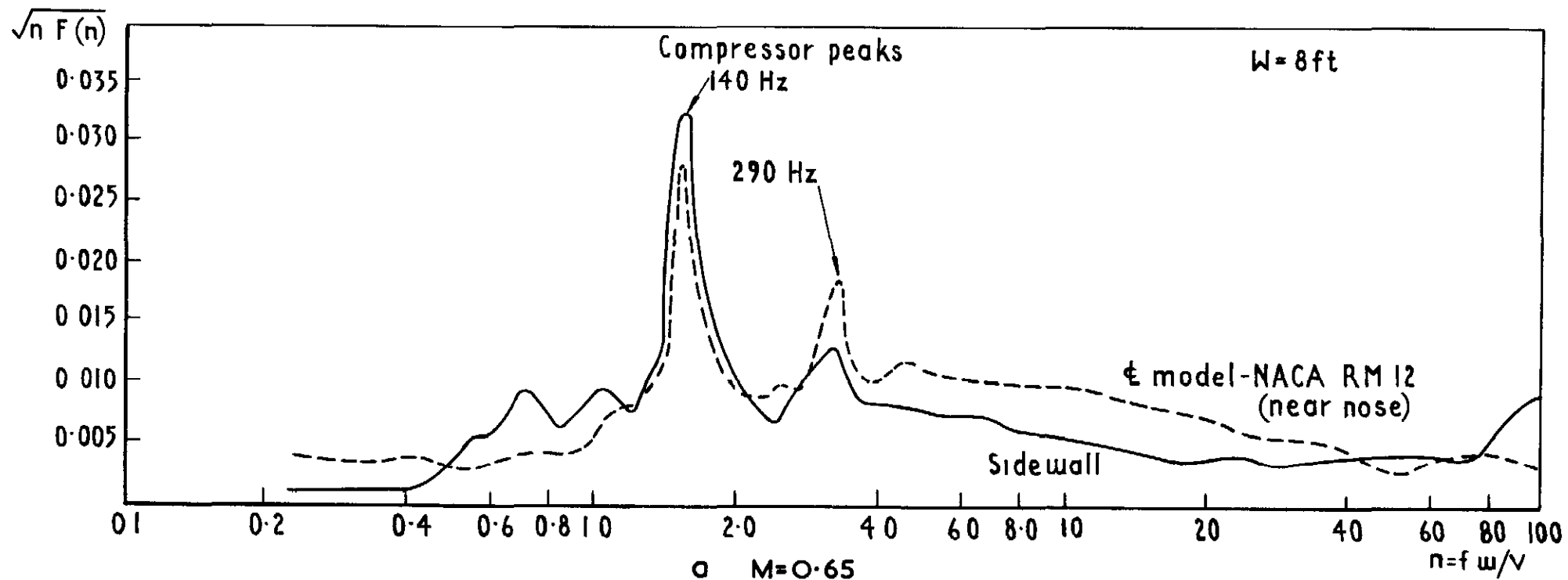


Fig 44a&b RAE 8ftx6ft slotted tunnel-comparison of pressure fluctuations on tunnel sidewall and centre line model

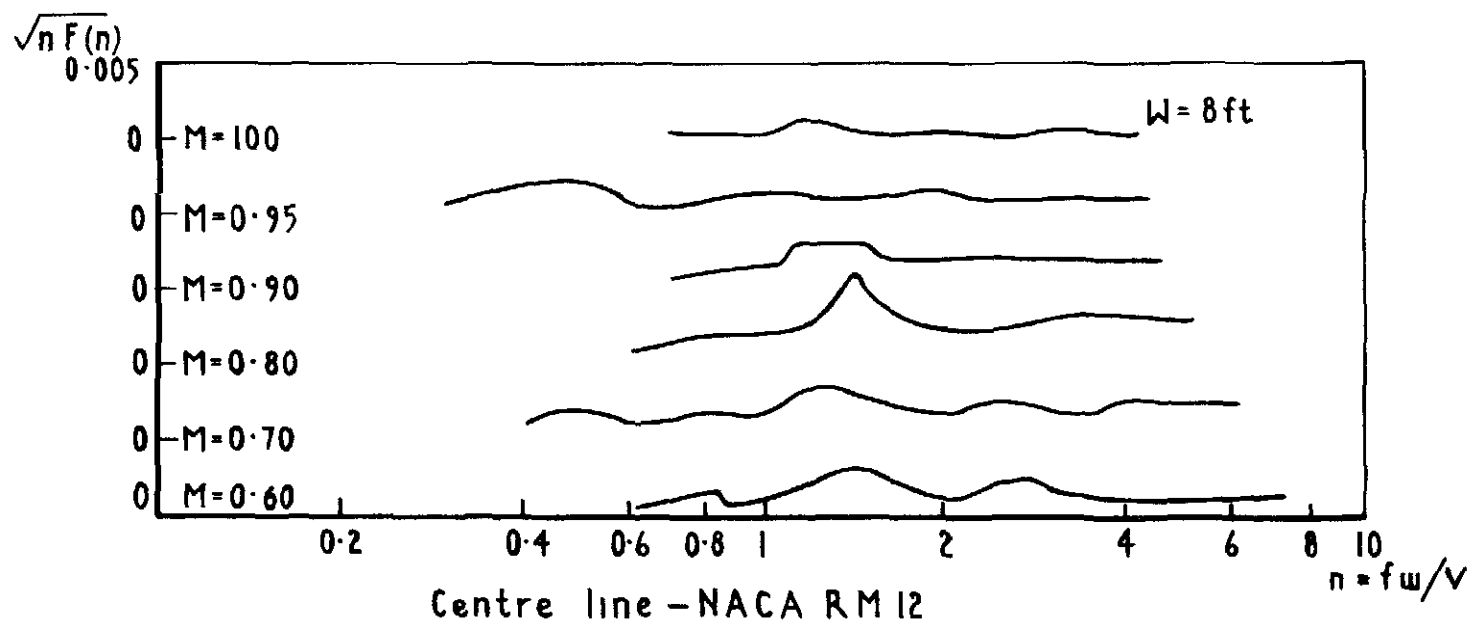


Fig 45 Unsteadiness in ARA 8ft x 9ft perforated tunnel

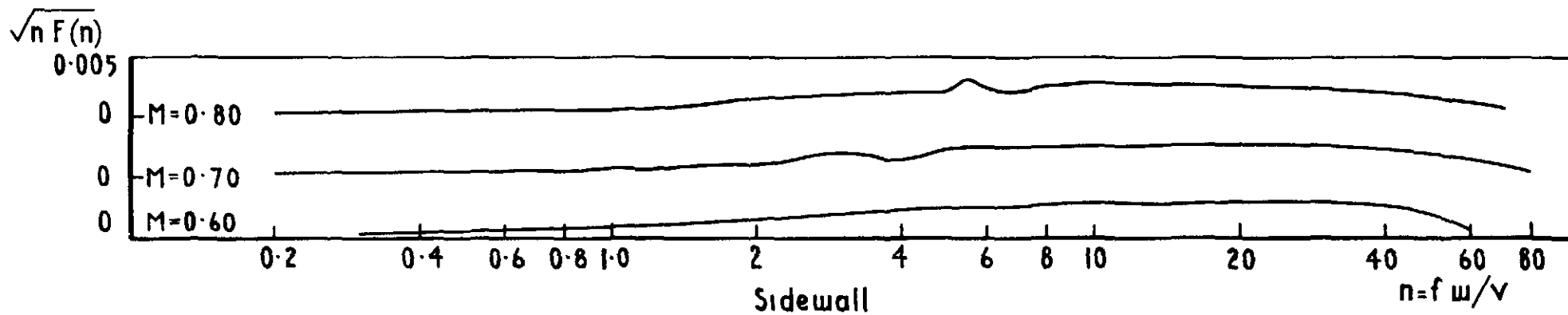


Fig.46 Unsteadiness in RAE 8ft x 8ft closed tunnel



## DETACHABLE ABSTRACT CARD

ARC CP No 1155  
October 1970

Mabey, D G

### FLOW UNSTEADINESS AND MODEL VIBRATION IN WIND TUNNELS AT SUBSONIC AND TRANSONIC SPEEDS

Flow unsteadiness and model vibration in the RAE 3ft x 3ft tunnel have impeded static and dynamic measurements at subsonic and transonic speeds. The unsteadiness was measured with pressure transducers both in the 3ft x 3ft tunnel and a 1/9 scale model of this tunnel and good agreement obtained.

For the closed 3ft x 3ft tunnel, successive modifications to the balance section and diffuser derived from tests of the model tunnel have reduced the unsteadiness at subsonic speeds to an acceptable level for dynamic tests.

The unsteadiness in the slotted tunnels operated by diffuser suction originated in the extraction region and was reduced in the 3ft x 3ft tunnel by covering the slots with perforated screens. The unsteadiness was still higher than in the closed tunnel and just

533 6 071 4  
532 5 013 6  
533 6 072  
534 13

(Over)

ARC CP No.1155  
October 1970

Mabey, D G.

### FLOW UNSTEADINESS AND MODEL VIBRATION IN WIND TUNNELS AT SUBSONIC AND TRANSONIC SPEEDS

Flow unsteadiness and model vibration in the RAE 3ft x 3ft tunnel have impeded static and dynamic measurements at subsonic and transonic speeds. The unsteadiness was measured with pressure transducers both in the 3ft x 3ft tunnel and a 1/9 scale model of this tunnel and good agreement obtained.

For the closed 3ft x 3ft tunnel, successive modifications to the balance section and diffuser derived from tests of the model tunnel have reduced the unsteadiness at subsonic speeds to an acceptable level for dynamic tests.

The unsteadiness in the slotted tunnels operated by diffuser suction originated in the extraction region and was reduced in the 3ft x 3ft tunnel by covering the slots with perforated screens. The unsteadiness was still higher than in the closed tunnel and just

533.6.071 4 .  
532.5.013.6 :  
533 6.072 :  
534.13

(Over)

(Over)

FLOW UNSTEADINESS AND MODEL VIBRATION IN  
 WIND TUNNELS AT SUBSONIC AND TRANSONIC SPEEDS  
 Flow unsteadiness and model vibration in the RAE 3ft x 3ft tunnel have impeded static and dynamic measurements at subsonic and transonic speeds. The unsteadiness was measured with pressure transducers both in the 3ft x 3ft tunnel and a 1/9 scale model of this tunnel and good agreement obtained.  
 For the closed 3ft x 3ft tunnel, successive modifications to the balance section and diffuser derived from tests of the model tunnel have reduced the unsteadiness at subsonic speeds to an acceptable level for dynamic tests.  
 The unsteadiness in the slotted tunnels operated by diffuser suction originated in the extraction region and was reduced in the 3ft x 3ft tunnel by covering the slots with perforated screens. The unsteadiness was still higher than in the closed tunnel and just

533 6 071.4  
 532.5 013.6  
 533 6 072  
 534 13

ARC CP No 1155  
 October 1970  
 Mabey, D G

(Over)

FLOW UNSTEADINESS AND MODEL VIBRATION IN  
 WIND TUNNELS AT SUBSONIC AND TRANSONIC SPEEDS  
 Flow unsteadiness and model vibration in the RAE 3ft x 3ft tunnel have impeded static and dynamic measurements at subsonic and transonic speeds. The unsteadiness was measured with pressure transducers both in the 3ft x 3ft tunnel and a 1/9 scale model of this tunnel and good agreement obtained.  
 For the closed 3ft x 3ft tunnel, successive modifications to the balance section and diffuser derived from tests of the model tunnel have reduced the unsteadiness at subsonic speeds to an acceptable level for dynamic tests.  
 The unsteadiness in the slotted tunnels operated by diffuser suction originated in the extraction region and was reduced in the 3ft x 3ft tunnel by covering the slots with perforated screens. The unsteadiness was still higher than in the closed tunnel and just

533 6 071.4  
 532.5 013 6  
 533 6 072 -  
 534 13

ARC CP No 1155  
 October 1970  
 Mabey, D G

acceptable in the 0.91m x 0.69m (3ft x 2.2ft) working section and unacceptable in the 0.91m x 0.91m (3ft x 3ft) working section

The perforated and closed working sections of the model tunnel had nearly the same unsteadiness and a similar result was achieved with the new perforated working section for the 3ft x 3ft tunnel in the frequency range normally of interest (from 20 to 900 Hz). Edge-tones generated at low unit Reynolds number were eliminated by a modification to the hole geometry.

Some comparative pressure fluctuation measurements in other closed, slotted and perforated tunnels are included in Appendices.

acceptable in the 0.91m x 0.69m (3ft x 2.2ft) working section and unacceptable in the 0.91m x 0.91m (3ft x 3ft) working section

The perforated and closed working sections of the model tunnel had nearly the same unsteadiness and a similar result was achieved with the new perforated working section for the 3ft x 3ft tunnel in the frequency range normally of interest (from 20 to 900 Hz). Edge-tones generated at low unit Reynolds number were eliminated by a modification to the hole geometry.

Some comparative pressure fluctuation measurements in other closed, slotted and perforated tunnels are included in Appendices.

acceptable in the 0.91m x 0.69m (3ft x 2.2ft) working section and unacceptable in the 0.91m x 0.91m (3ft x 3ft) working section

The perforated and closed working sections of the model tunnel had nearly the same unsteadiness and a similar result was achieved with the new perforated working section for the 3ft x 3ft tunnel in the frequency range normally of interest (from 20 to 900 Hz). Edge-tones generated at low unit Reynolds number were eliminated by a modification to the hole geometry.

Some comparative pressure fluctuation measurements in other closed, slotted and perforated tunnels are included in Appendices.

acceptable in the 0.91m x 0.69m (3ft x 2.2ft) working section and unacceptable in the 0.91m x 0.91m (3ft x 3ft) working section.

The perforated and closed working sections of the model tunnel had nearly the same unsteadiness and a similar result was achieved with the new perforated working section for the 3ft x 3ft tunnel in the frequency range normally of interest (from 20 to 900 Hz). Edge-tones generated at low unit Reynolds number were eliminated by a modification to the hole geometry.

Some comparative pressure fluctuation measurements in other closed, slotted and perforated tunnels are included in Appendices.





C.P. No. 1155

© *Crown copyright 1971*

Published by  
HER MAJESTY'S STATIONERY OFFICE

To be purchased from  
49 High Holborn, London WC1 V 6HB  
13a Castle Street, Edinburgh EH2 3AR  
109 St Mary Street, Cardiff CF1 1JW  
Brazennose Street, Manchester M60 8AS  
50 Fairfax Street, Bristol BS1 3DE  
258 Broad Street, Birmingham B1 2HE  
80 Chichester Street, Belfast BT1 4JY  
or through booksellers

C.P. No. 1155

SBN 11 470423 6